Fifth High-Lift Prediction Workshop (HLPW-5)

Fixed-Grid Reynolds-Averaged Navier-Stokes (RANS)

Technical Focus Group (TFG)

August 2, 2024

Key Questions

- **HLPW-5 Key Questions**
  - Test Case 1: Can consistency of integrated CFD forces/moments be achieved for simple high-lift configurations?
  - Test Case 2: Does consistency of CFD forces/moments change in configuration buildup?
  - Test Case 3: Does consistency of CFD forces/moments change with variation of Reynolds number?
  - Are there unique CFD modeling requirements (e.g., mesh, solver, etc.)?
- **Fixed-Grid RANS TFG Key Questions**
  - Can grid-converged solution be achieved with practical RANS solvers for high-lift configurations?
  - Can different solvers using the same RANS model agree on grid-converged solution?
  - What are requirements for different RANS solvers to agree on grid-converged solutions?
  - What insight RANS solutions can provide for experiments and turbulence models?

Outline

- **Statistics of Fixed-Grid RANS Solutions**
- **Test Case 1: Verification**
- **Test Case 2 : Configuration buildup**
- **Test case 3 : Reynolds Number Effects**
- **Conclusion: Responses to Key Questions**

Fixed-Grid RANS TFG Statistics

- **96 E-mail Addresses on Fixed-Grid RANS TFG Distribution List**
- **26 Teams Submitted RANS Solutions on Fixed-Grid Families**
  - 23 R- teams and H-005, L-004, and L-005 teams
  - R- teams/codes listed at https://hiliftpw.larc.nasa.gov/Workshop5/TFG_rans.html
  - 10 countries
  - Government labs, major aerospace companies, academic institutions, commercial software developers, and small businesses
  - 224 independent sets of fixed-grid solutions

Fixed-Grid RANS Solutions

- **Discretization Approaches**
  - Node-centered, finite-volume, 2nd order : 6 solvers, 69 sets
  - Cell-centered, finite-volume, 2nd order : 16 solvers, 141 sets
  - Node-centered, continuous finite-element : 2 solvers, 14 sets
- **RANS Models**
  - Spalart-Allmaras (SA) equations, including SA-neg and SA-noft2 variants : 22 solvers, 150 sets
  - SA-R(C_{rot}=1)-QCR2000 equations : 13 solvers, 32 sets
  - Other models : 9 solvers, 42 sets
- **Fixed-Grid Families**
  - POINTWISE, mixed-element (1.R.01, 1.R.09, 2.R.03, 3.R.01) : 18 solvers, 83 sets
  - HELDENMESH, mixed-element (1.R.03, 1.R.05, 1.R.07, 2.R.01, 3.R.02) : 11 solvers, 76 sets
  - ANSYS ICEM CFD, hex-dominant (1.R.04, 1.L.01, 1.H.04, 2.L.01) : 10 solvers, 31 sets
  - STAR-CCM+, mixed-element (2.R.04) : 2 solvers, 9 sets
  - Custom grids : 6 solvers, 18 sets
- **RANS solutions on adapted grids are shown for reference**

Solution Assessment Criteria

- **Iterative Convergence Criteria**
  - Machine-zero meanflow and turbulence-model residuals for steady-state solutions are desirable
    - ✓ Rarely achieved for complex geometries (2.2-2.4, 3.1-3.4) and high angles of attack
  - Relaxed criteria of 1% variation in established convergence pattern of forces and pitching moment (F&M) over last 20% of iterations
    - ✓ Illustrated later on Case 1 example

- **Grid Convergence**
  - Solutions on three or more grids in family, including fine enough grids
  - Smaller variation between solutions on finer grids
  - Aerodynamic coefficients are plotted versus characteristic mesh size $\mathrm{h} = \mathrm{N}^{(-1/3)}$
    - ✓ N is degrees of freedom: nodes for node-centered and cells for cell-centered solutions

Test Case 1

Verification Case

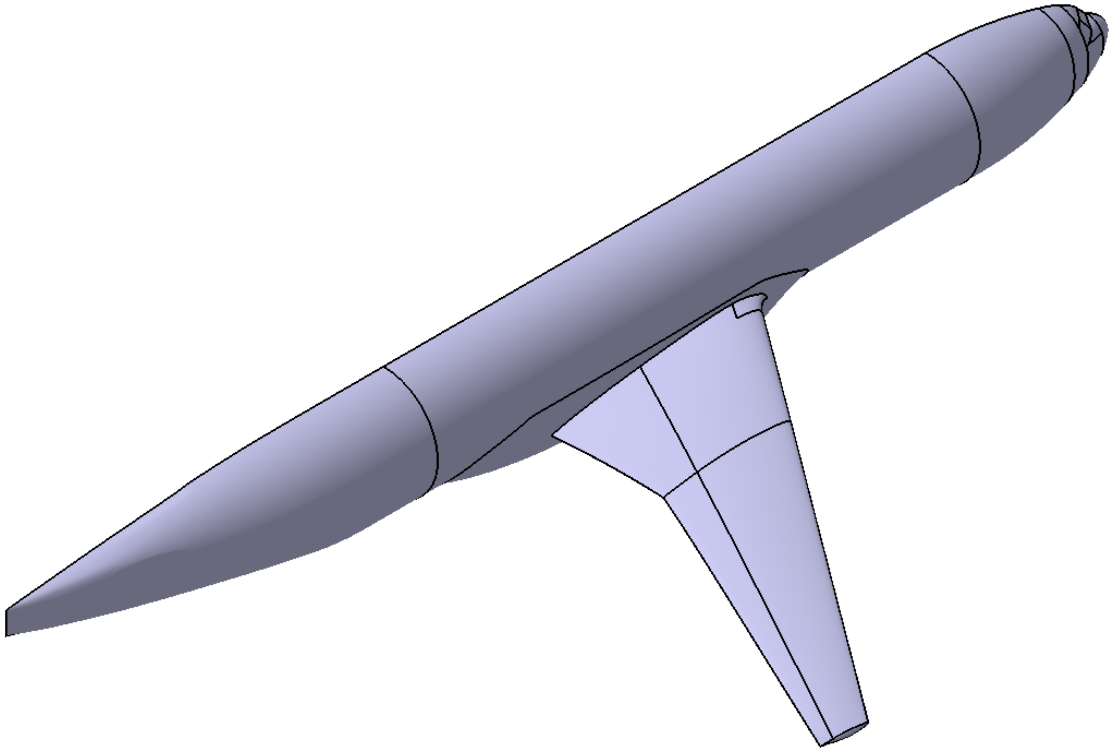

CRM-HL-WB

Flow Conditions: $M_\infty = 0.2$, $Re_{MAC} = 5.6\times10^6$, $T_{ref} = 521°R$, $\alpha = 11°$

F&M Grid Convergence, All RANS Solutions

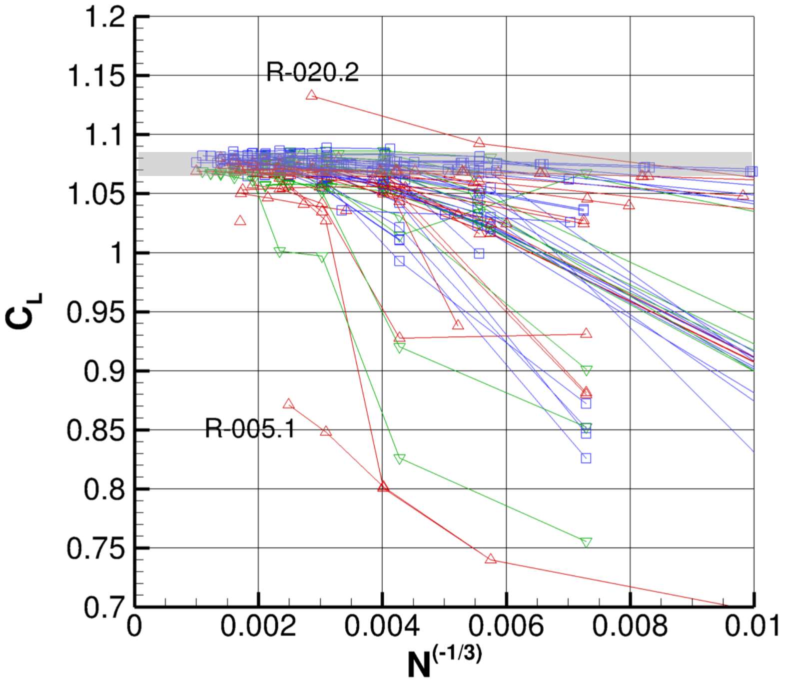

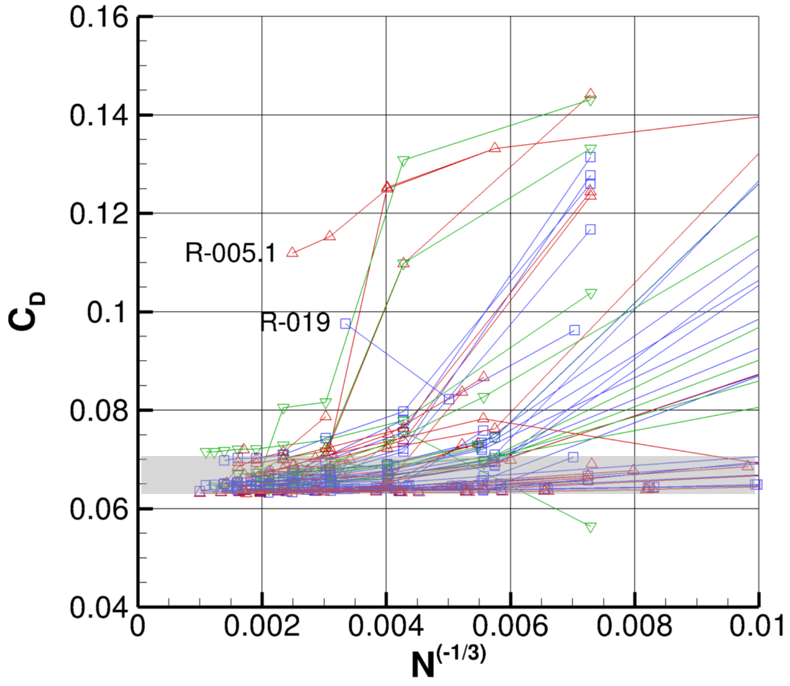

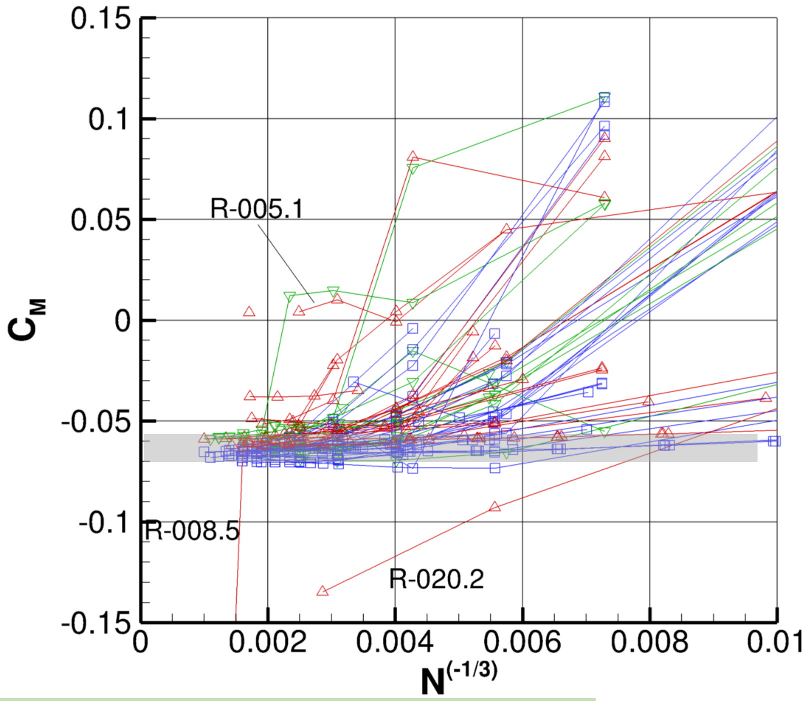

Blue = SA
Red = SA-R(c_{rot}=1)-QCR2000
Green = other

Global view:

- With exception of outliers, relatively tight grouping of aerodynamic coefficients in grid refinement
- Hard to discern more details

Grid-size reference:

N =	1,000,000	$N^{(-1/3)} \sim 0.01$
N =	5,000,000	$N^{(-1/3)} \sim 0.006$
N =	10,000,000	$N^{(-1/3)} \sim 0.005$
N =	100,000,000	$N^{(-1/3)} \sim 0.002$
N =	300,000,000	$N^{(-1/3)} \sim 0.0015$
N =	500,000,000	$N^{(-1/3)} \sim 0.0013$
N =	1,000,000,000	$N^{(-1/3)} \sim 0.001$

F&M Grid Convergence (Zoomed), All RANS Solutions

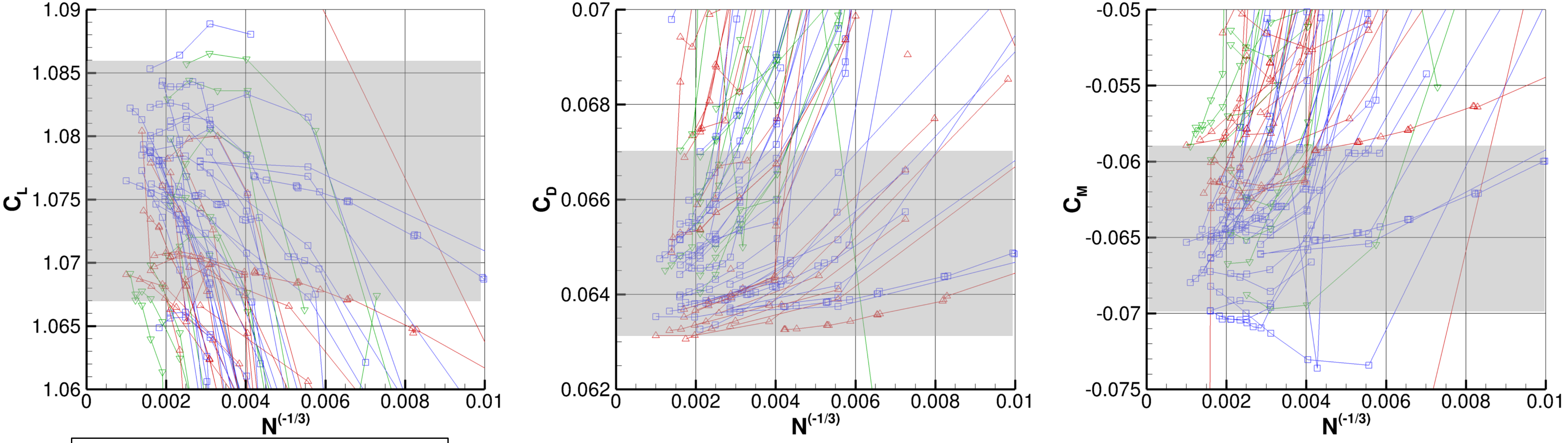

Blue = SA
Red = SA-R(c_{rot}=1)-QCR2000
Green = other

C_L: 2% range [1.065, 1.086] (shaded)
C_D: 6% range [0.063, 0.067] (40 counts, shaded)
C_M: 20% range [-0.070, -0.058] (shaded)

- Only two models have multiple submissions
- Selection is needed to assess agreement between solutions in grid refinement

Selection process:

1. Solutions computed with the same RANS model
2. Solutions converged iteratively on nominal grids
3. Solutions demonstrated grid convergence

Iterative Convergence, All RANS Solutions

Iterative convergence criteria: 1% variation in established convergence pattern of lift and pitching moment over last 20% of iterations

- Steady-state solution: mean varies by less than 1% and standard deviation is less than 1%
- Established oscillatory solution: mean and standard deviation vary by less than 1%

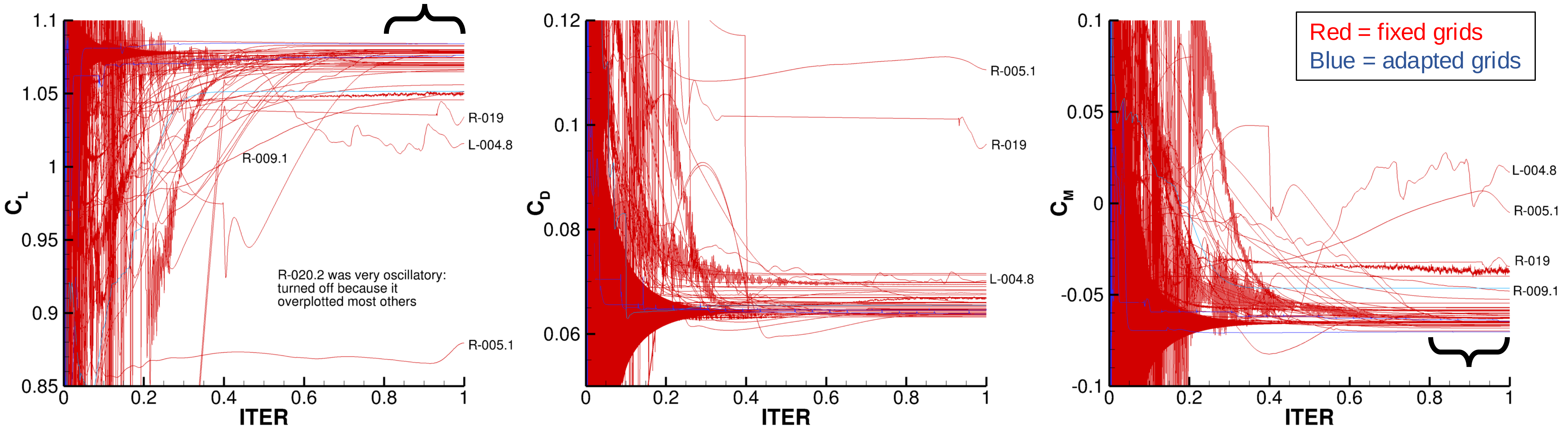

- With exception of outliers, solutions satisfy iterative convergence criteria
- Most solutions converged to steady state
- Many solutions converged residuals to low levels comparable with machine zero

F&M Grid Convergence, SA Solutions

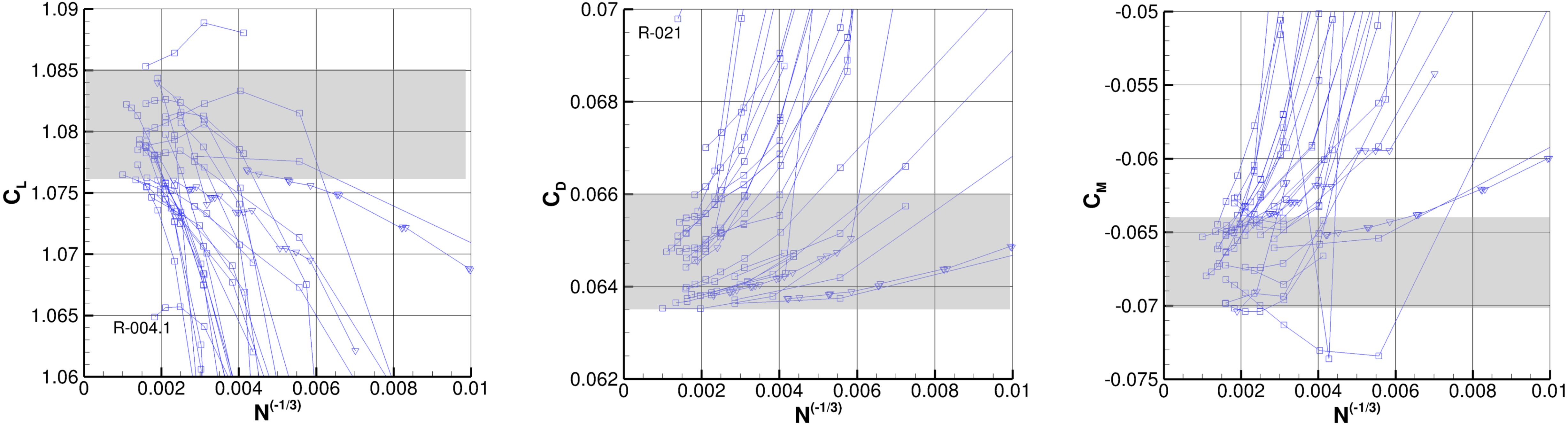

All RANS solutions (shown for reference)

C_L: 2% range [1.065, 1.086]
C_D: 6% range [0.063, 0.067] (40 counts)
C_M: 20% range [-0.070, -0.058]

SA solutions

C_L: 0.9% range [1.075, 1.085] (shaded)
C_D: 4% range [0.0635, 0.0660] (25 counts, shaded)
C_M: 9% range [-0.070, -0.064] (shaded)

- Grid-convergence trend, i.e., smaller solution variation on finer grids
- F&M ranges for SA solutions reduced by more than factor 2 for C_L and C_M; by 15 counts for C_D

Selected SA Solutions

Grid-converged solution established with high confidence

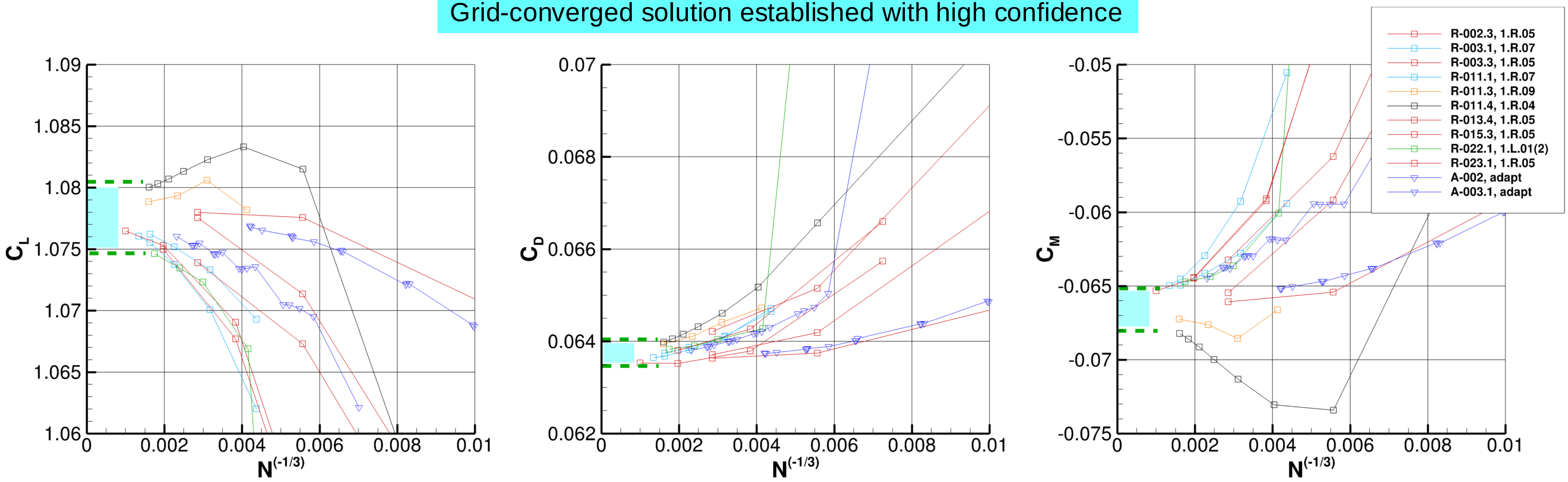

All SA solutions (shown for reference)

C_L: 0.9% range [1.075, 1.085]
C_D: 4% range [0.0635, 0.0660] (25 counts)
C_M: 9% range [-0.070, -0.064]

- Solutions not satisfying iterative convergence criteria and solutions on 1.R.01 grids removed
- Grid-convergence plots colored by grid family

Selected SA solutions

C_L: 0.45% range [1.075, 1.080]
C_D: 0.8% range [0.0635, 0.0640], (5 counts)
C_M: 4.5% range [-0.068, -0.065]

- Ranges of C_L and C_M reduced by factor 2
- Range of C_D reduced by 20 counts
- Residuals are well converged

Selected SA-R(c_{rot}=1)-QCR2000 Solutions

Grid-converged solution established with high confidence

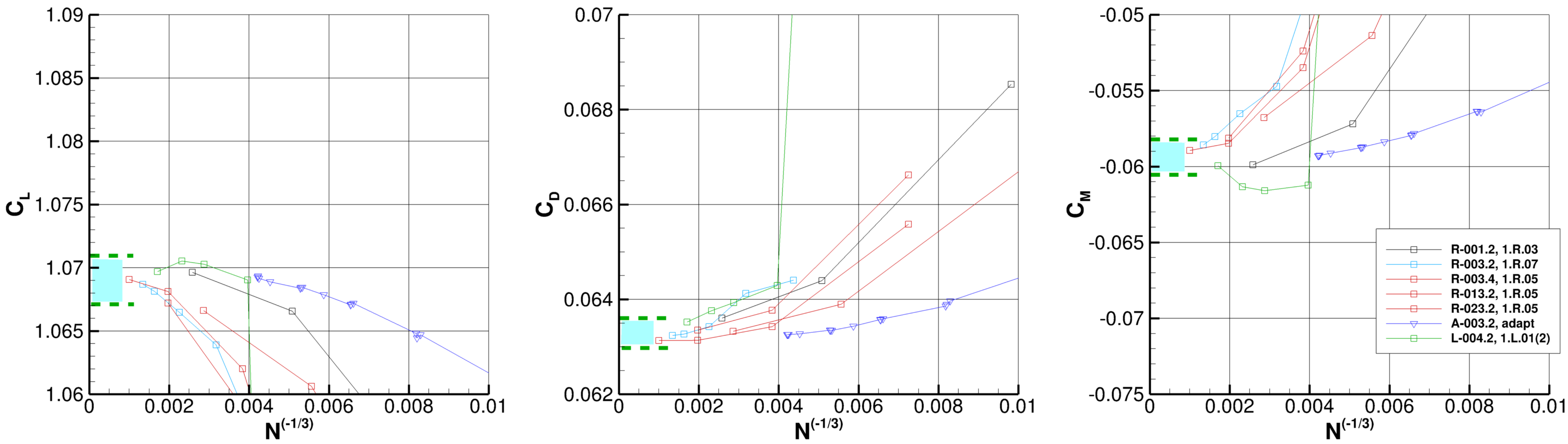

- Ranges for C_L and C_M in SA and SA-R(c_{rot}=1)-QCR2000 solutions do not overlap
- Distinctly different grid-converged solutions for each model
- Grid-convergence plots colored by grid family

All SA-R(c_{rot}=1)-QCR2000 solutions

C_L: 2.3% range [1.066, 1.081]
C_D: 10% range [0.0630, 0.0694] (64 counts)
C_M: 12% range [-0.063, -0.056]

Selected SA-R(c_{rot}=1)-QCR2000 solutions

C_L: 0.4% range [1.067, 1.071]
C_D: 1% range [0.0630, 0.0636], (6 counts)
C_M: 5% range [-0.061, -0.058]

SP1.1 View: Outboard Wing Trailing-Edge Streamlines

Looking outboard at glancing angle, fuselage turned off

SA model

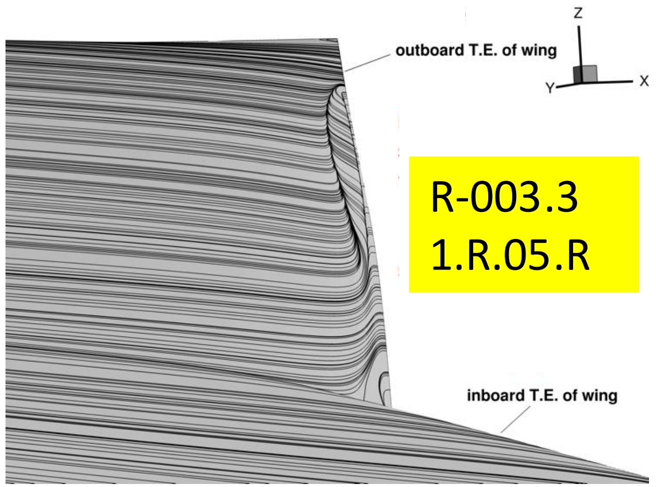

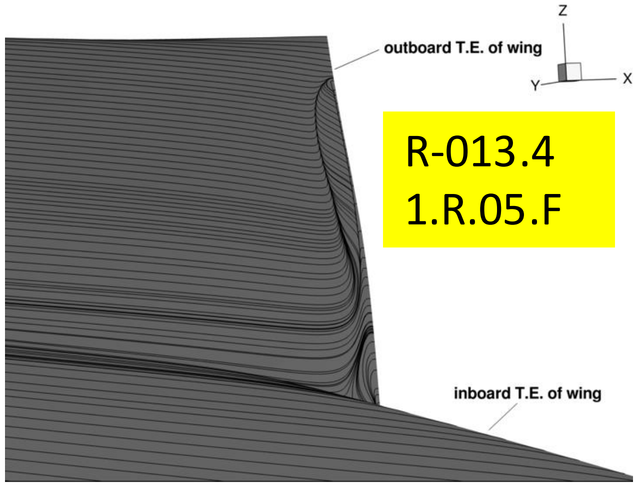

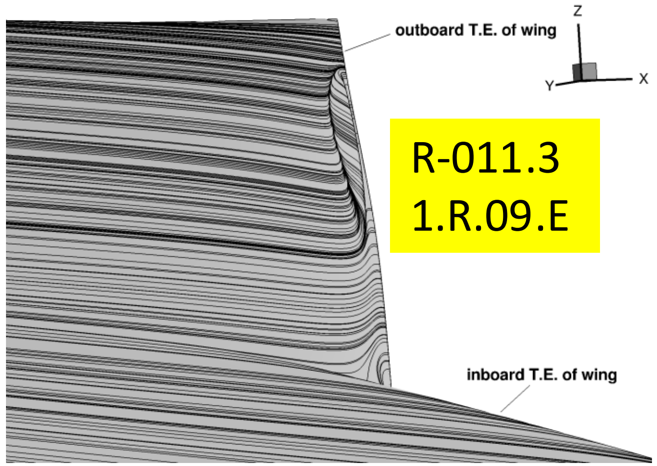

SA-R(c_{rot}=1)-QCR2000 model

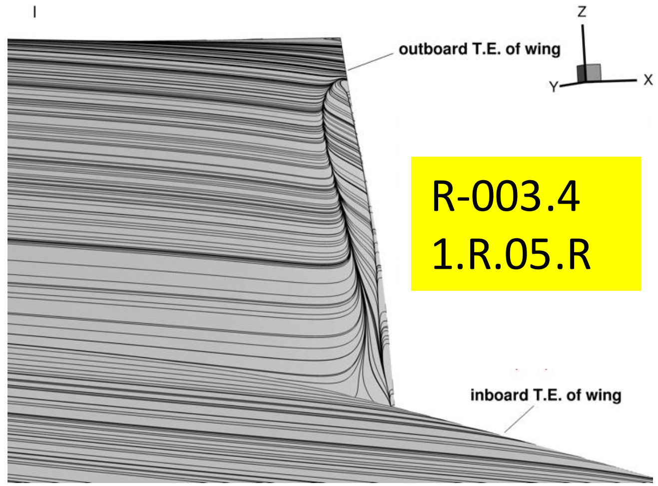

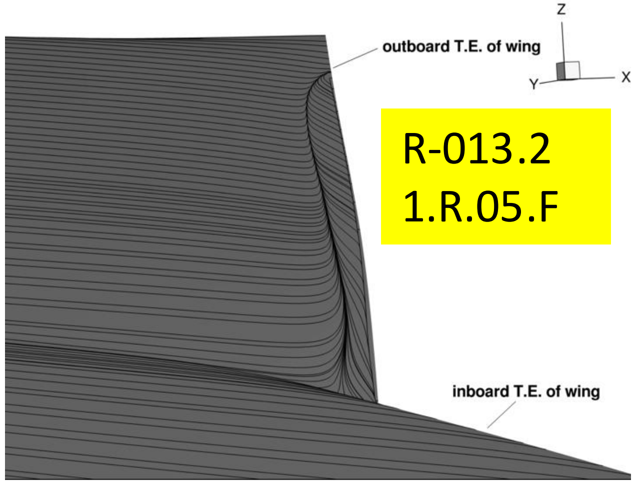

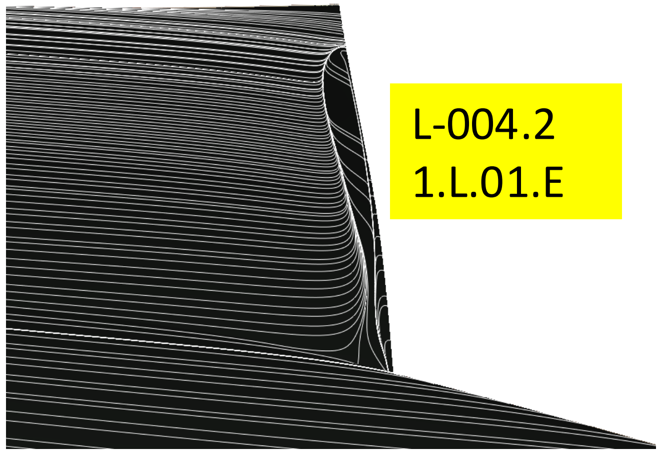

Distinctly different streamlines in SA and SA-R(c_{rot}=1)-QCR2000 solutions

Streamlines in Selected SA Solutions

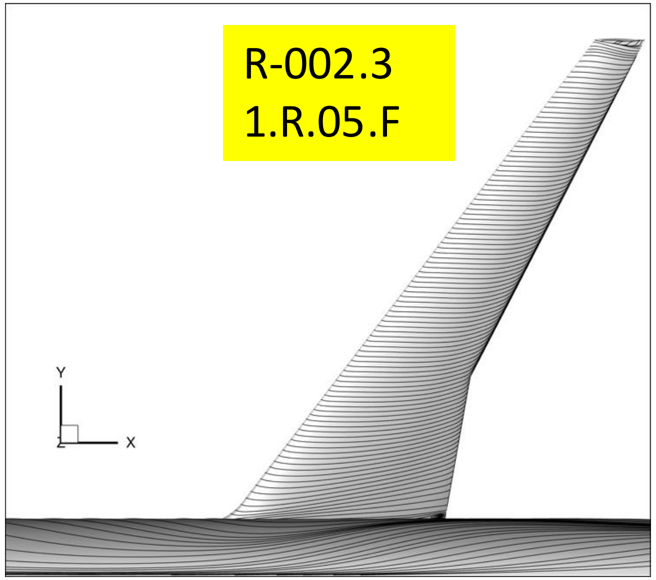

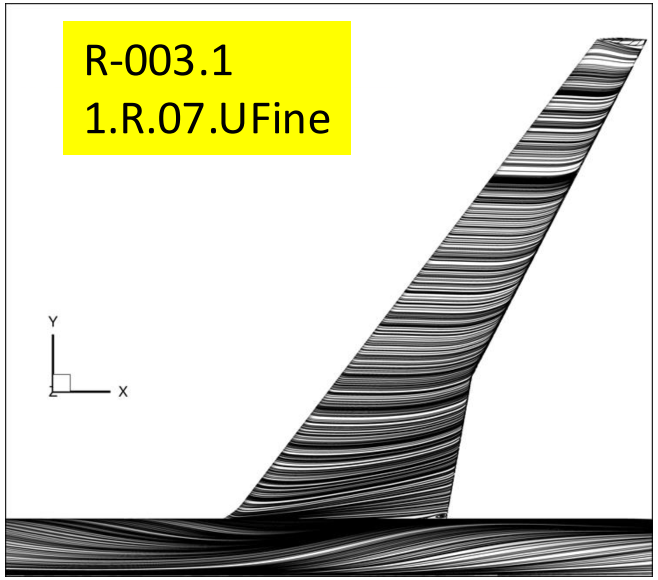

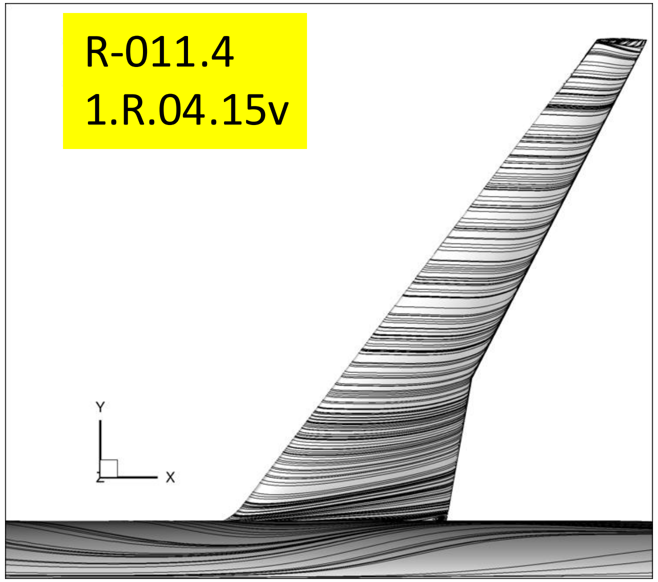

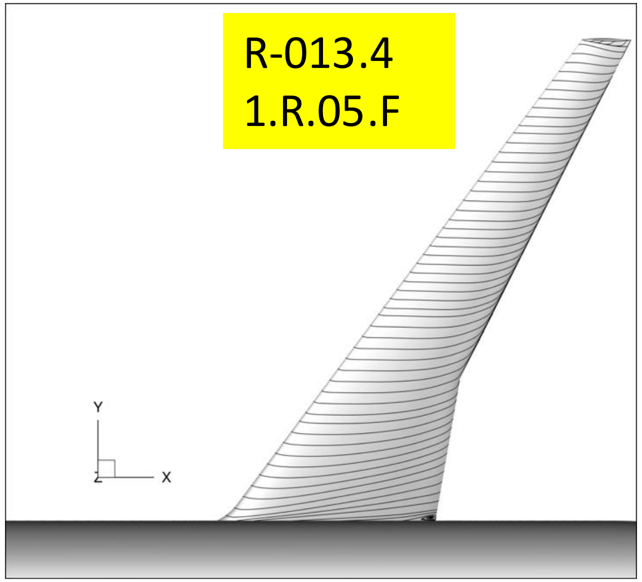

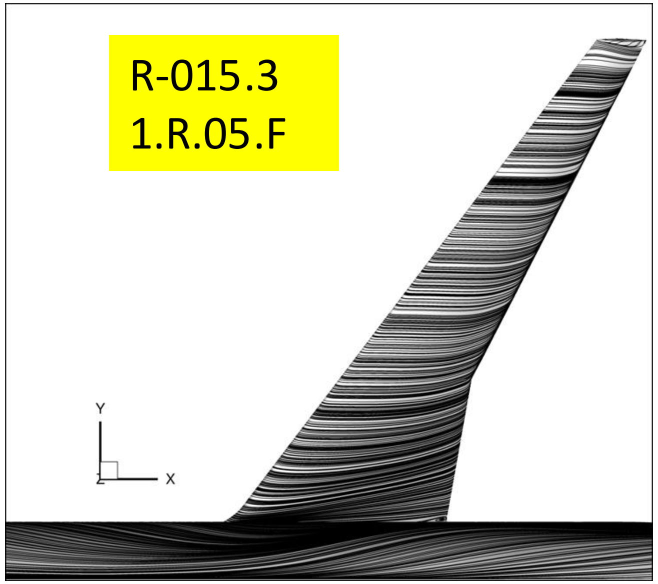

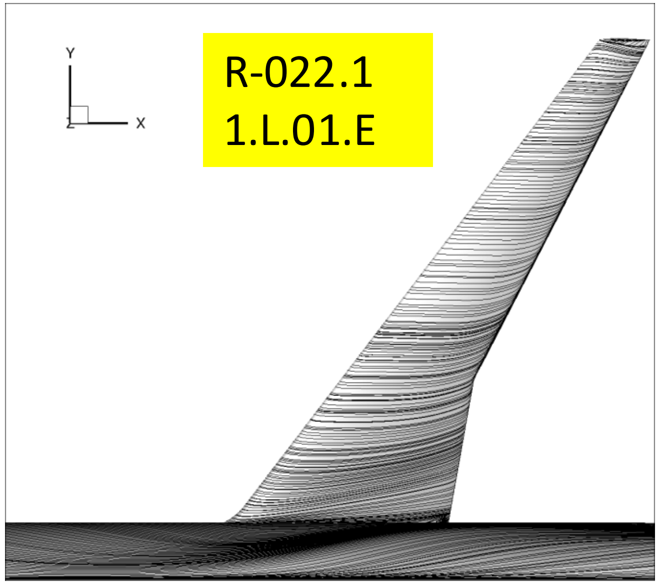

- Similar streamlines in selected SA solutions

Skin-Friction Contours in Selected SA Solutions

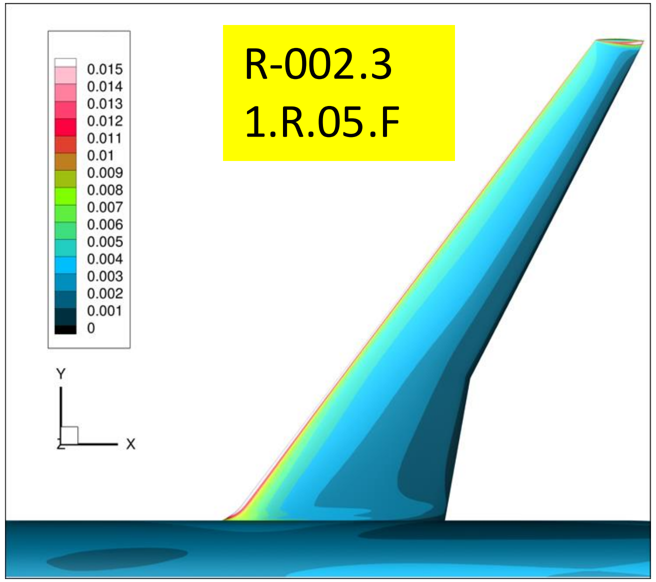

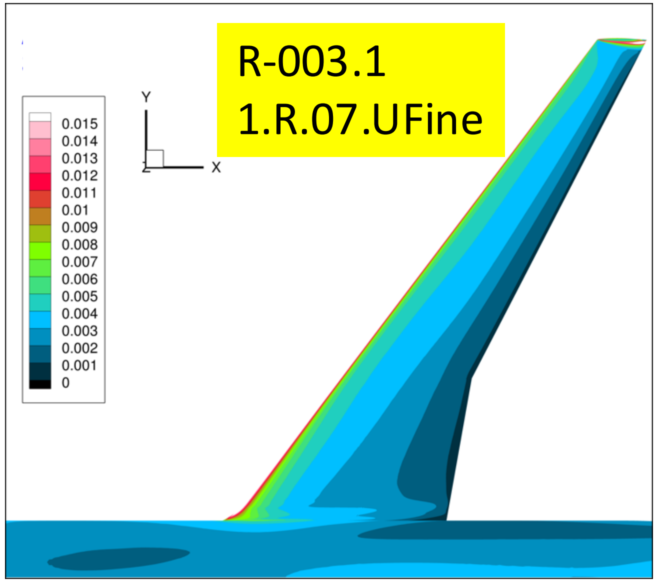

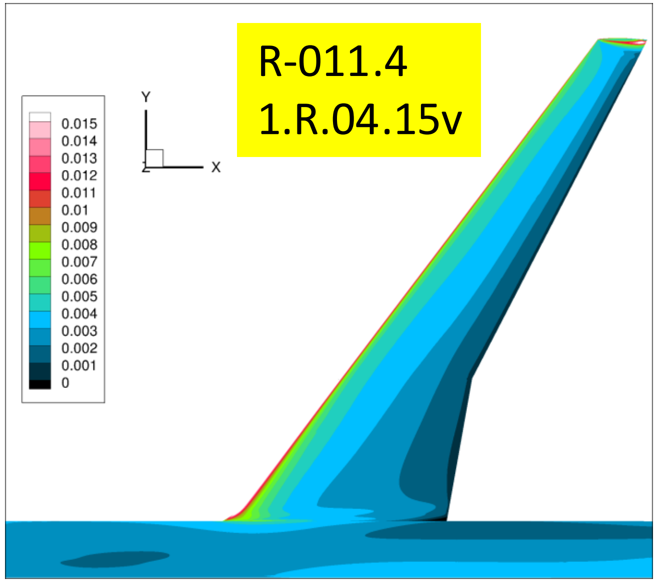

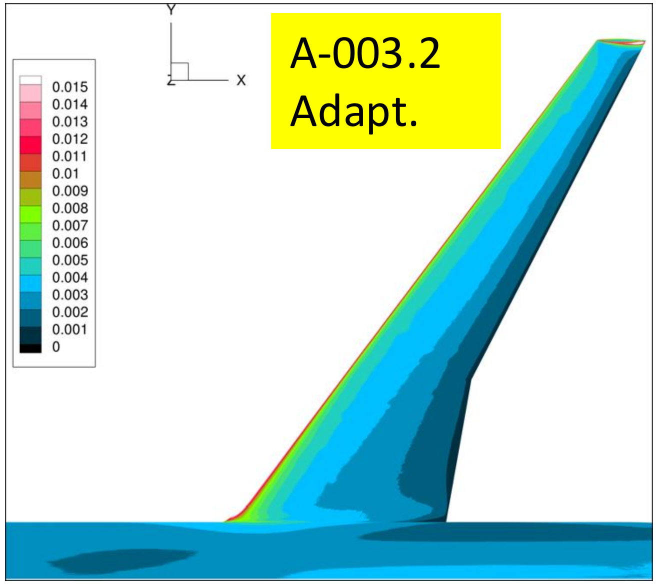

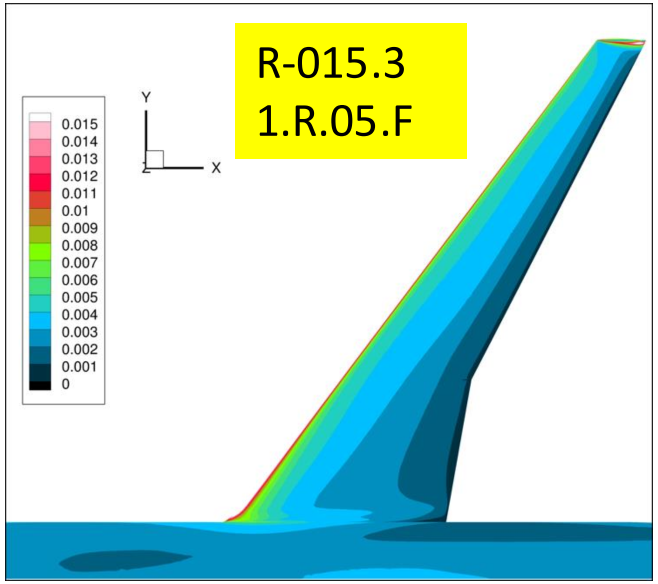

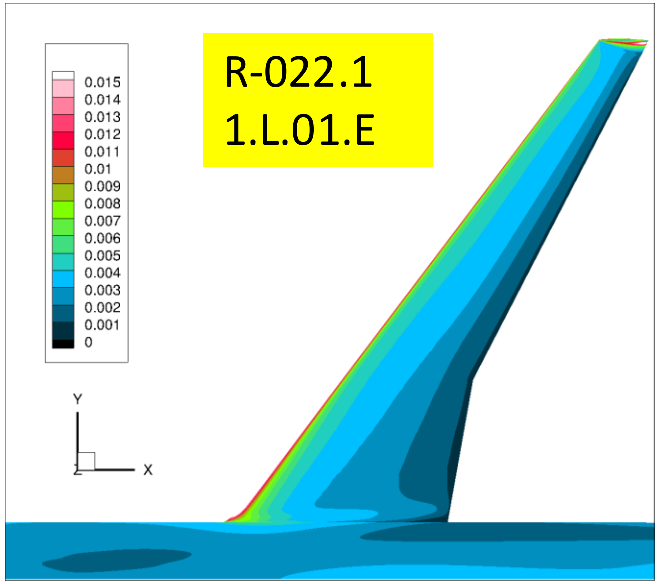

- Similar skin-friction patterns in selected SA solutions

Surface Pressure, All RANS Solutions

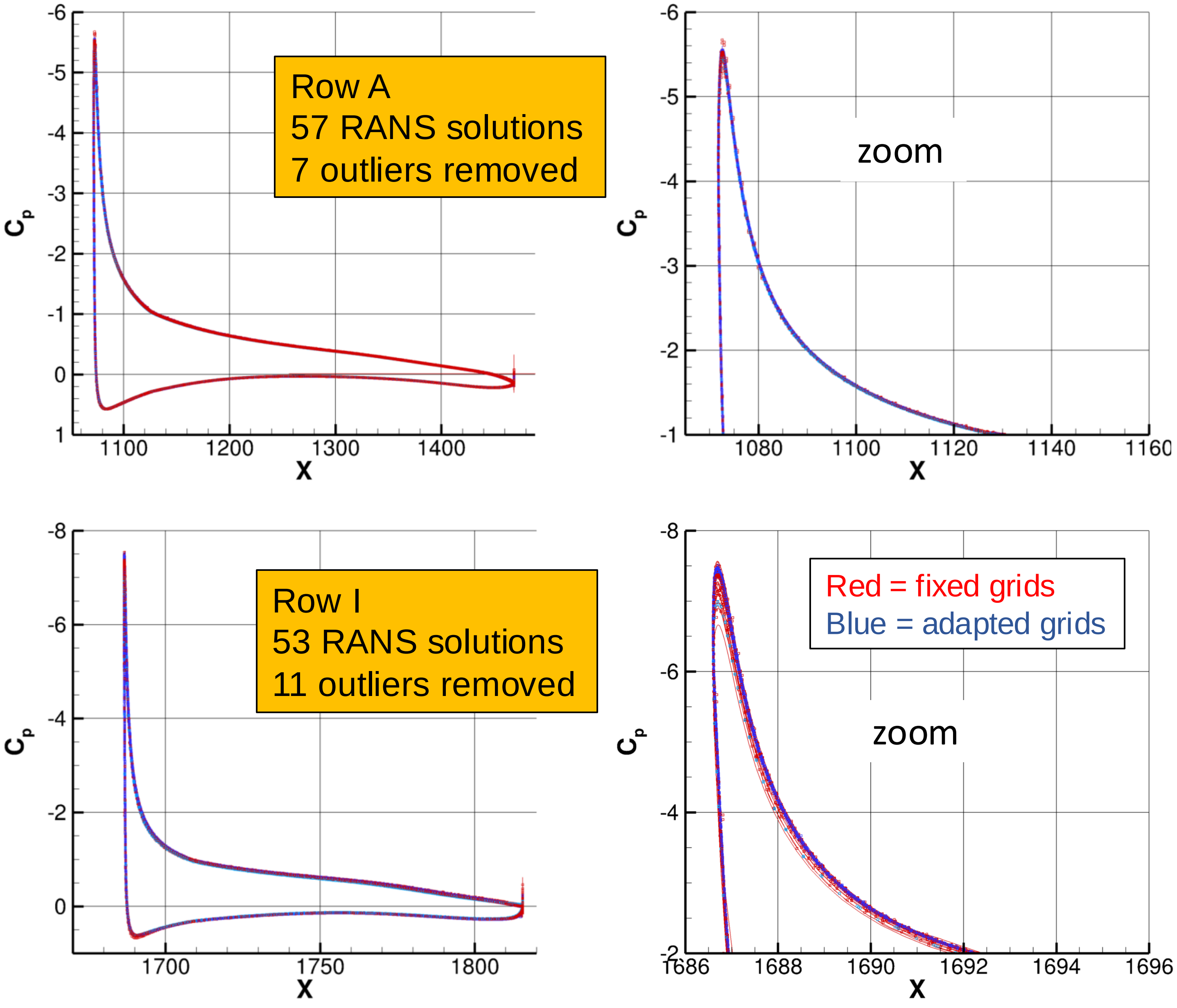

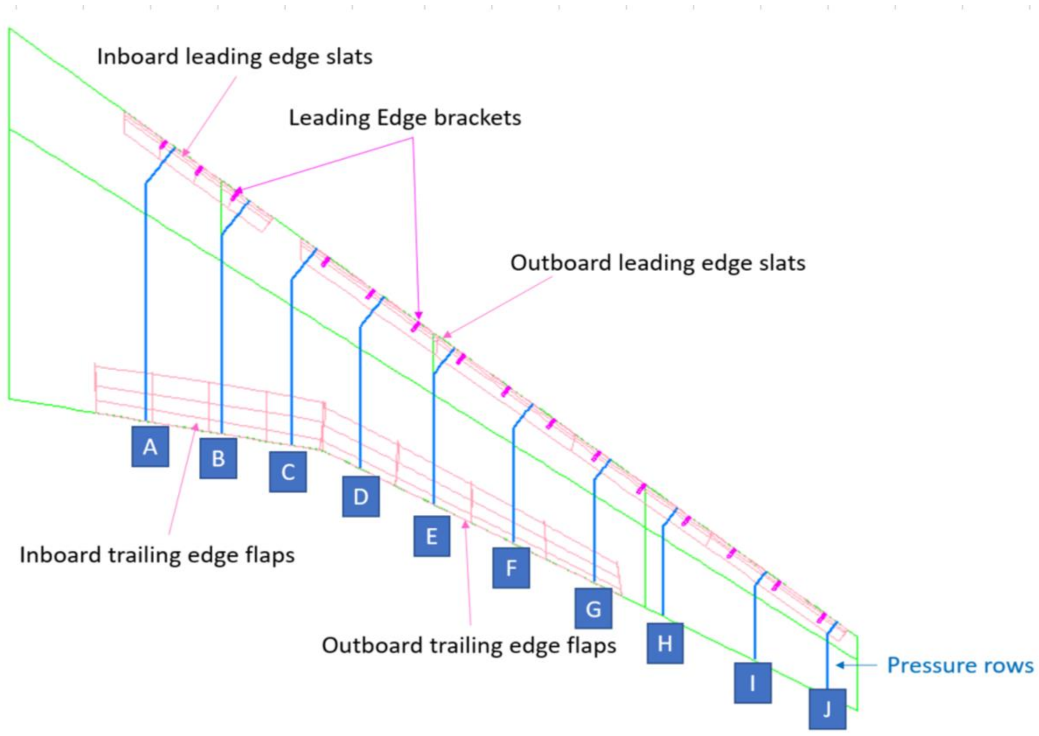

- Good agreement in surface pressure among most solutions at inboard sections
- Some deterioration for outboard sections

Surface Pressure Suction Peak, Selected Solutions

- Excellent agreement between surface pressures in selected solutions at all sections, including suction peak and trailing edge (not shown)

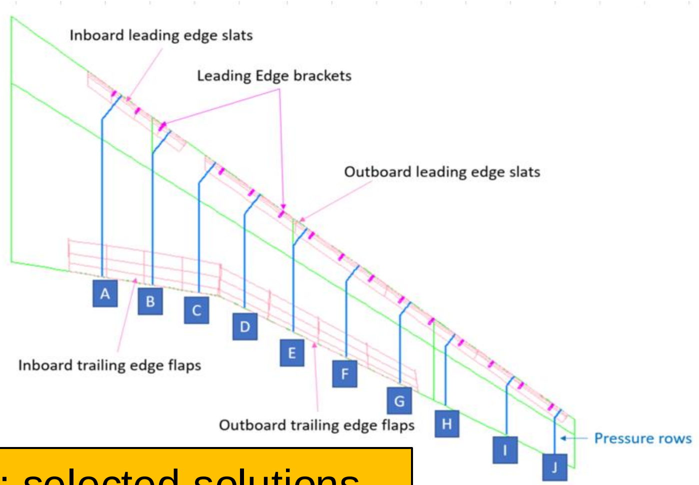

Zoomed suction-peak view

Row I: RANS solutions (shown for reference)

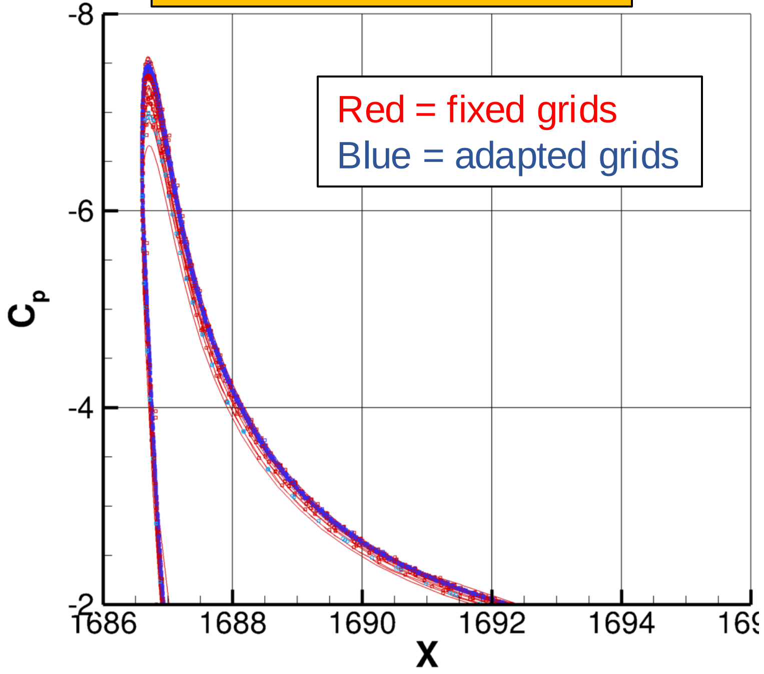

Row I: selected solutions SA

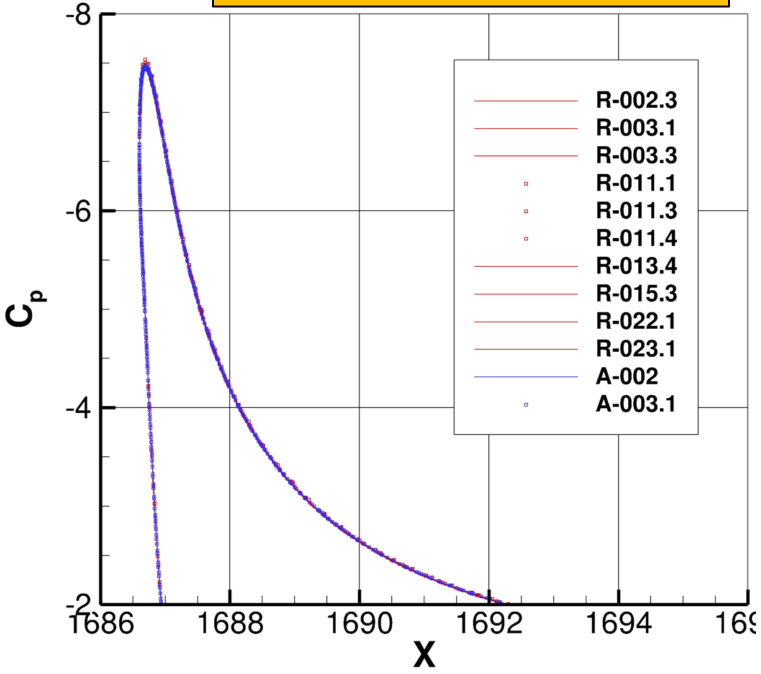

Row I: selected solutions SA-R(c_{rot}=1)-QCR2000

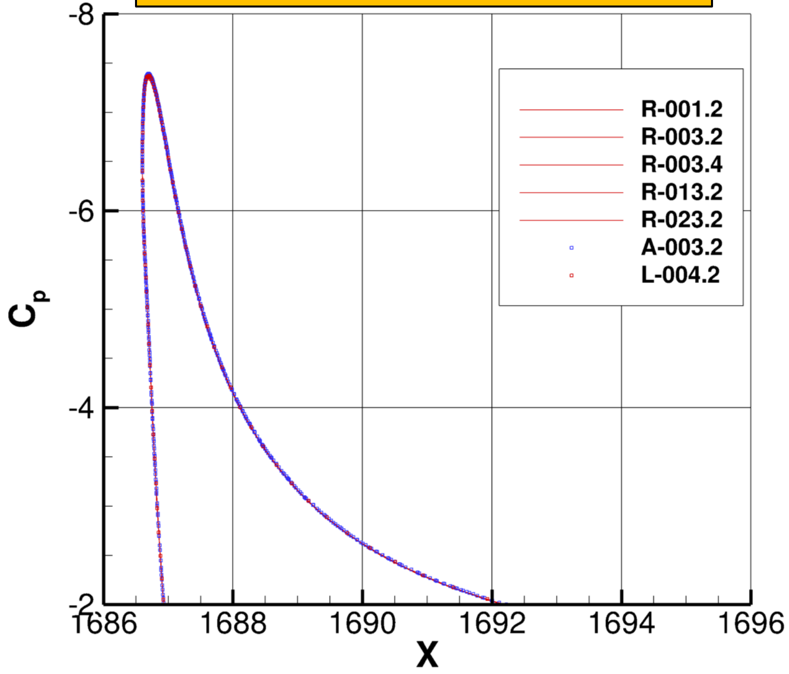

Case 1

Miscellaneous Observations

Eddy-viscosity profiles

Blue = SA
Red = SA-R(c_{rot}=1)-QCR2000
Green = other

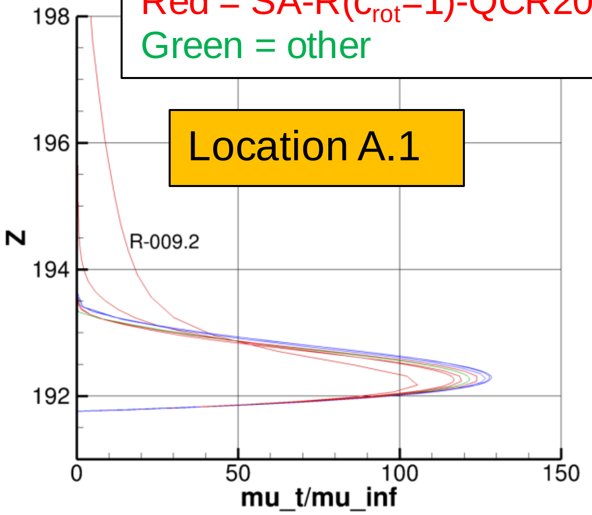

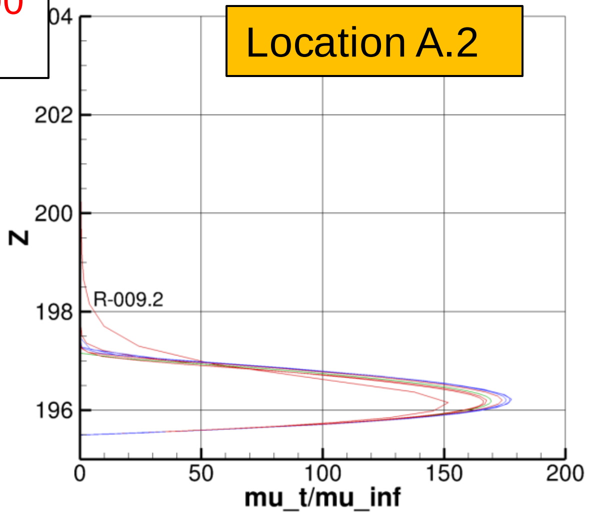

Submissions from:
R-009.1-2
R-015.1-4
R-017.5
R-020.1-2
A-006

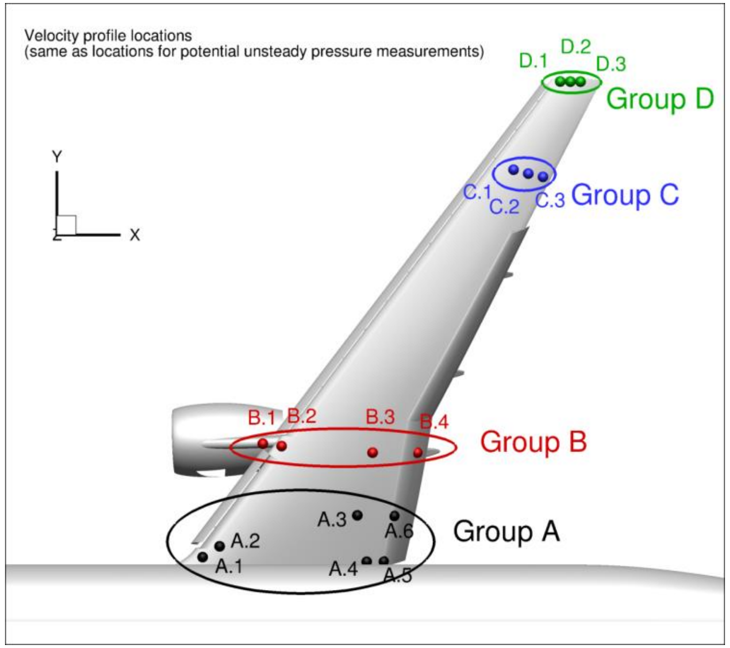

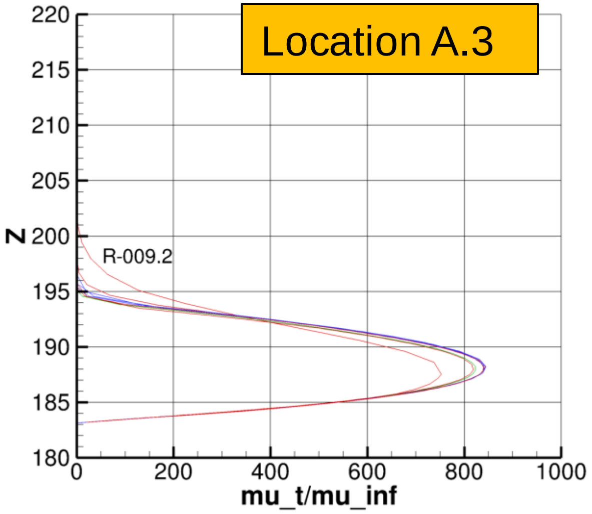

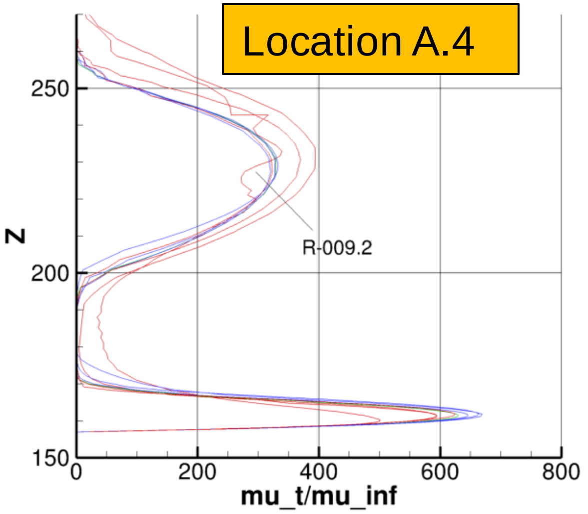

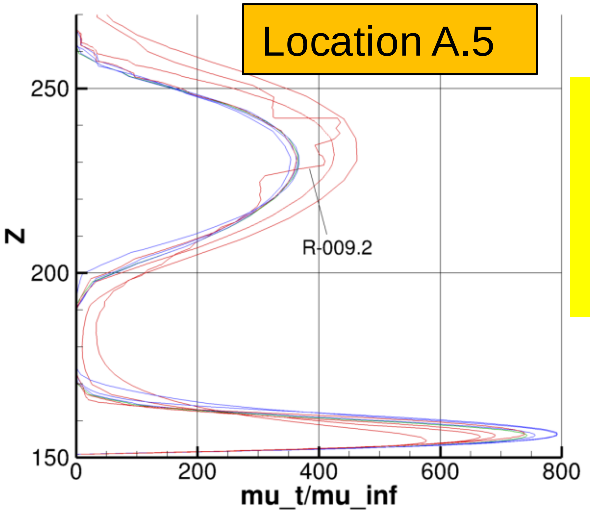

- Few eddy-viscosity profiles
  - SA solutions agree well
  - SA-R(c_{rot}=1)-QCR2000 solutions show more variation

Red = fixed grids
Blue = adapted grids

Velocity Profiles

Location B.2

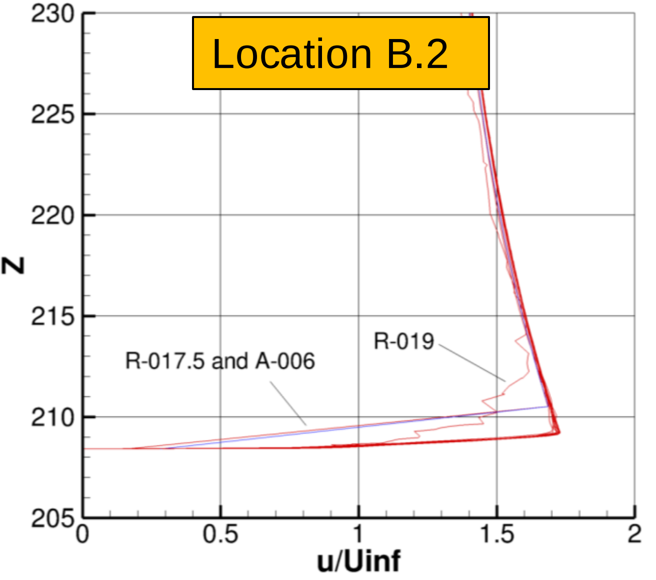

Location B.3

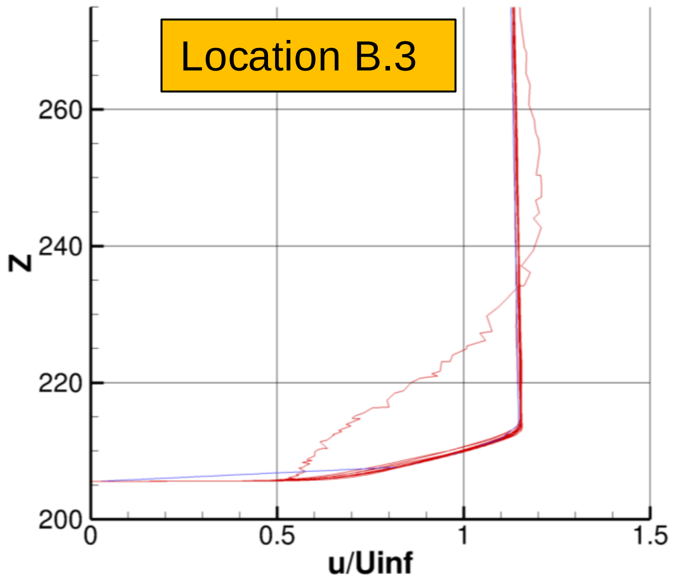

RANS
Submissions from:
R-009.1-2
R-015.1-4
R-016.1-2
R-017.5
R-019
R-020.1-2
R-022.1-2
A-006
(also L-004.1,2,8)

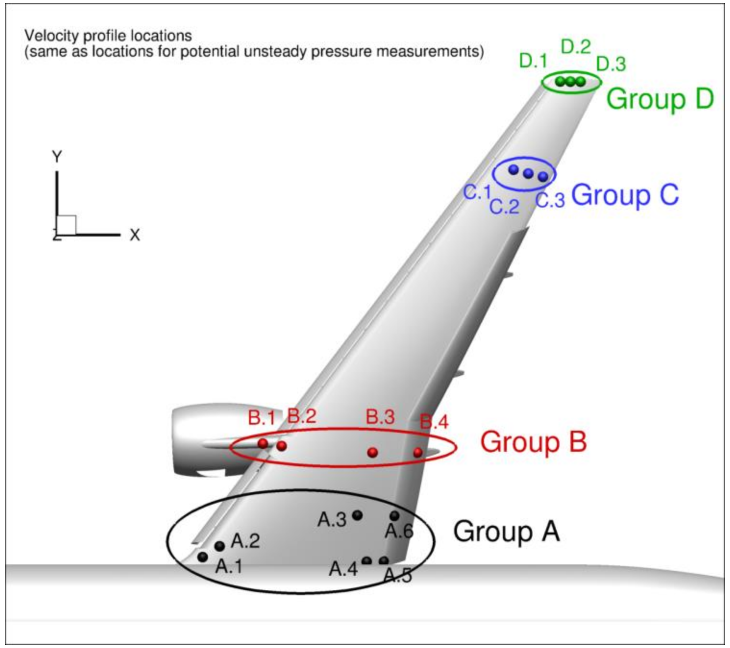

Location C.1

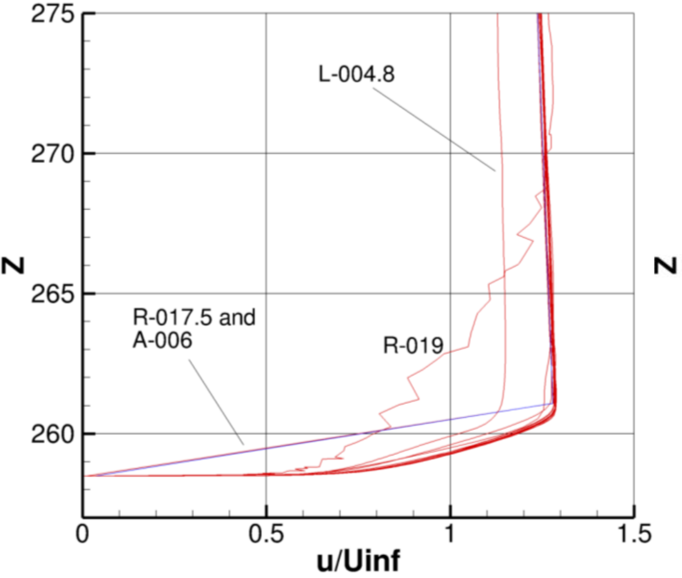

Location C.2

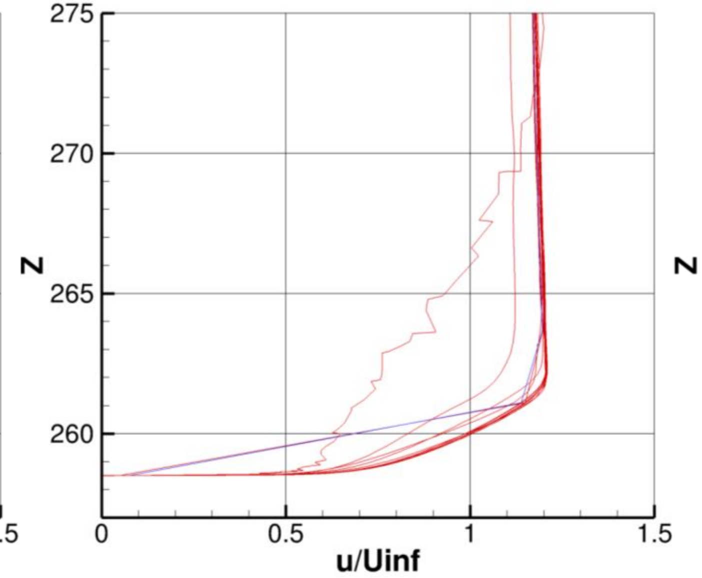

Location C.3

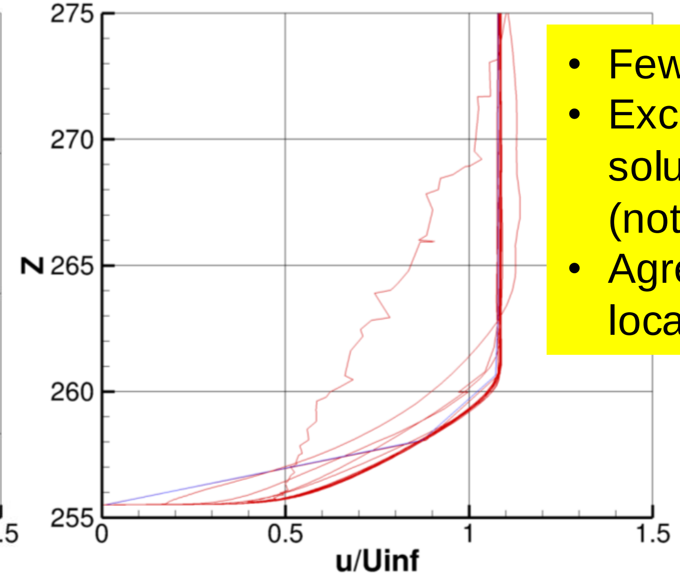

- Few velocity profiles
- Except for several outliers, RANS solutions agree at locations A (not shown) and B
- Agreement gets worse at locations C and D (not shown)

Test Case 1: Summary

- **RANS solvers agree on grid-converged solutions if**
  - Solutions computed with the same RANS model
    - ✓ Importance of well-posed RANS models (PDE solution exists, is unique, and continuously depends on input parameters)
  - Grid families place sufficient degrees of freedom in critically important areas
    - ✓ Importance of mesh-generation and aerodynamics experts in loop
  - Iterative convergence is sufficient
    - ✓ Importance of strong nonlinear iterative solvers
- **Case 1 grid-converged solutions established with high confidence for SA and SA-R(c_{rot}=1)-QCR2000 models**
  - Different solvers computing on different grid families with the same RANS model converge aerodynamic coefficients within narrow ranges
  - Grid-converged solutions distinguish between different RANS models, in aerodynamic coefficients and separation patterns
  - Can be used for validation

Test Case 2

Configuration Build-Up

Case 2.1

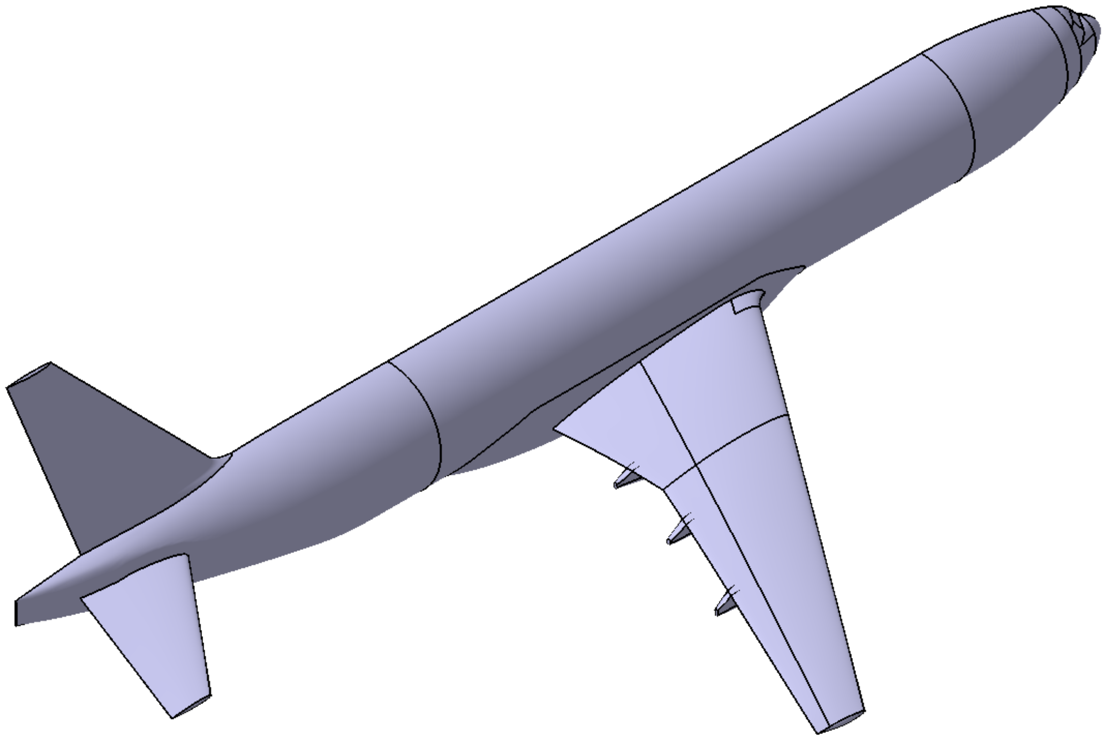

CRM-HL-WBHV

Flow Conditions: M_∞ = 0.2, Re_{MAC} = 5.4×10^6, T_{ref} = 518.67°R,

α = 6°,10°, 12°, 13°, 14°, 15°, 16°

F&M Polars on Nominal Grids, All RANS Solutions

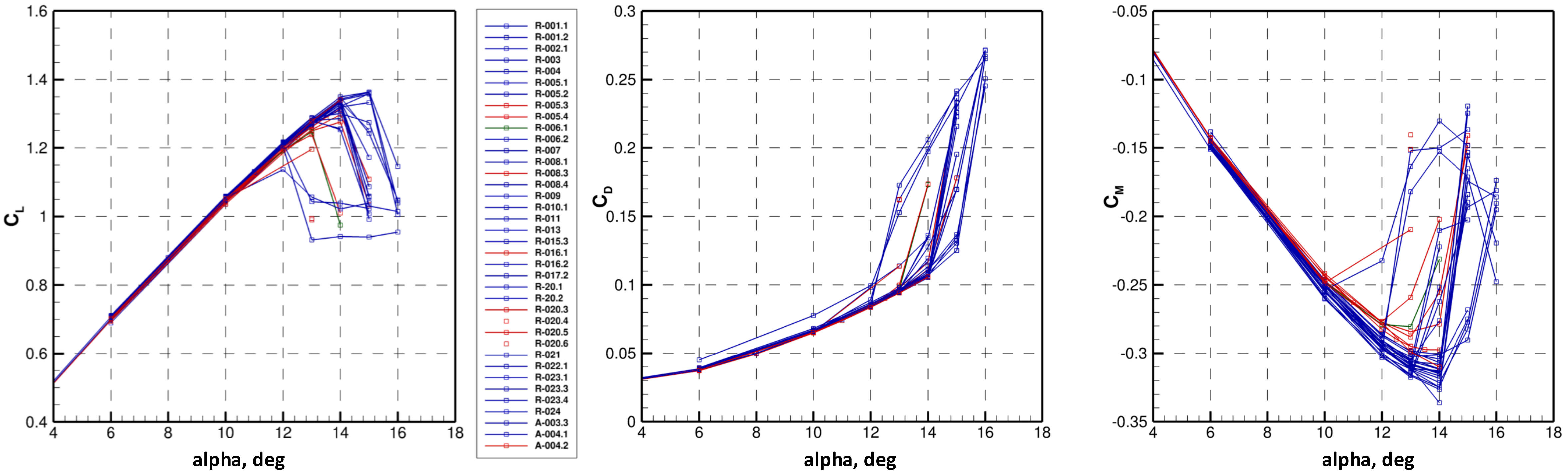

Blue = SA
Red = SA-R(c_{rot}=1)-QCR2000
Green = other

Global view:

- With exception of outliers, relatively good F&M agreement for $\alpha \leq 12°$
- Larger discrepancy at high angles of attack
- Some agreement for after-stall conditions, $\alpha = 16°$; more studies needed

F&M Polars on Nominal Grids
SA Solutions Iteratively Converged at α = 14°

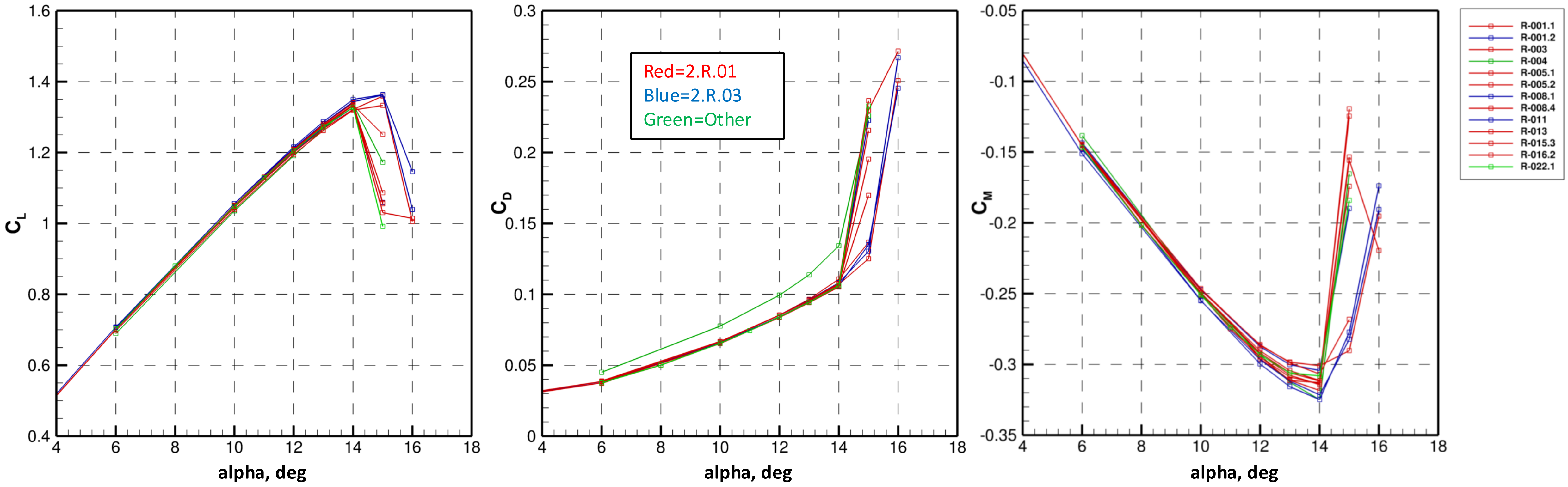

Global view:

- Relatively good C_L agreement up to α = 14°
- With single exception, relatively good C_D agreement up to α = 14°
    - at α = 6°, C_D range is [0.0371, 0.0390], 19 counts
    - at α = 14°, C_D range is [0.1055, 0.1108], 53 counts
- Reasonable C_M agreement for low angles of attack
    - Larger discrepancy at high angles of attack

F&M Grid Convergence, All RANS Solutions, α = 10° and α = 12°

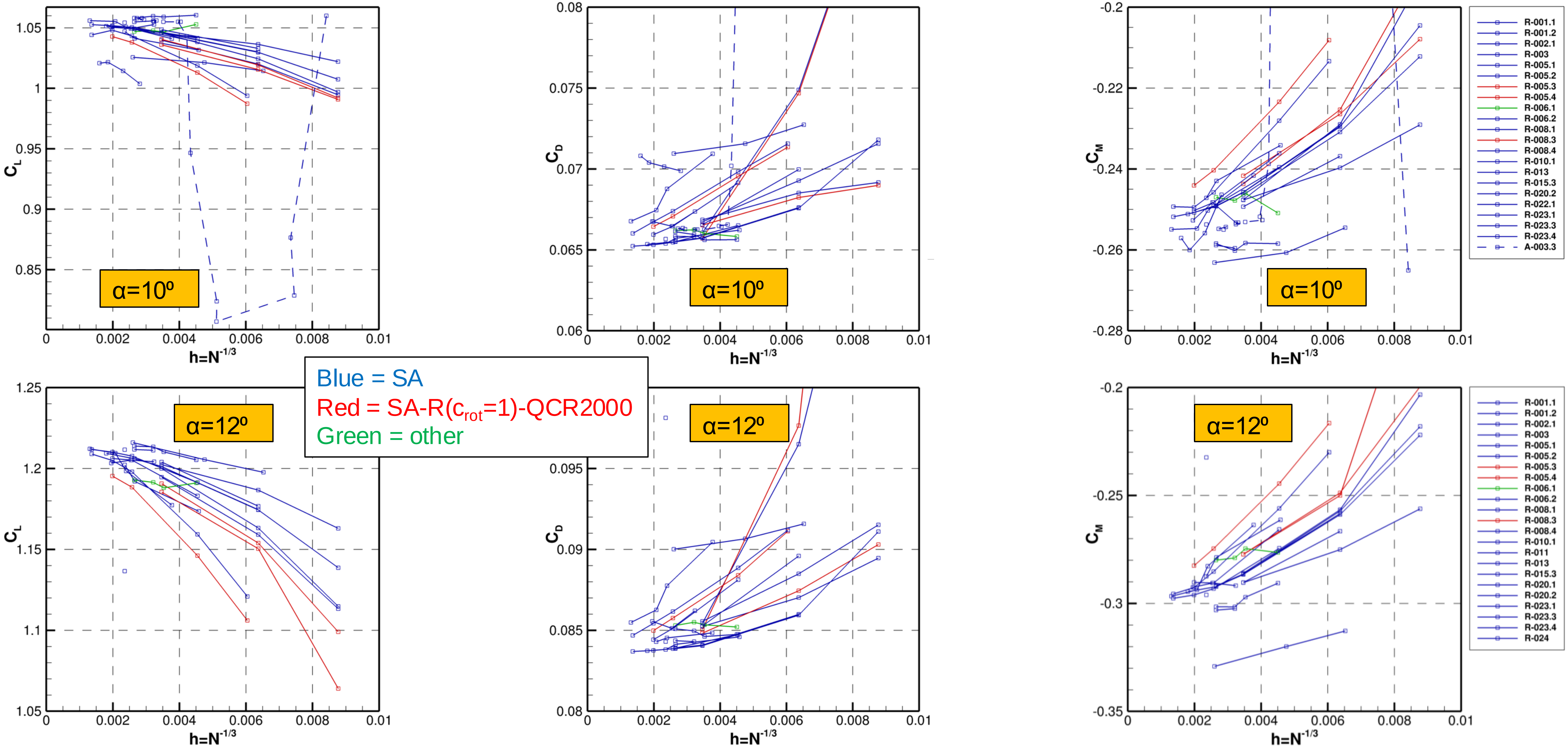

- With exception of outliers, F&M grid-convergence trend starts from coarse grids

F&M Grid Convergence, All RANS Solutions, α = 14° and α = 15°

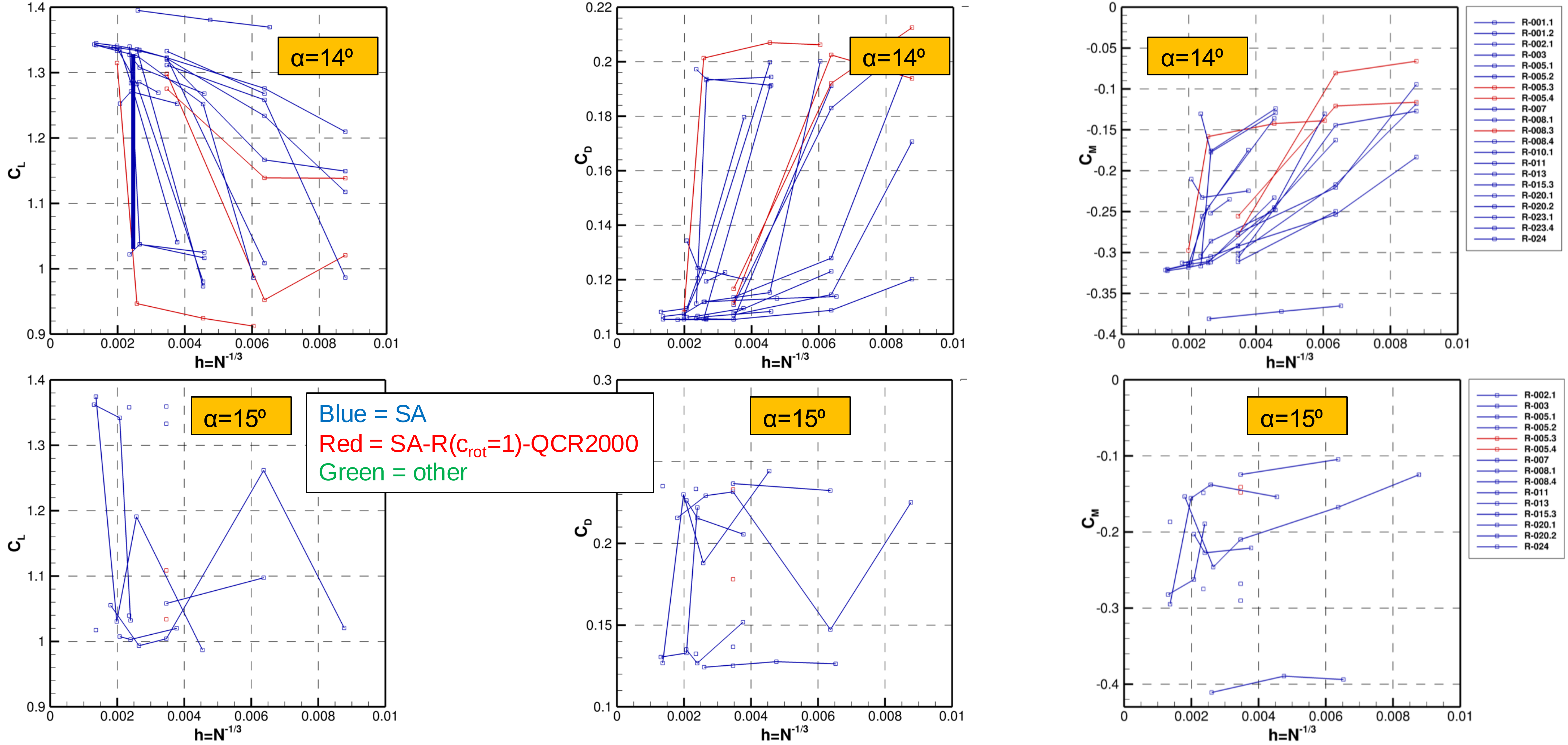

- Solutions at α = 14° require finer grids to show grid convergence
- Solutions at α = 15° do not show grid convergence

Selected SA Solutions, $\alpha = 12°$

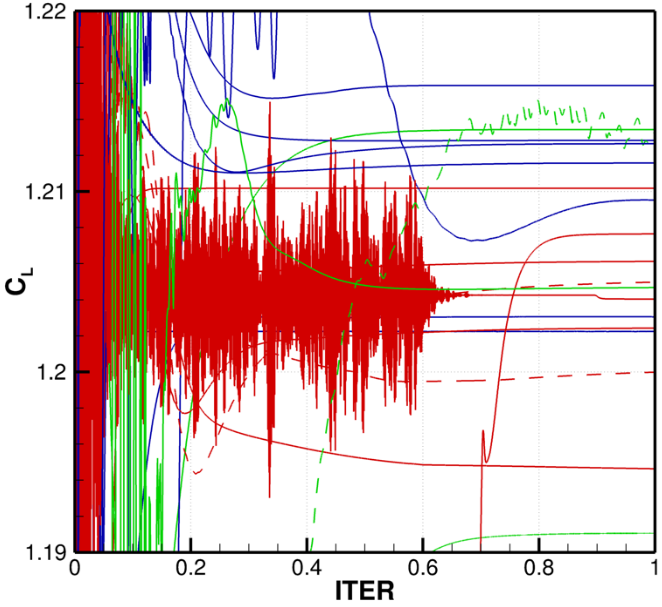

C_L: 1.7% range [1.195, 1.215] (shaded)
C_D: 2.1% range [0.0837, 0.0855] (18 counts, shaded)
C_M: 5.4% range [-0.302, -0.286] (shaded)

- Many solutions converge to steady state
  - Deep residual convergence shown by 5 solutions on nominal grids
  - Dash-line solutions have not converged sufficiently
- F&M variation ranges wider than in Case 1
- F&M agreement improves on finer grids
  - 0.25% C_L range, 18 counts C_D range, and 0.66% C_M range on grid with 400M degrees of freedom

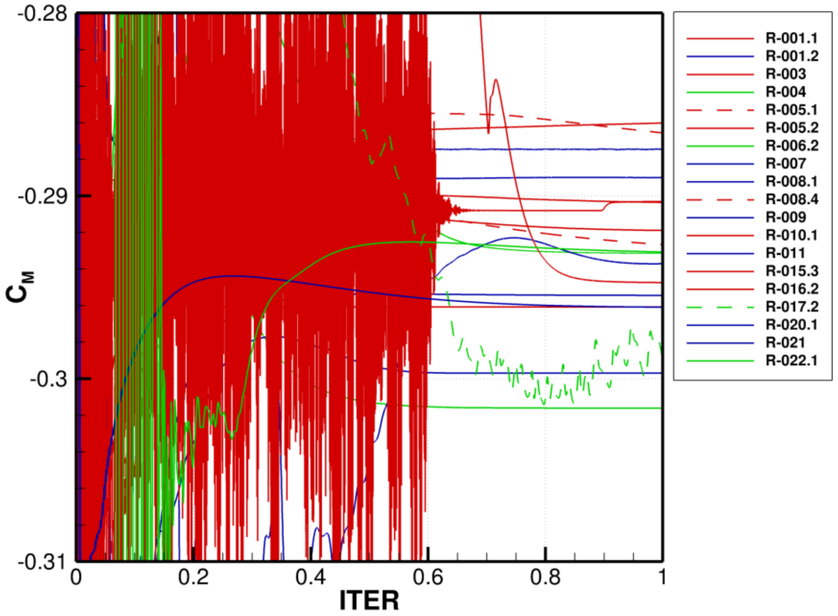

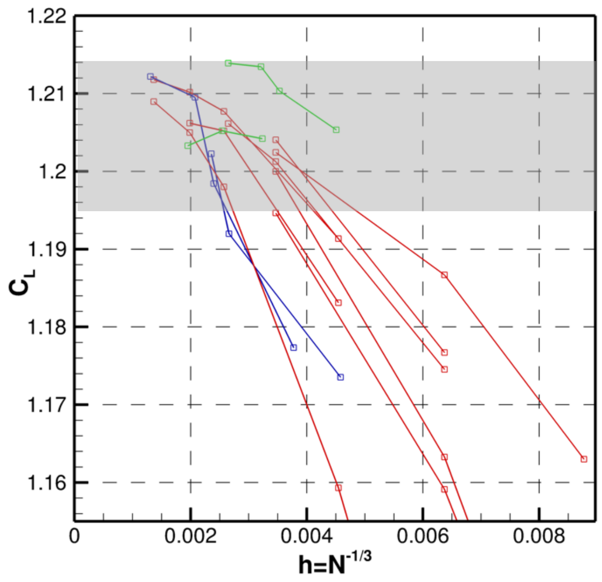

Red=2.R.01
Blue=2.R.03
Green=Other

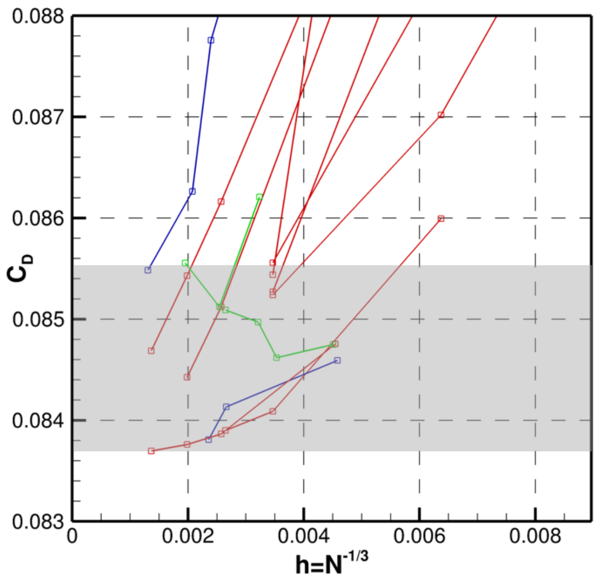

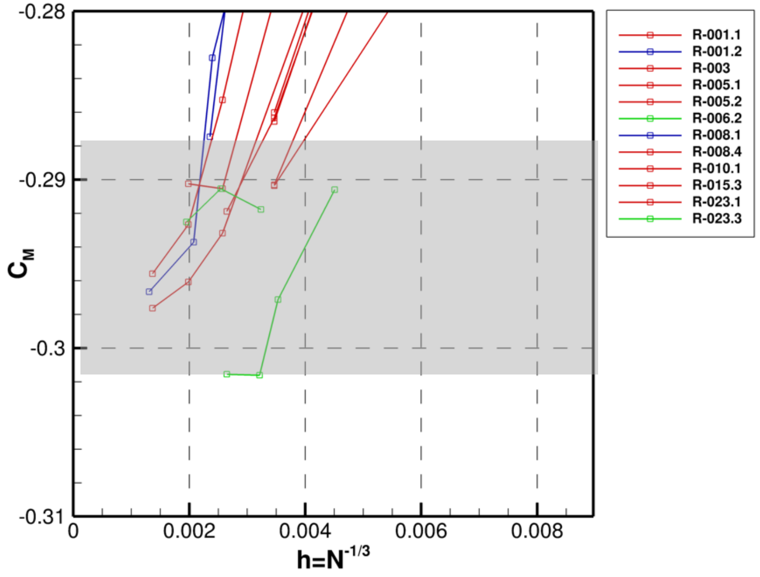

Streamlines in Selected SA Solutions, $\alpha = 12°$

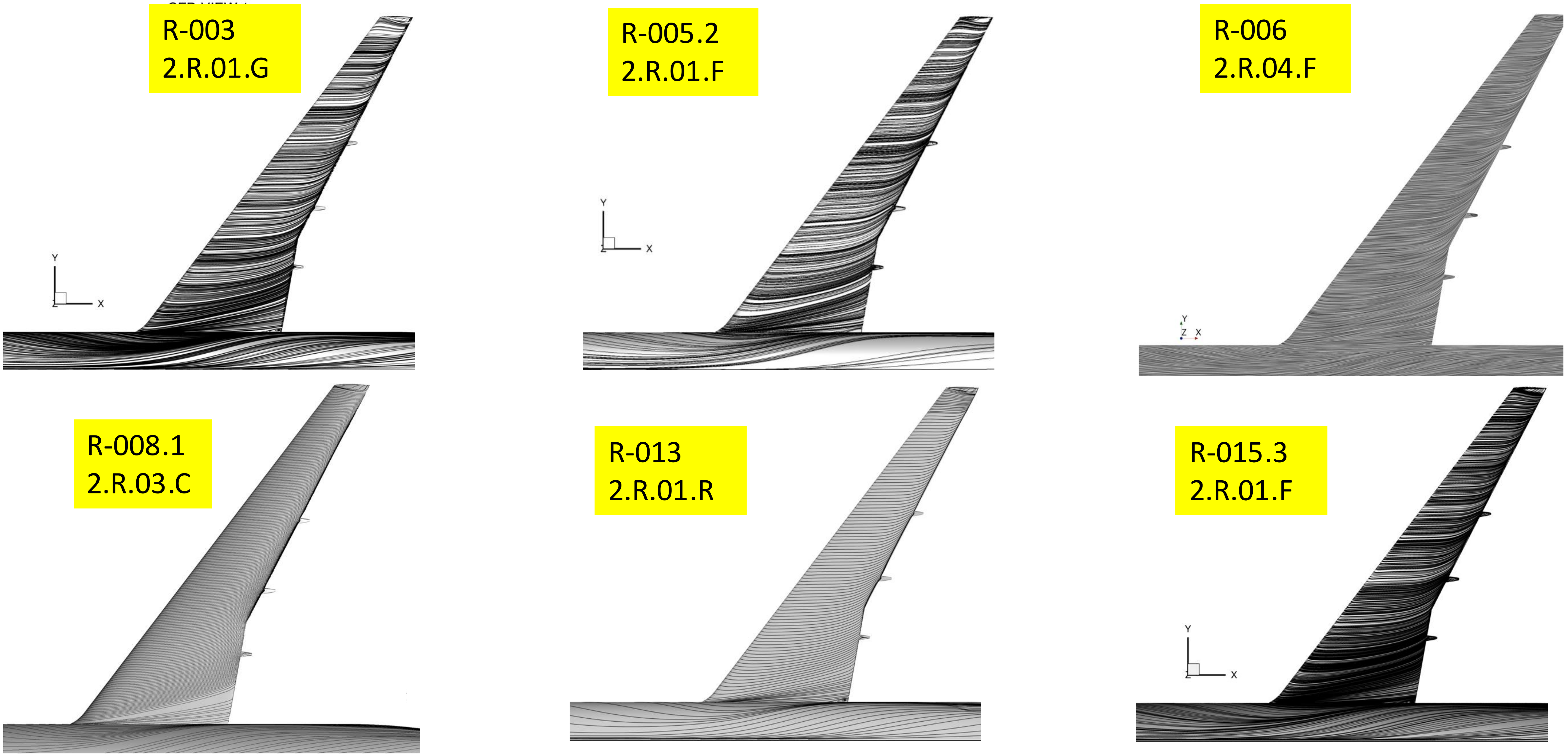

- Similar mostly attached streamlines in selected solutions

Surface Pressure, α = 12°

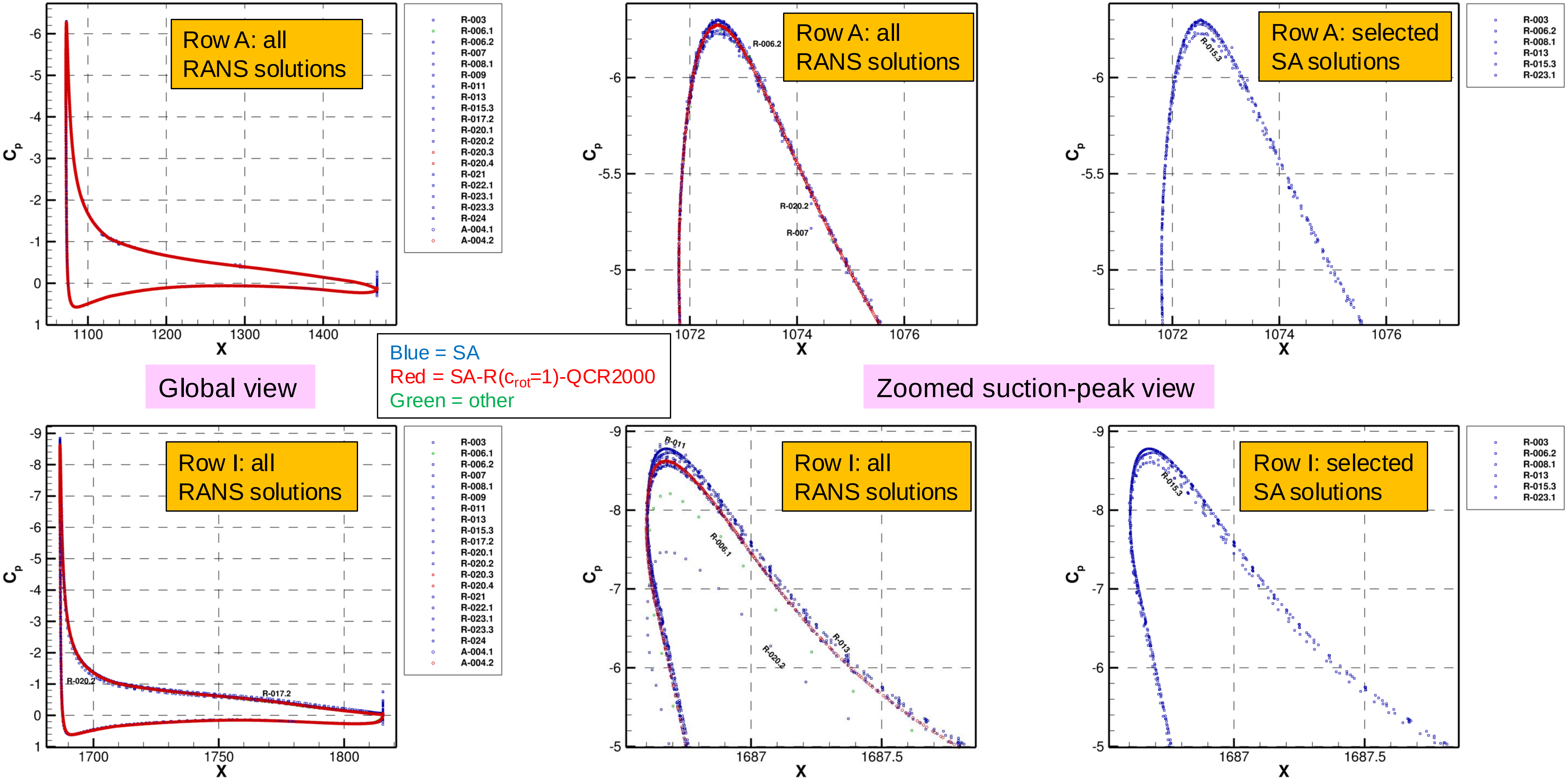

- Good agreement between surface pressure in selected SA solutions at all sections

Selected SA Solutions α = 14°

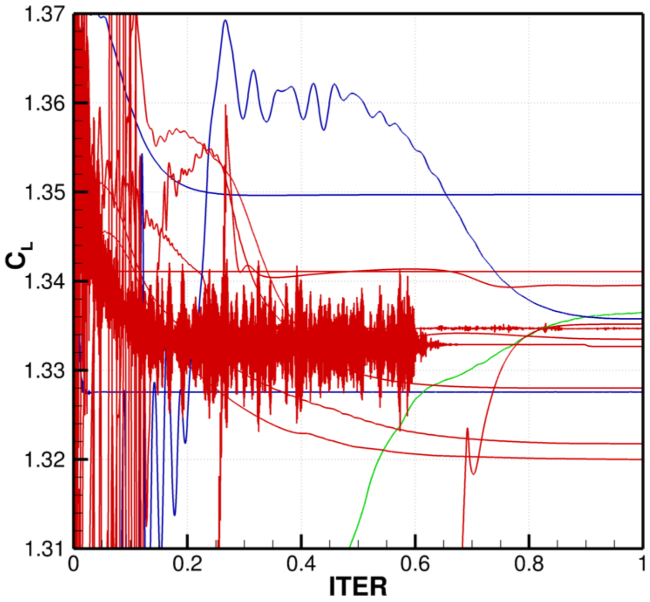

C_L: 1.8% range [1.320, 1.344] (shaded)
C_D: 6% range [0.105, 0.111] (60 counts, shaded)
C_M: 7.6% range [-0.325, -0.301] (shaded)

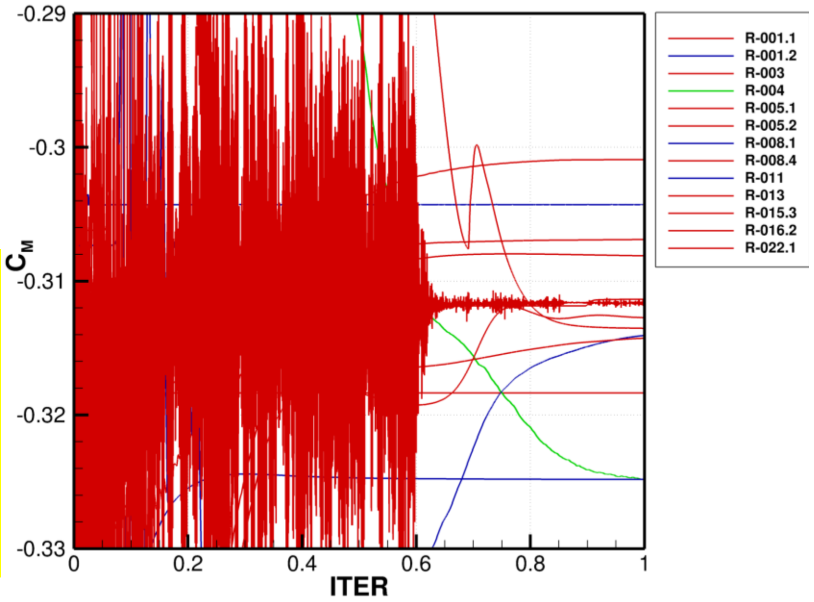

- F&M variation ranges wider than for α = 12°
- Fewer solutions iteratively converged
  - 3 solutions reported deep residual convergence on nominal grids
  - 7 iteratively-converged solutions computed on 3 or more grids
- F&M agreement improves on finer grids
  - 0.37% C_L range, 13 counts C_D range, and 3.1% C_M range on grids with 170M+ degrees of freedom

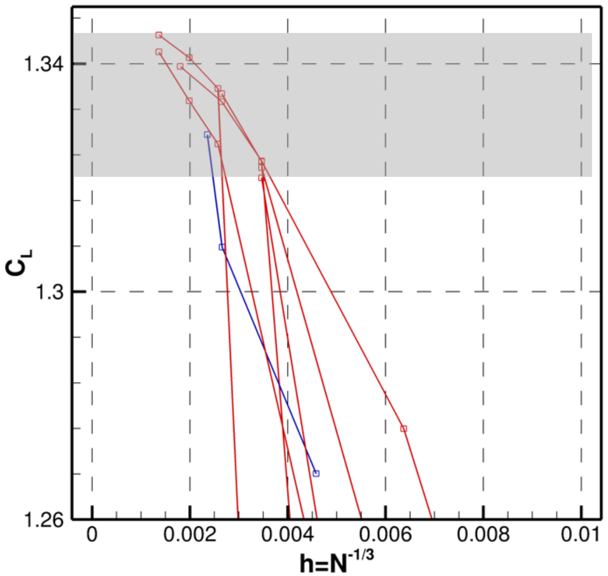

Red=2.R.01
Blue=2.R.03
Green=Other

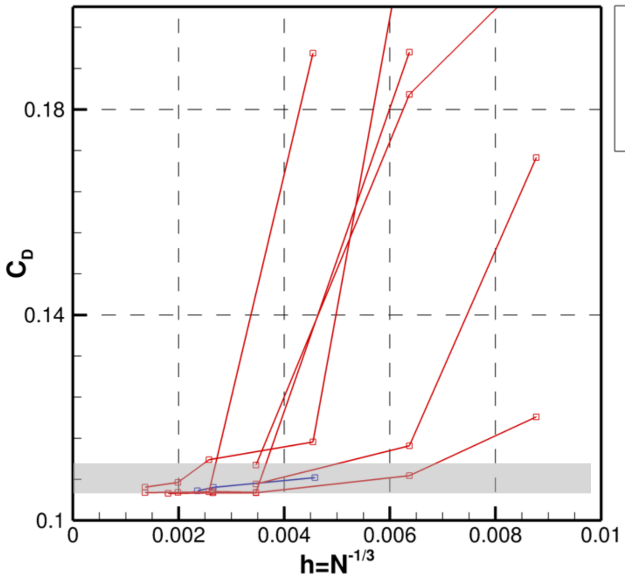

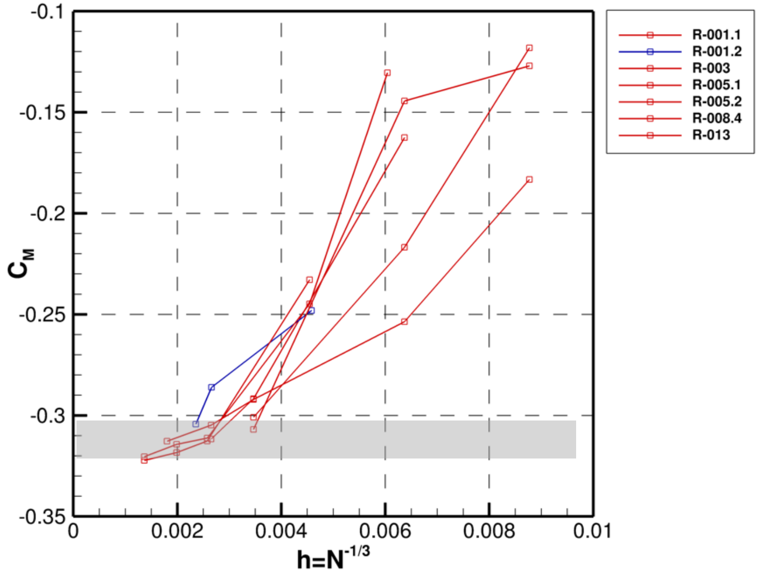

Streamlines in Selected SA Solutions, $\alpha = 14°$

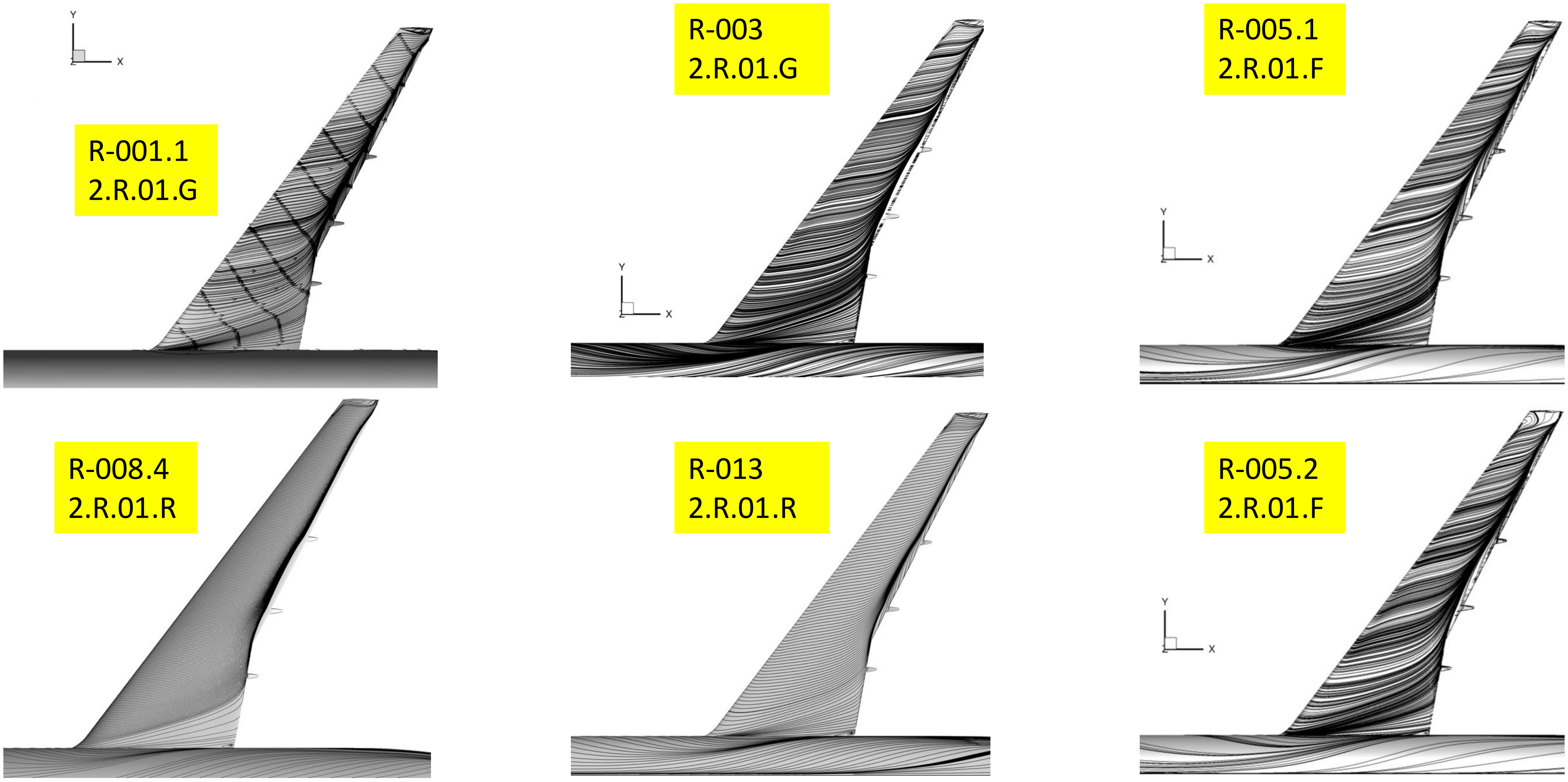

- Small differences in separation extent at trailing edge and wing tip

Skin-friction Contours in Selected SA Solutions, $\alpha = 14°$

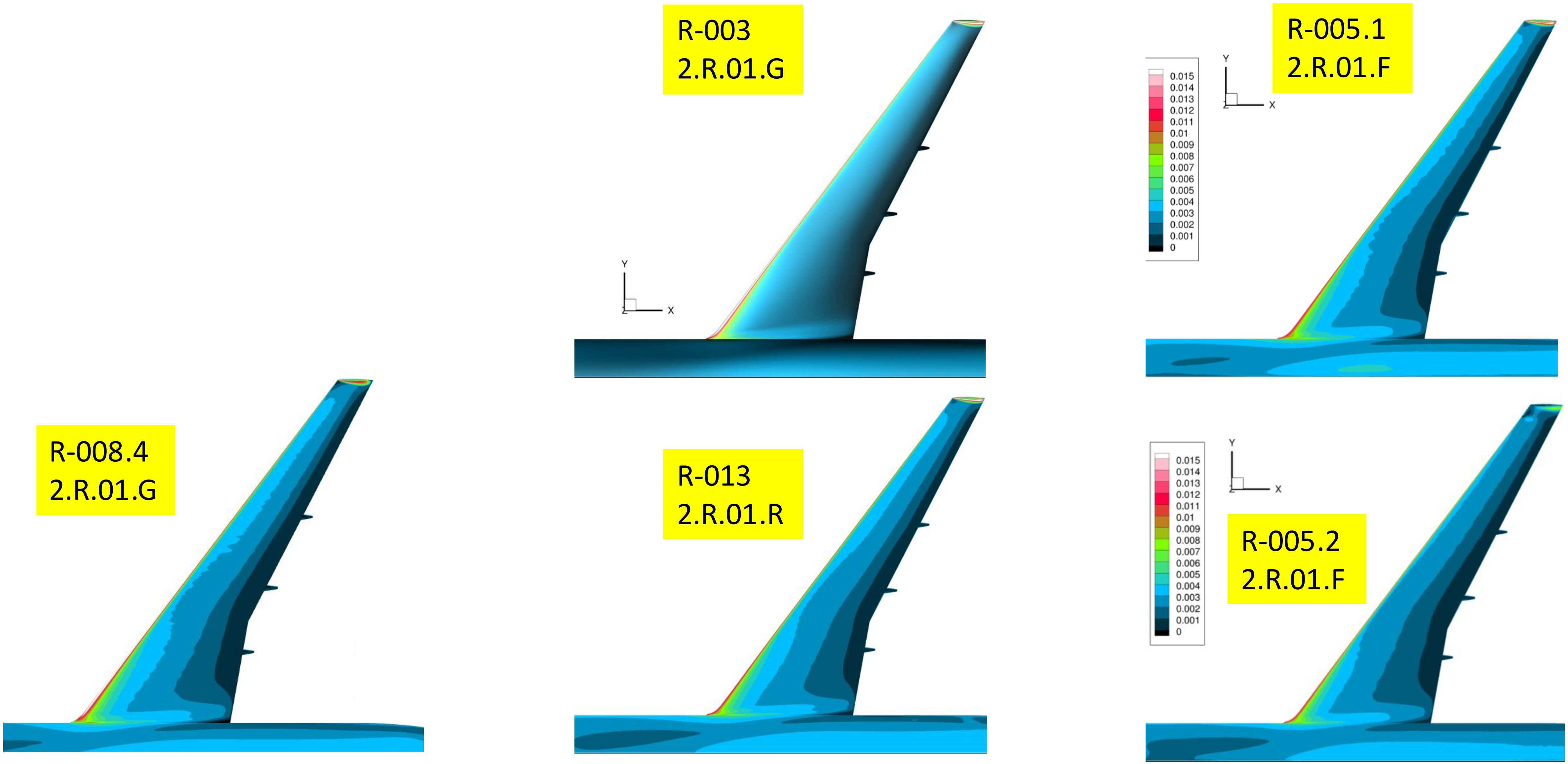

- Similar skin-friction contours in selected SA solutions

Surface Pressure, α = 14°

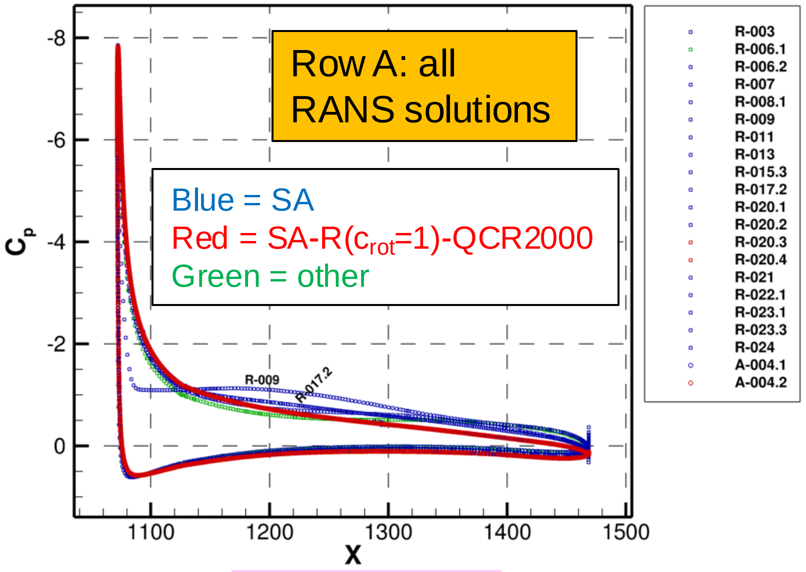

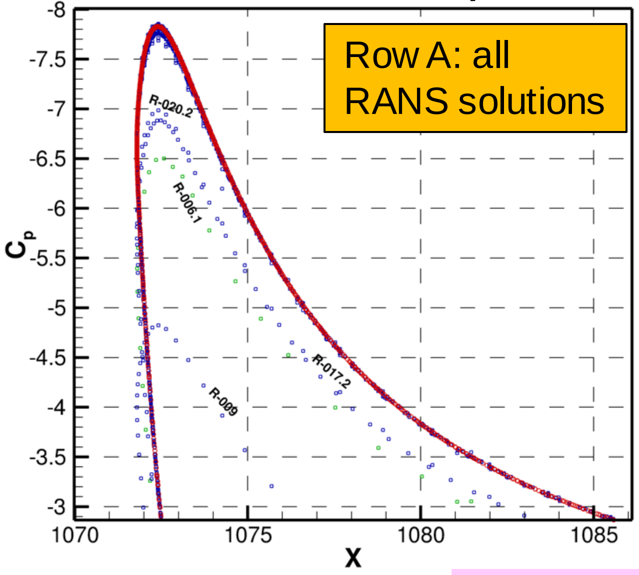

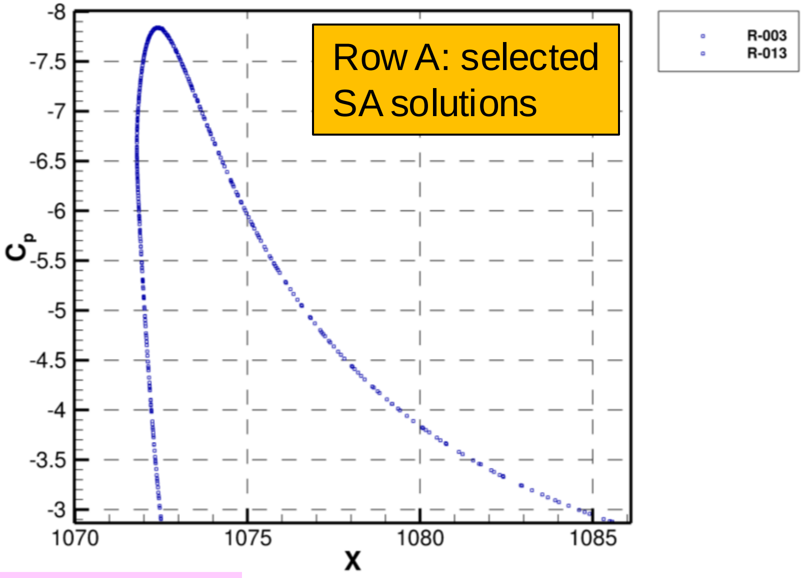

Global view

Zoomed suction-peak view

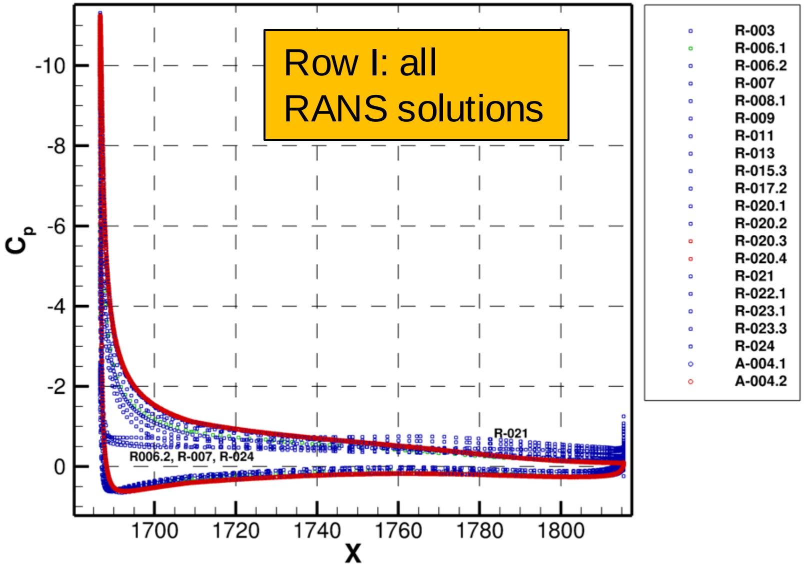

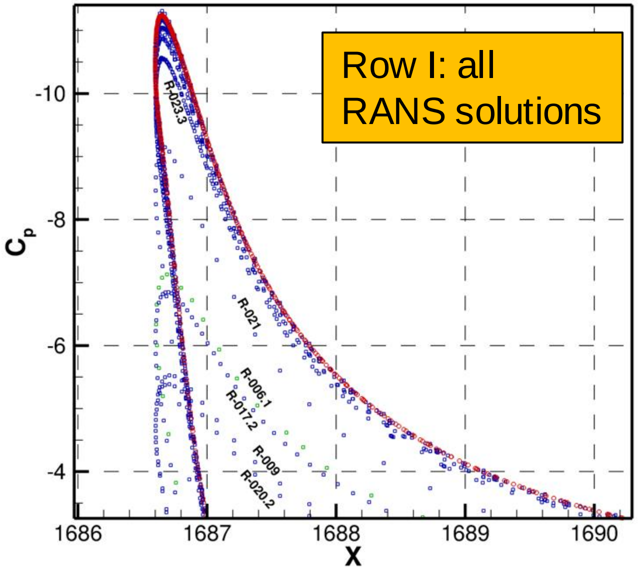

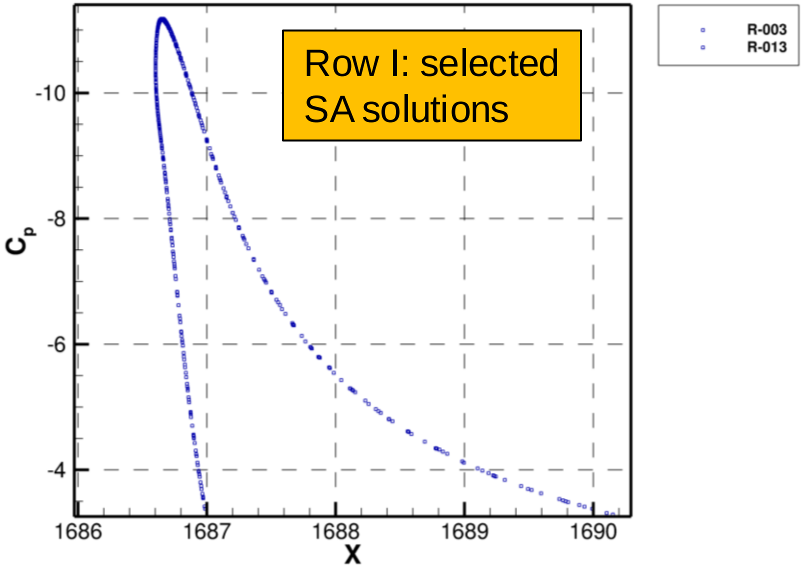

- All-solution agreement deteriorates, especially outboard
- Only two Cp for selected SA solutions, agree well

No Selected Solutions at α = 15°

- Few solutions
- Poor iterative convergence
- Grid convergence cannot be assessed
- Poor surface-pressure agreement at all sections

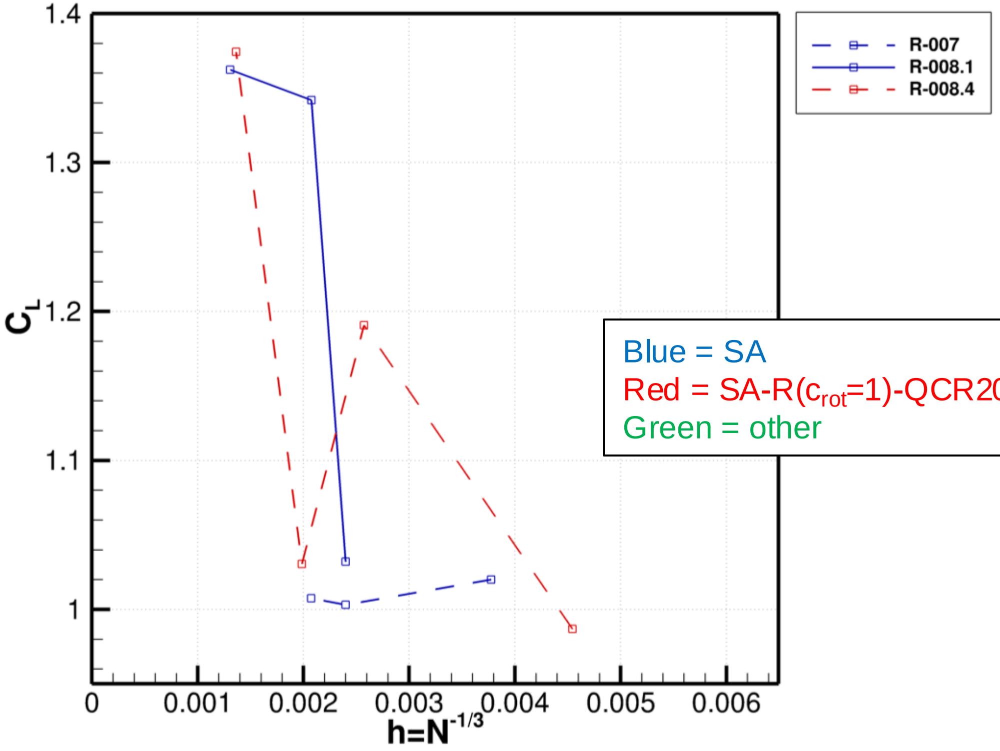

Blue = SA
Red = SA-R(c_{rot}=1)-QCR2000
Green = other

Global view

Zoomed suction-peak view

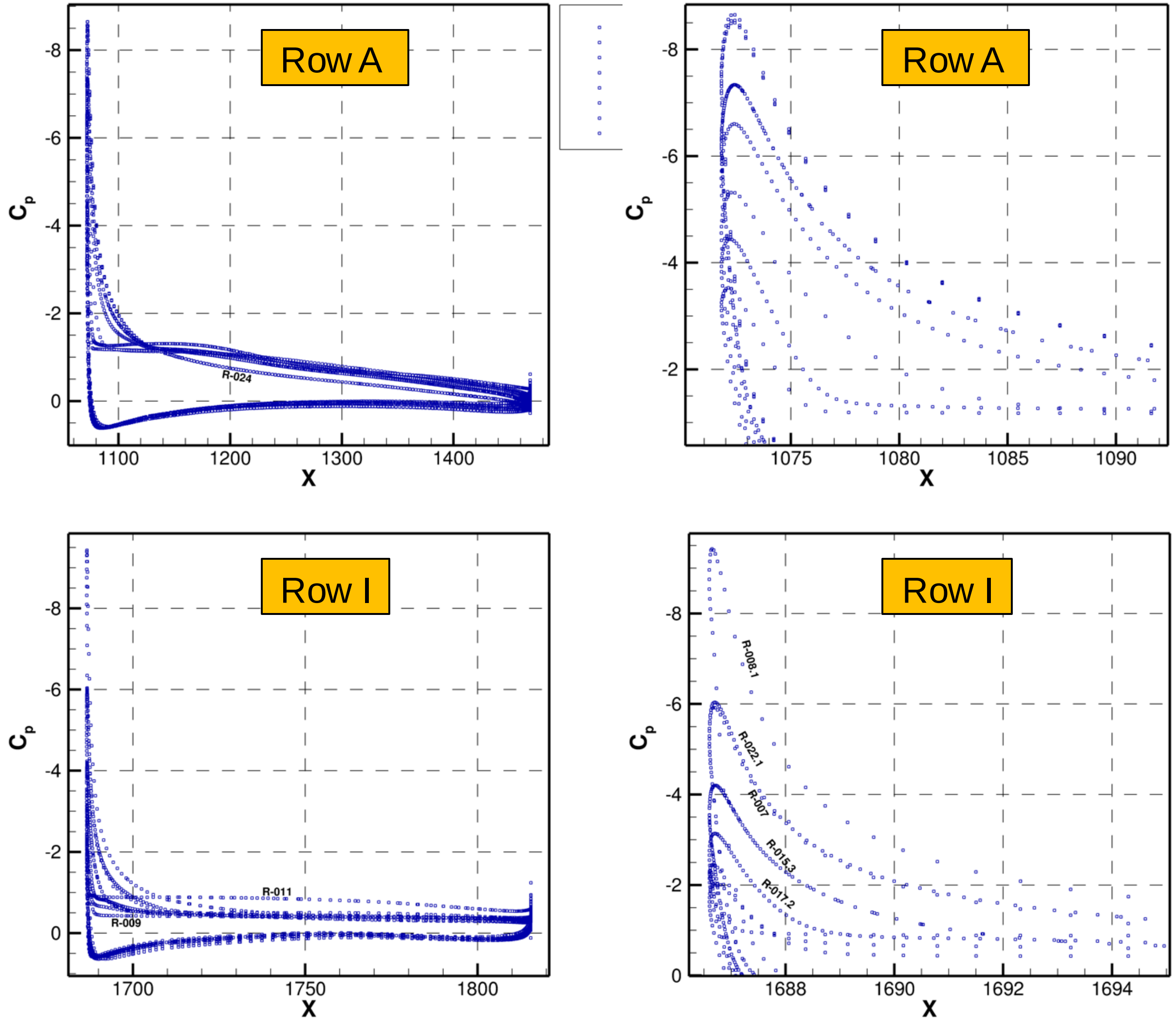

Streamlines, α = 15°

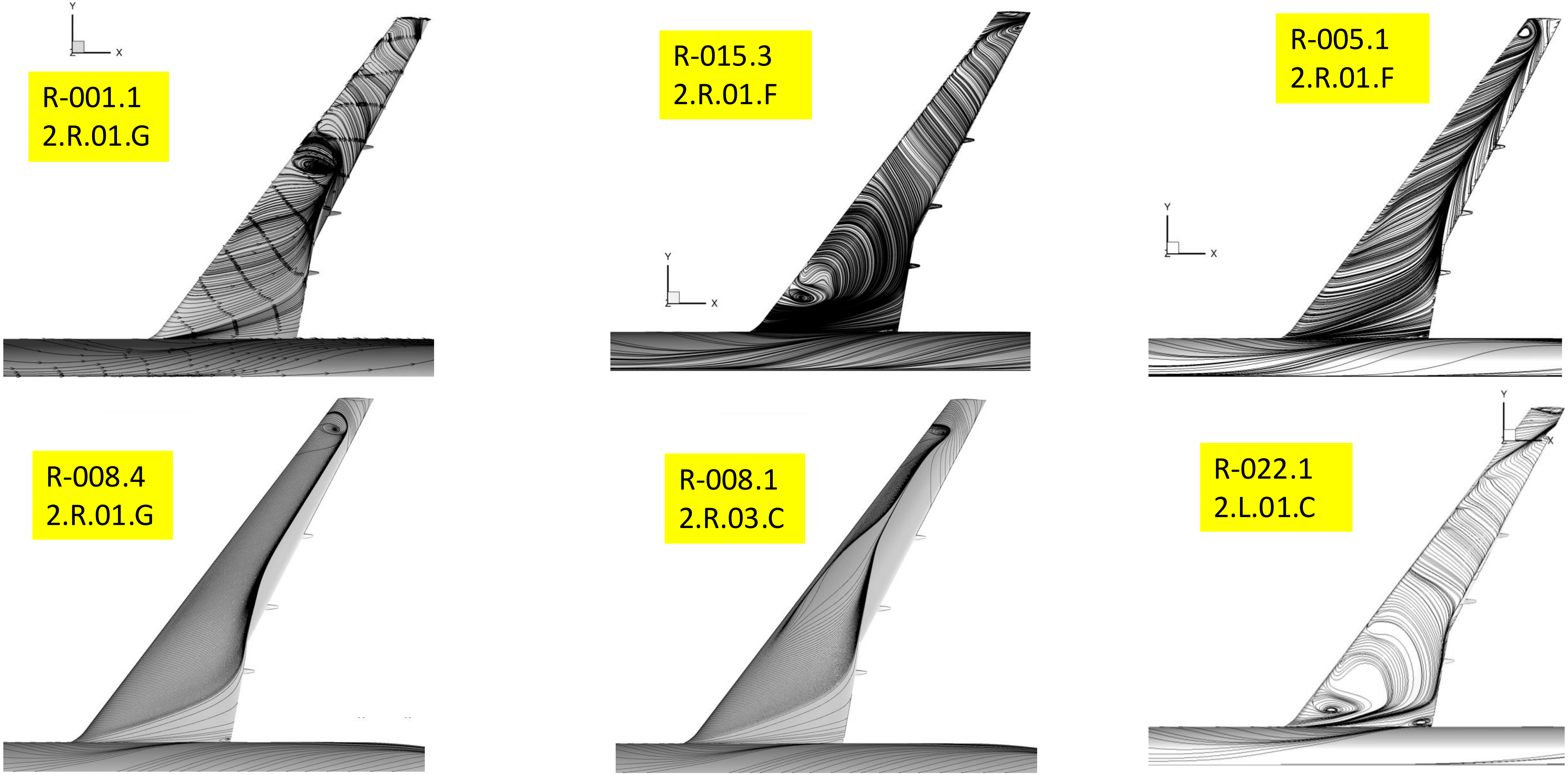

- Surface streamlines for solutions that agreed at α = 12° and α = 14° do not agree at α = 15°

Test Case 2.1: Summary

- **Selected grid-converged SA solutions agree to each other for $\alpha \leq 14°$**
- **Good iterative convergence for selected SA solutions for $\alpha \leq 14°$**
  - Several solvers reported machine-zero residuals on nominal grids
  - Many solutions converged to steady state
- **Insufficient data at $\alpha = 15°$**
  - Few solutions have data on grid convergence and iterative convergence
  - Iterative convergence is worse than for lower angles of attack
    - ✓ Deep residual convergence is elusive
  - No solutions selected
  - No agreement between solutions

Case 2.2

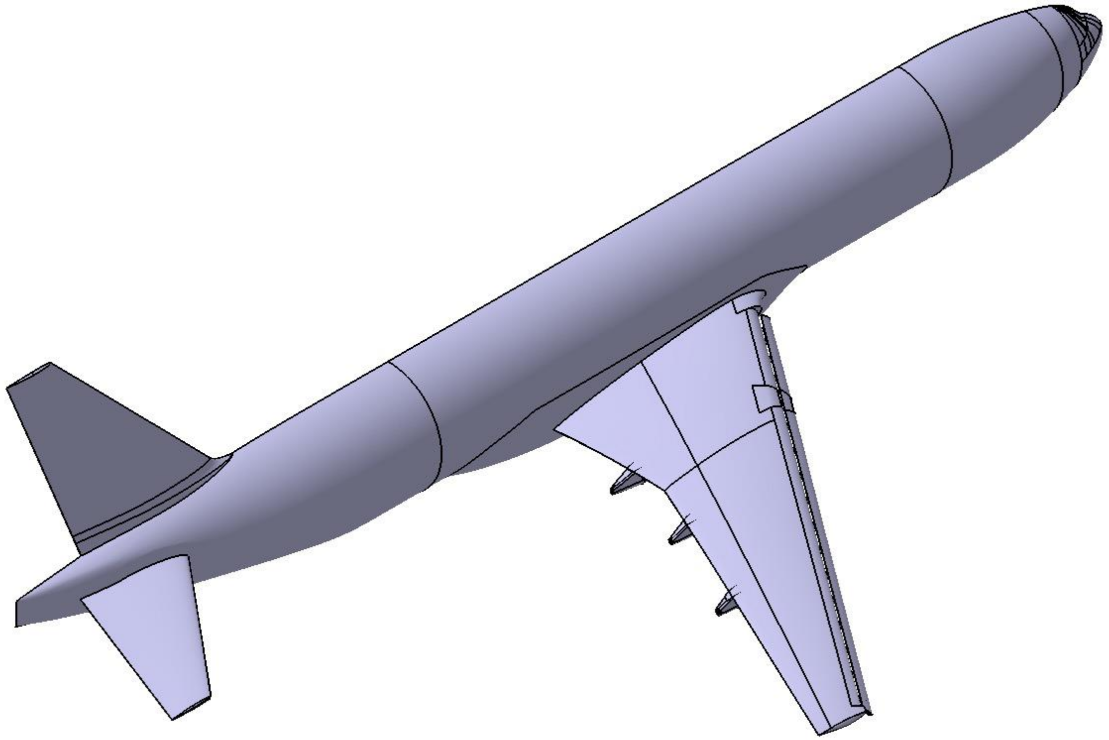

ONERA_LRM-WBSHV

Flow Conditions: M_∞ = 0.2, Re_{MAC} = 5.9×10^6, T_{ref} = 518.67°R,

α = 6°,10°, 12°, 17.7°, 20°, 21.5°, 23°, 23.8°

F&M Polars on Nominal Grids, All RANS Solutions

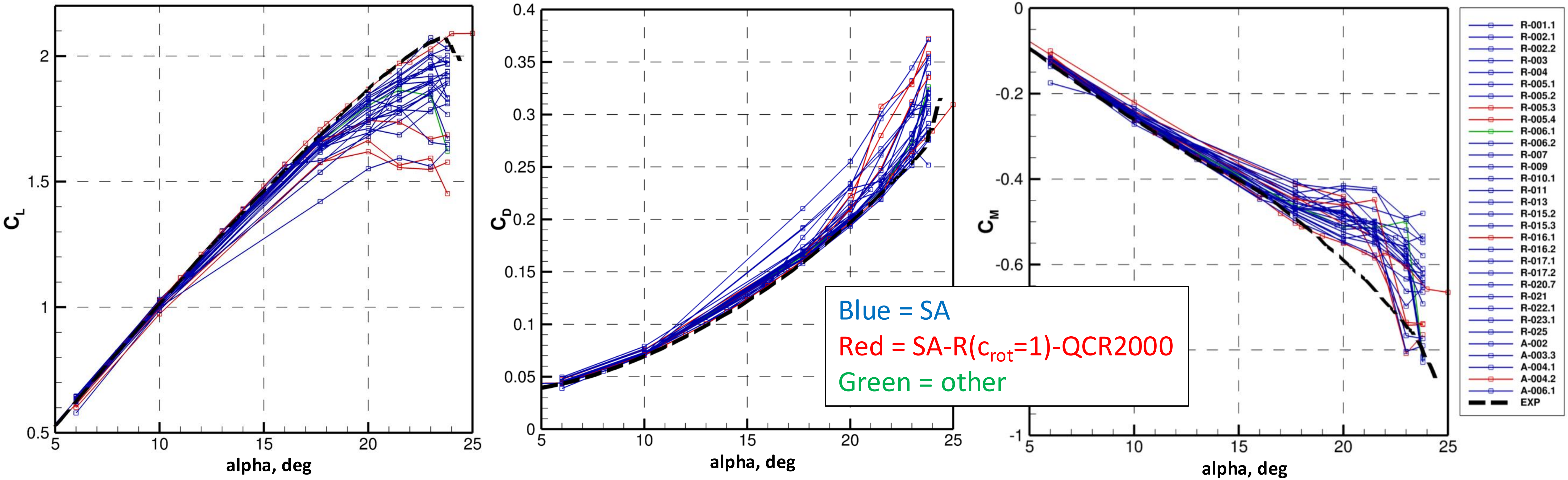

Global View:

- Reasonable agreement between F&M for low angles of attack
- Large discrepancy for medium to high angles of attack
- In comparison to ONERA experiment
  - Reasonable agreement in F&M at low angles of attack
  - At high angles of attack, $C_{L,max}$ is lower, C_D is higher, and C_M is less negative than ONERA experiment
  - Some solutions have good agreement in C_L and C_D at all angles of attack
  - No agreement in CM at high angles of attack

F&M Polars on Nominal Grids
SA Solutions Iteratively Converged at α = 23.8°

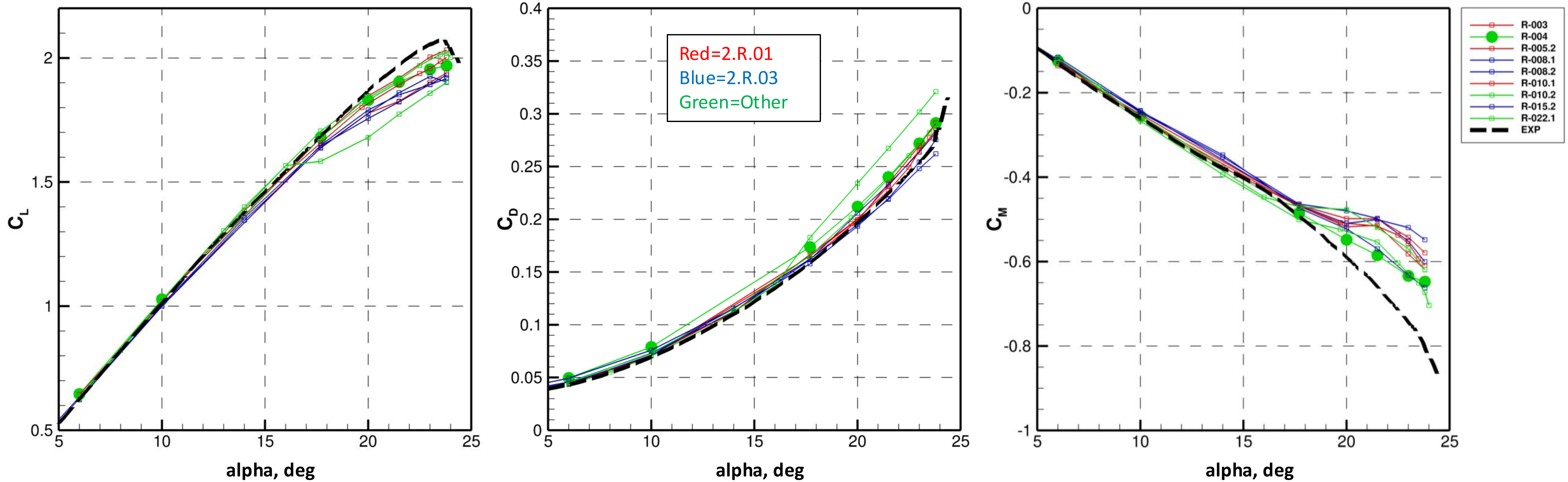

Global view:

- Green circles mark R-004 solutions that converge to steady state and show deep residual convergence for Case 2.2 at all angles of attack
- With two exceptions, C_L variation is less than 10% up to α = 23°
- With a few exceptions, good agreement in C_D; at α = 23°, C_D range is [0.2637 , 0.2698], 61 counts
- With one exception, reasonable C_M agreement up to α = 17.7°; larger discrepancy at high angles of attack

F&M Grid Convergence, All RANS Solutions, α = 10° and α = 17.7°

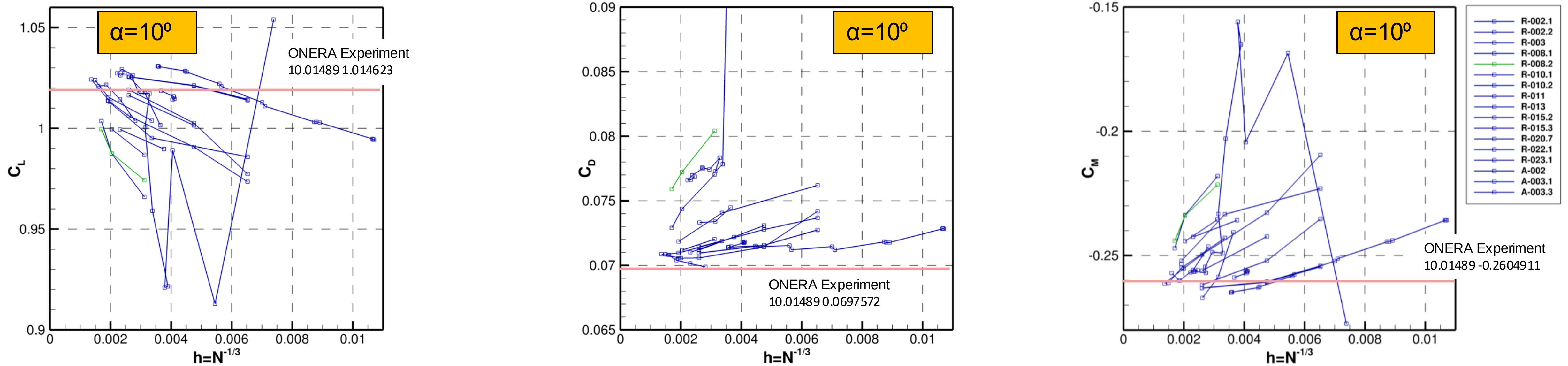

- At α = 10°, C_L and C_D converge to values higher than experiment, C_M converges close to experiment

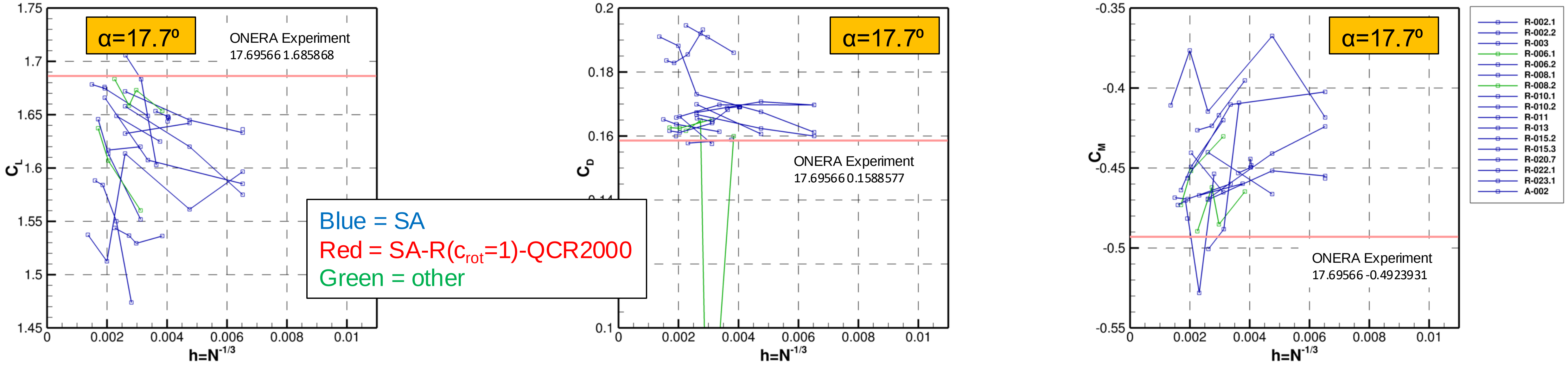

- At α = 17.7°, grid convergence is not clear; subset of solutions appear converging near experiment

F&M Grid Convergence, All RANS Solutions, α = 21.5°

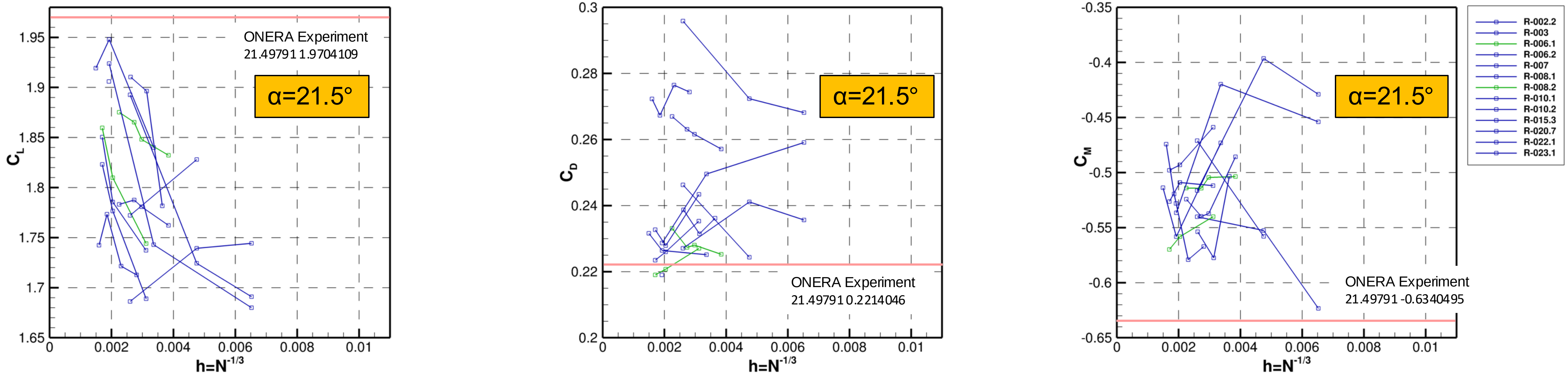

- At α = 21.5°, no grid convergence can be discerned

Blue = SA
Red = SA-R(c_{rot}=1)-QCR2000
Green = other

Selected SA Solutions, α = 10°

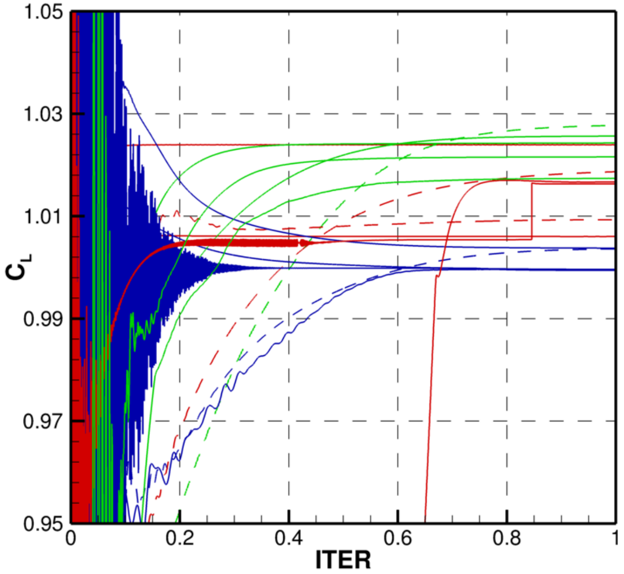

C_L: 1.5% range [1.015, 1.030]
C_D: 7.8% range [0.0708, 0.0765], 57 counts
C_M: 5.4% range [-0.265, -0.251]

- F&M variation ranges comparable to Case 2.1
- Several solutions converged to steady state
- Few solutions on 100M+ grids
- F&M agreement improves on fine grids
  - 0.34% C_L range, 0.5 count C_D range, and 1.6% C_M range on grids with 250M+ degrees of freedom

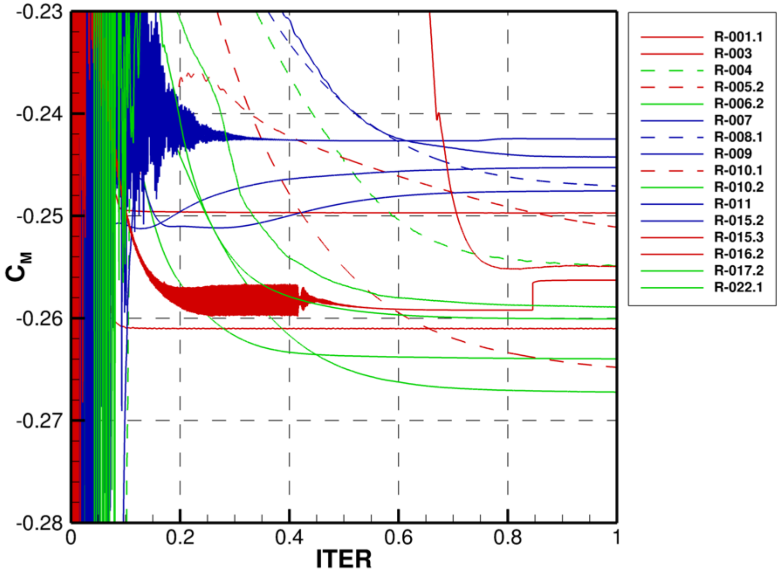

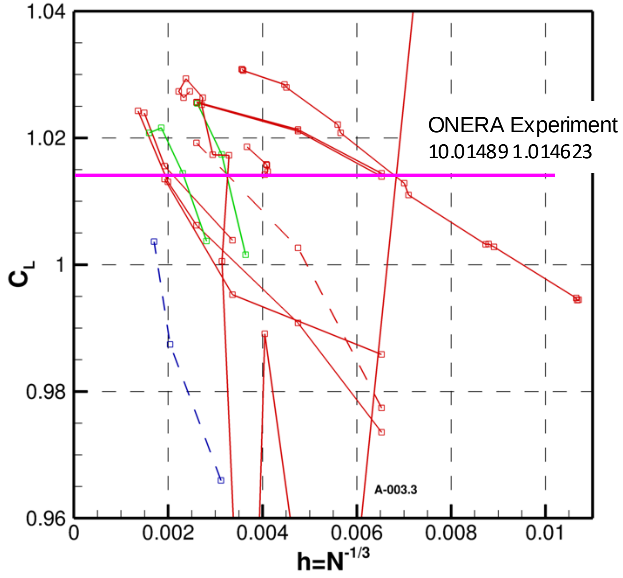

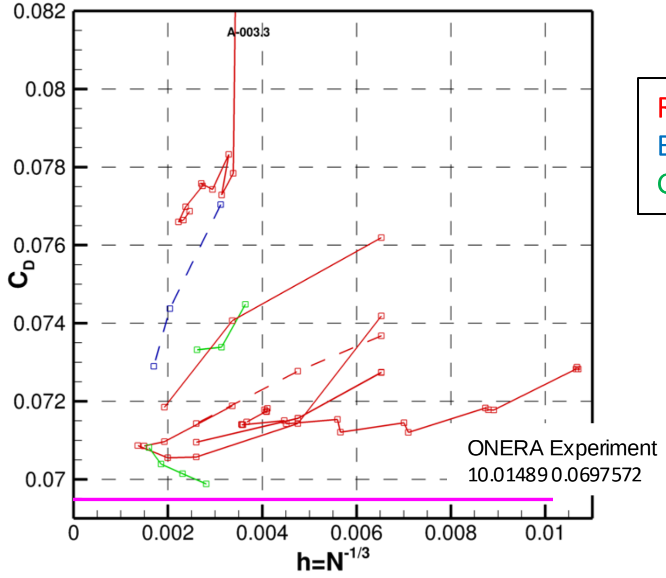

Red=2.R.01
Blue=2.R.03
Green=Other

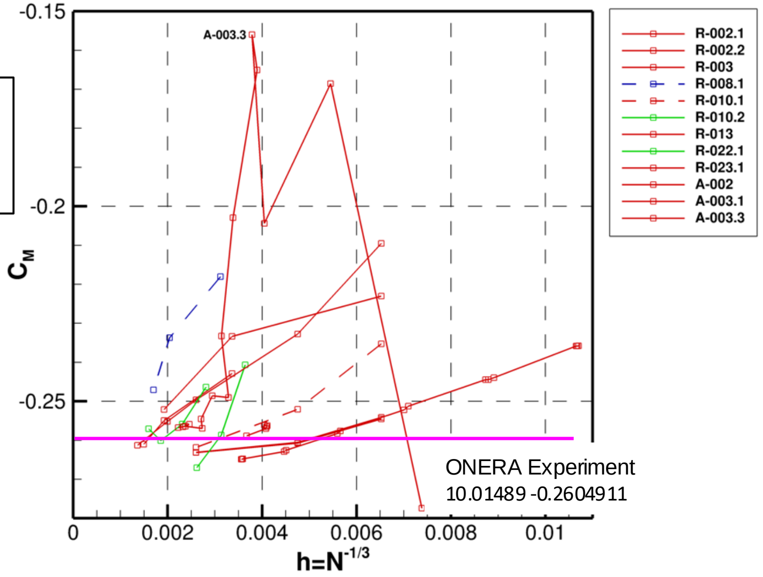

Streamlines in Selected SA Solutions, $\alpha = 10°$

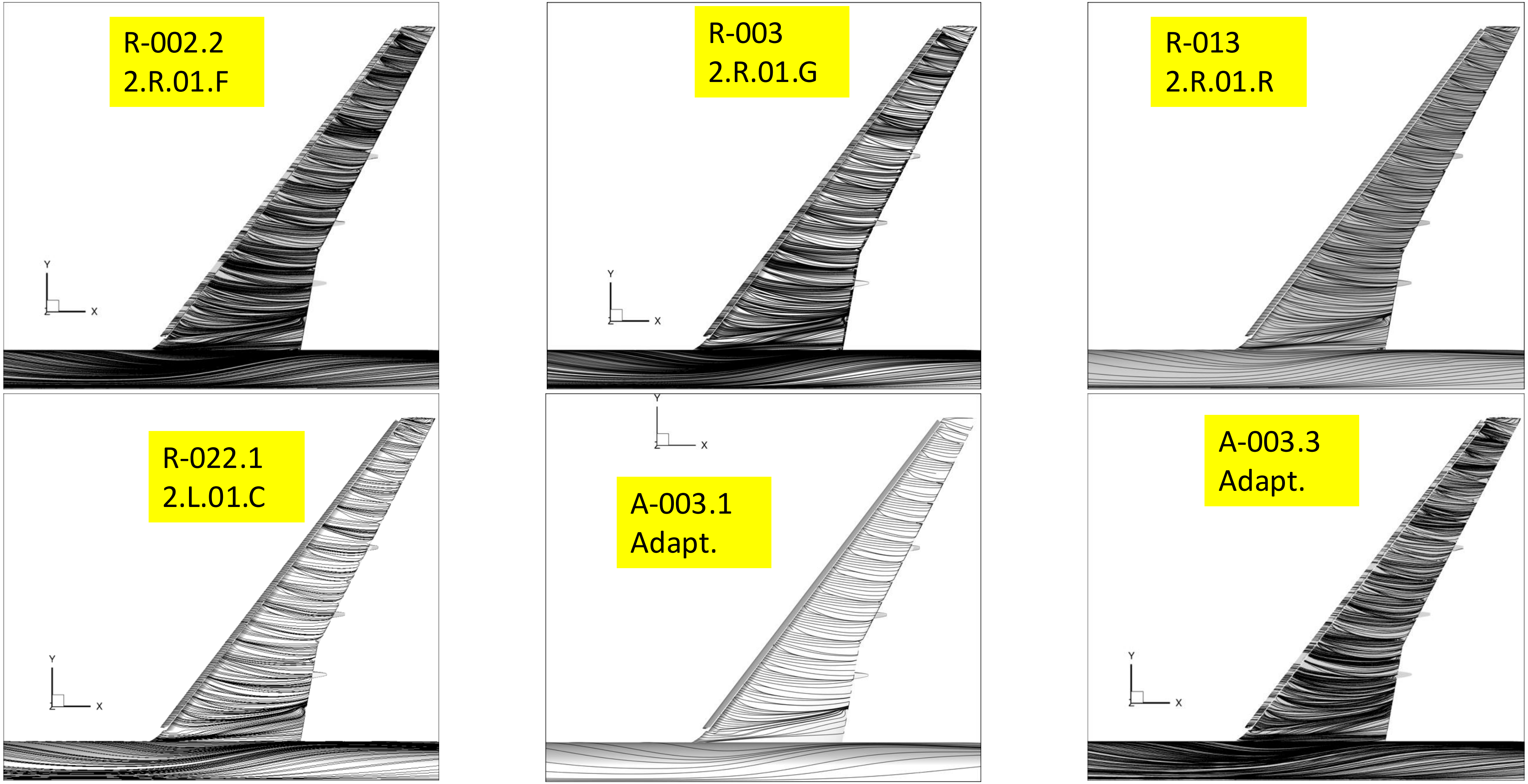

- Similar mostly attached streamlines in selected SA solutions

Skin-Friction Contours in Selected SA Solutions, α = 10°

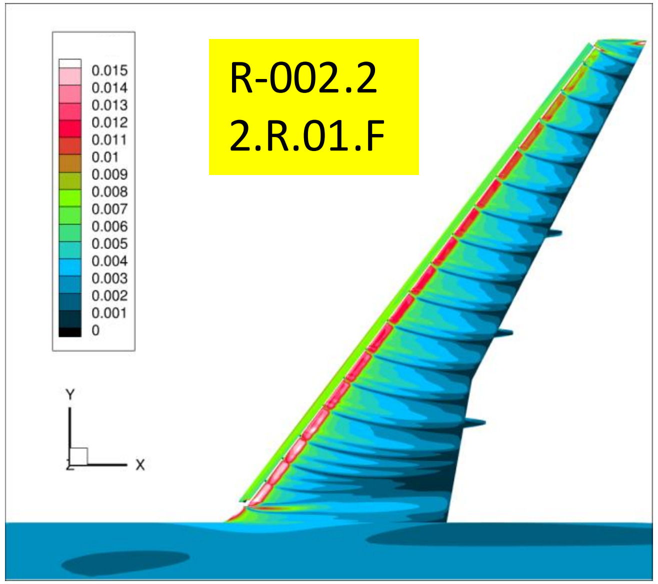

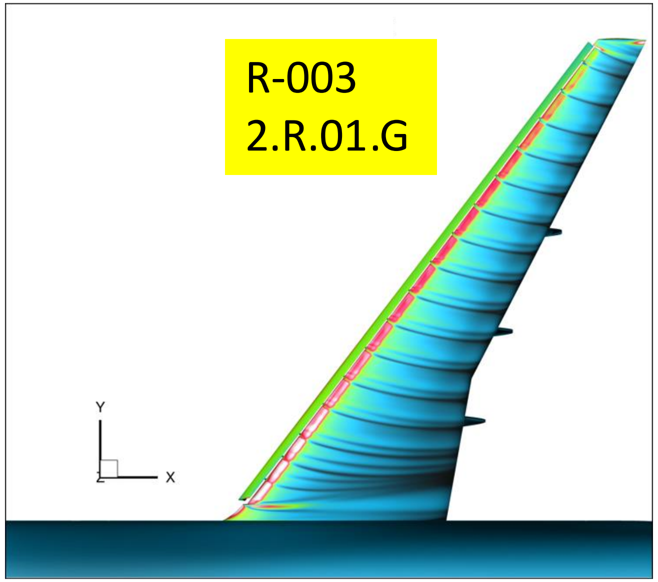

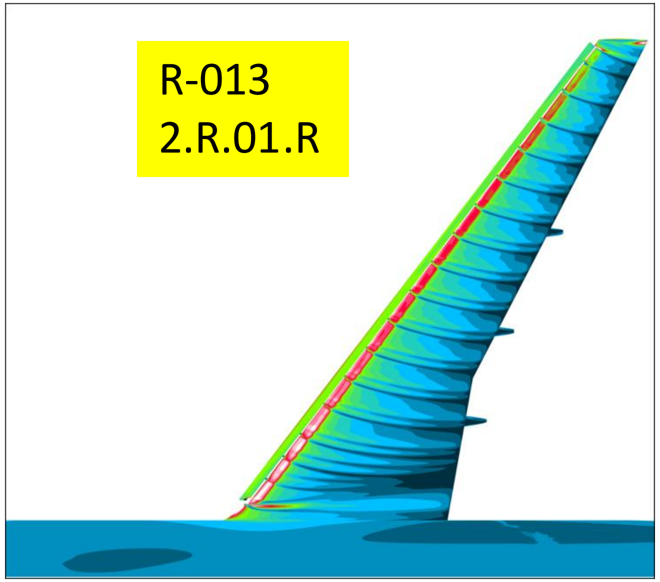

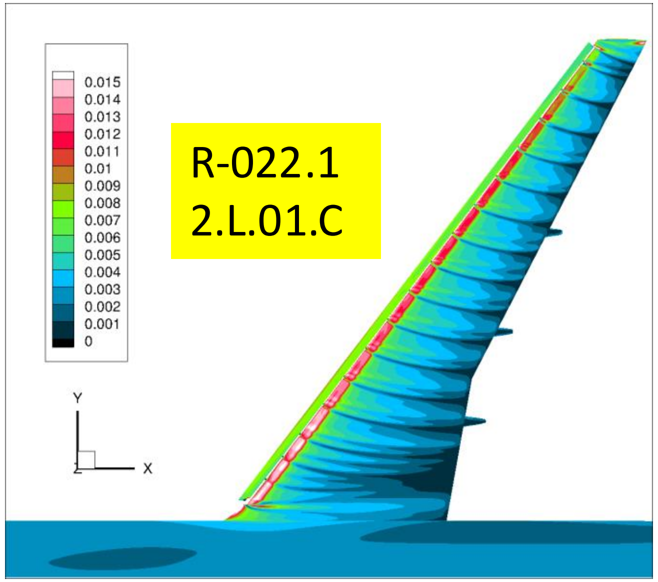

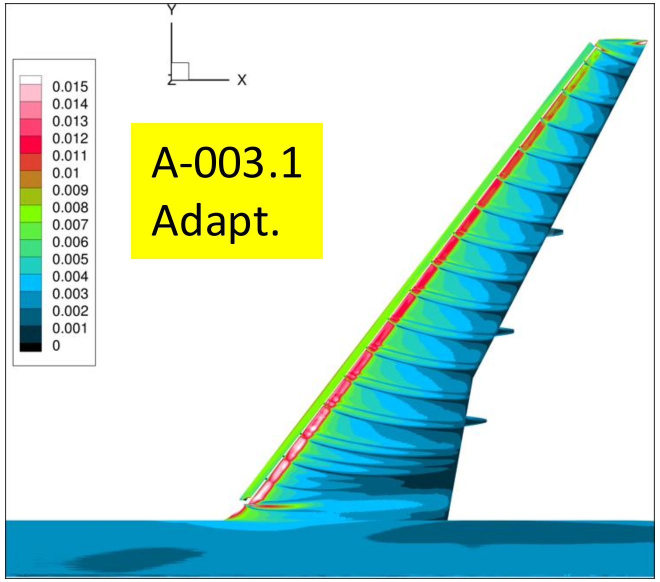

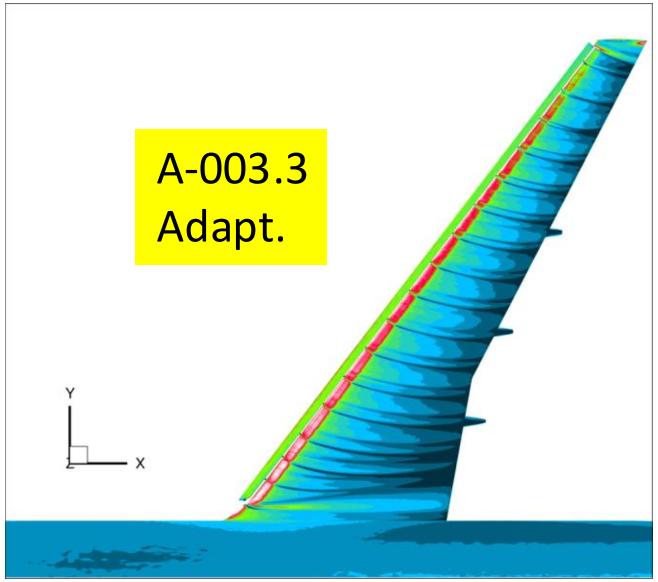

- Similar skin-friction contours in selected solutions
- No significant outboard separation

Selected SA Solutions, α = 17.7°

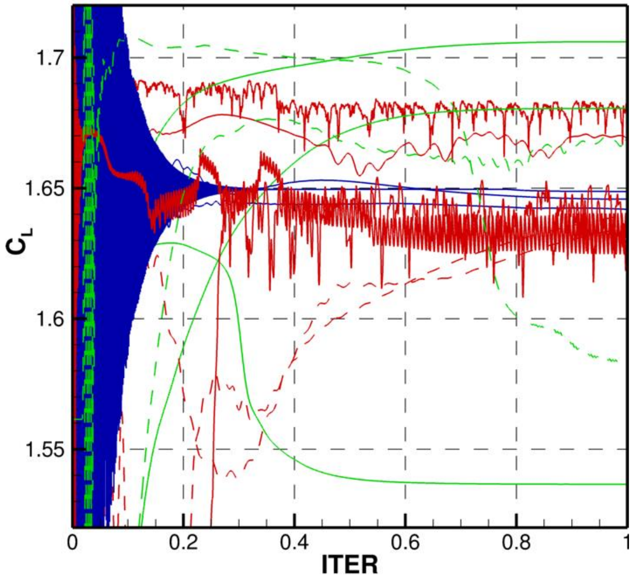

C_L: 4.8% range [1.63, 1.71]
C_D: 4.5% range [0.1615, 0.1690], 75 counts
C_M: 10% range [-0.502, -0.454]

- F&M ranges increased compared to α = 10°
- Very few solutions converged to steady state
  - Most established solutions oscillate
  - R-013 appears as outlier; good agreement for other angles
- F&M agreement improves on fine grids
  - 2% C_L range, 41 count C_D range, and 2.6% C_M range on grids with 200M+ degrees of freedom

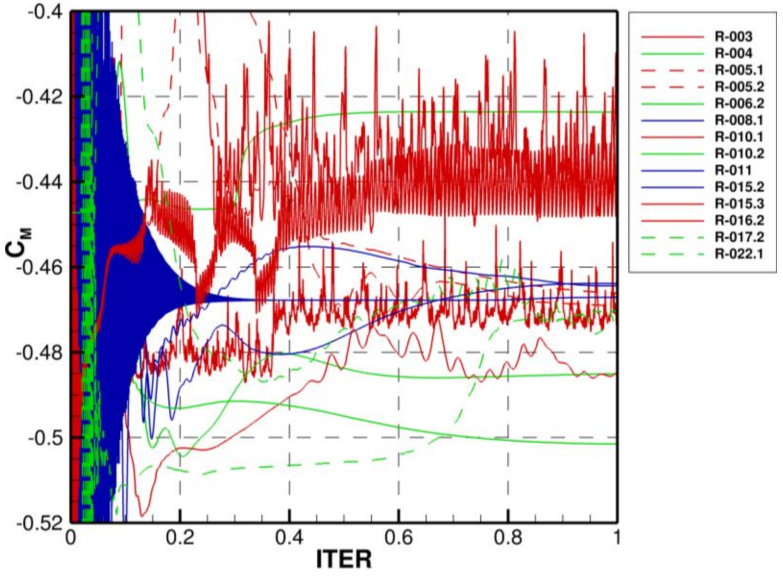

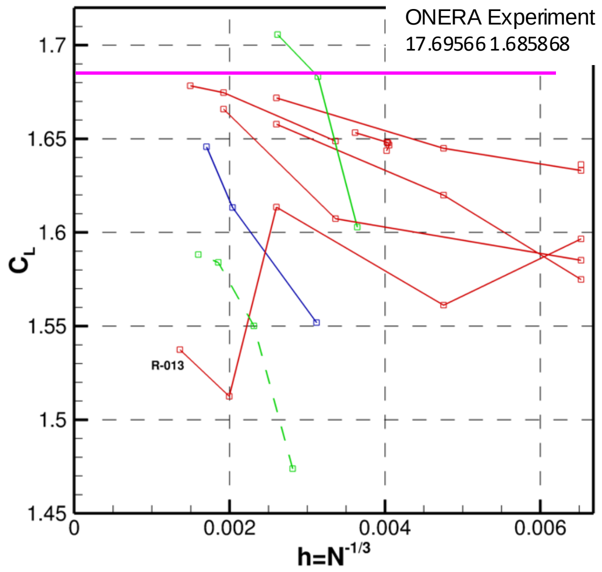

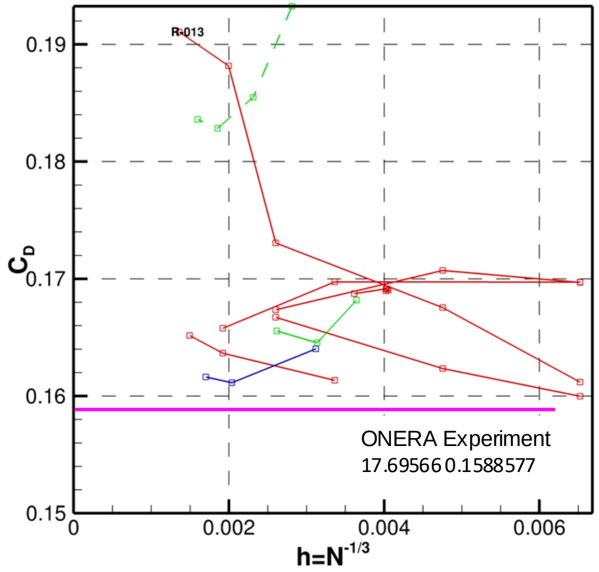

Red=2.R.01
Blue=2.R.03
Green=Other

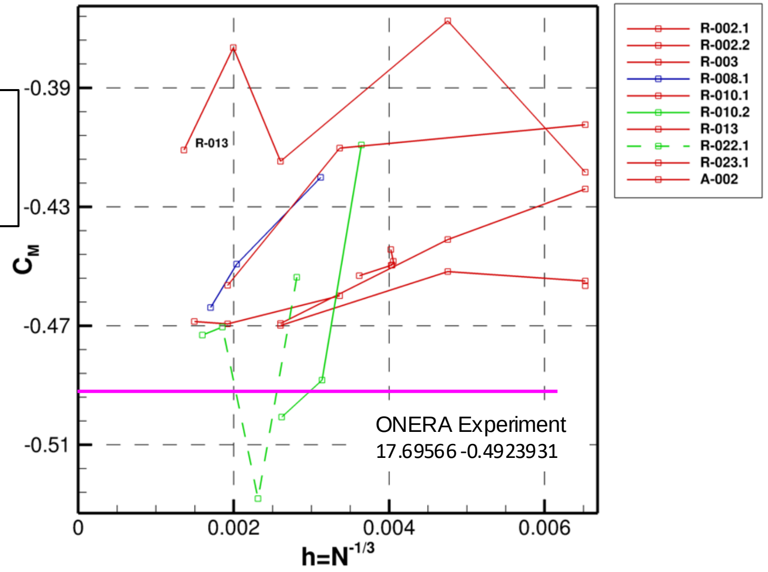

Skin-Friction Contours in Selected SA Solutions, $\alpha = 17.7°$

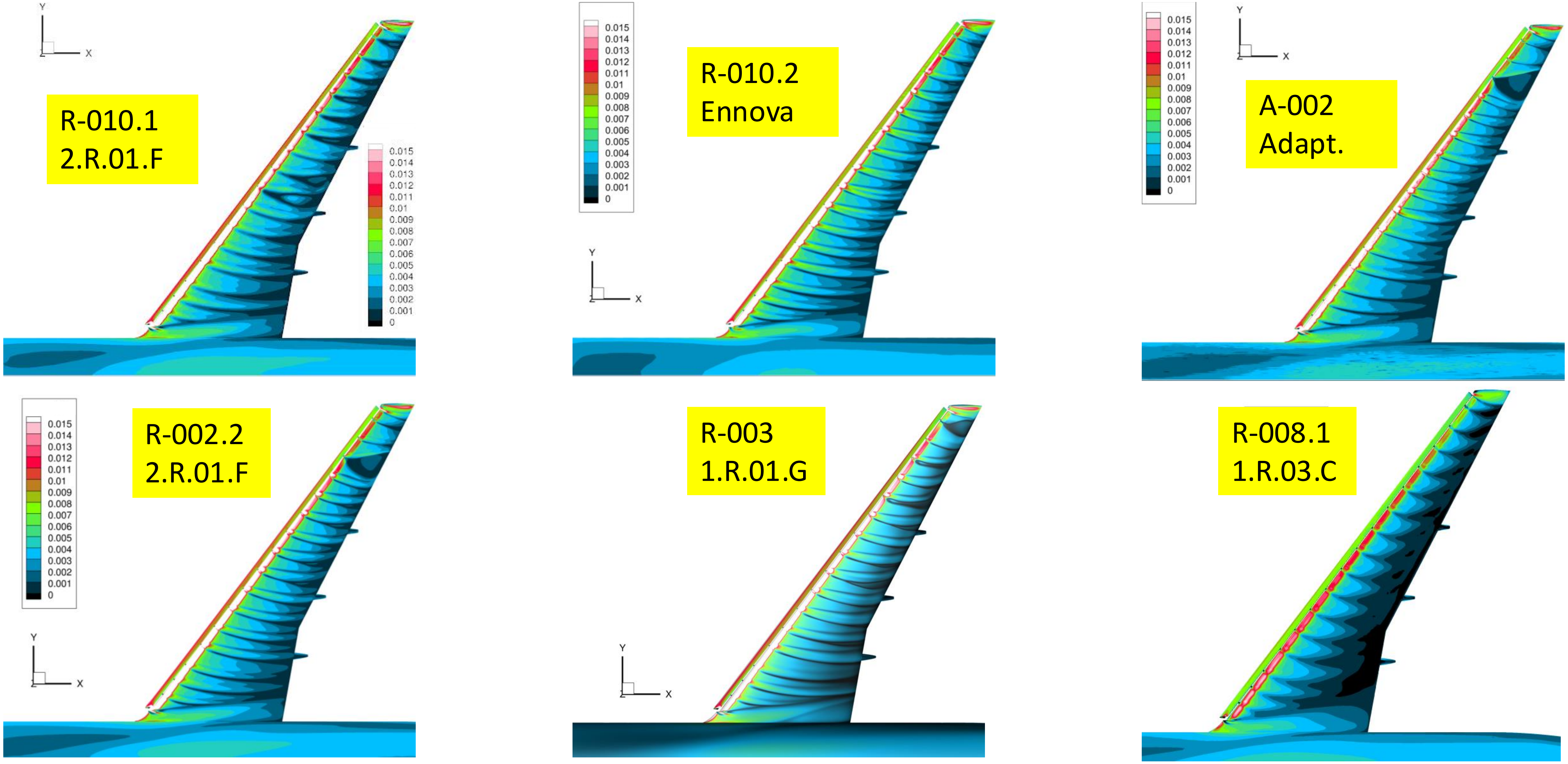

- Significant differences in skin-friction contours midspan and outboard
- “Pizza” disturbance appears outboard, at different slat brackets

Selected SA Solutions, α = 21.5°

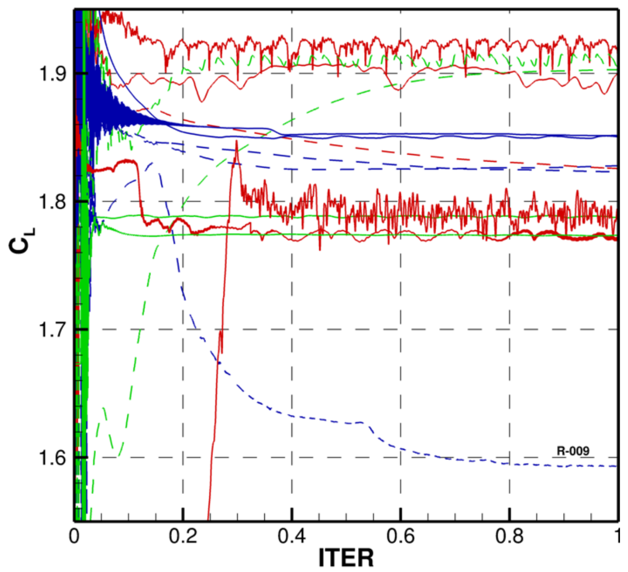

C_L: 13% range [1.69, 1.925]
C_D: 30% range [0.229, 0.296], 670 counts
C_M: 18% range [-0.57, -0.475]

- 2 solutions appear converged to steady state
  - Most established solutions strongly oscillate
- Insignificant improvements on fine grids
  - No grid convergence observed
  - Finer grids are needed

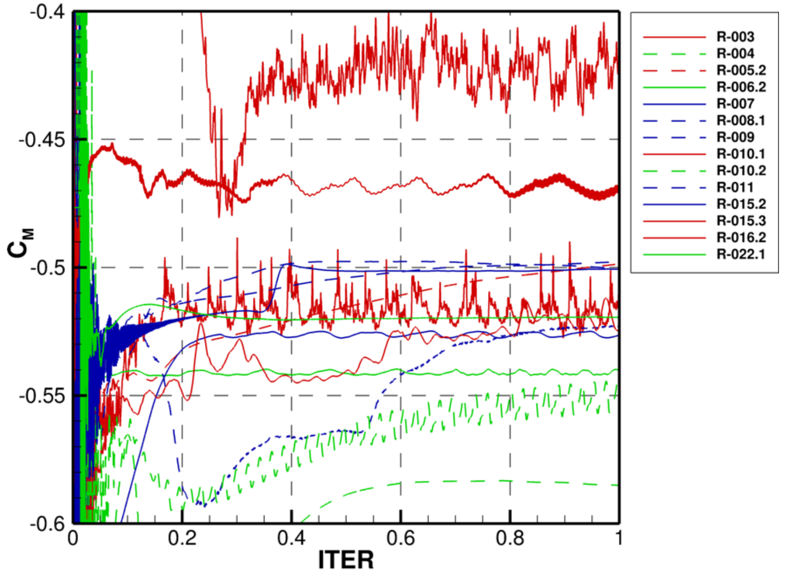

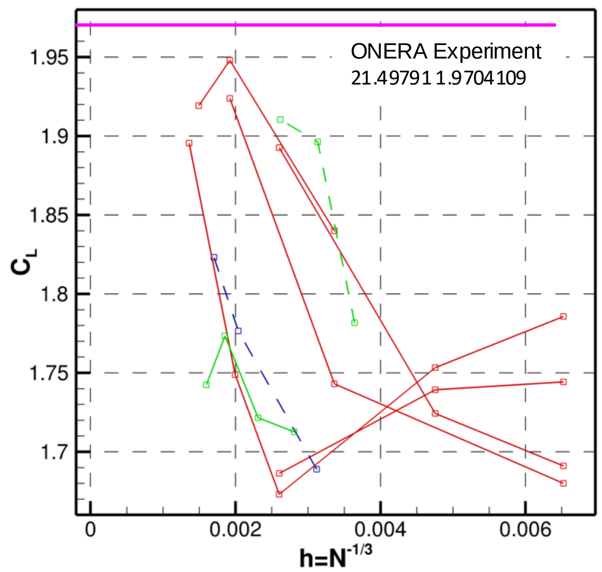

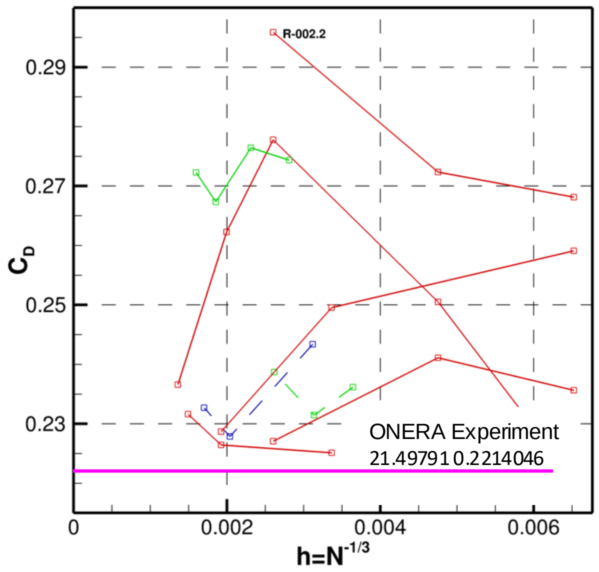

Red=2.R.01
Blue=2.R.03
Green=Other

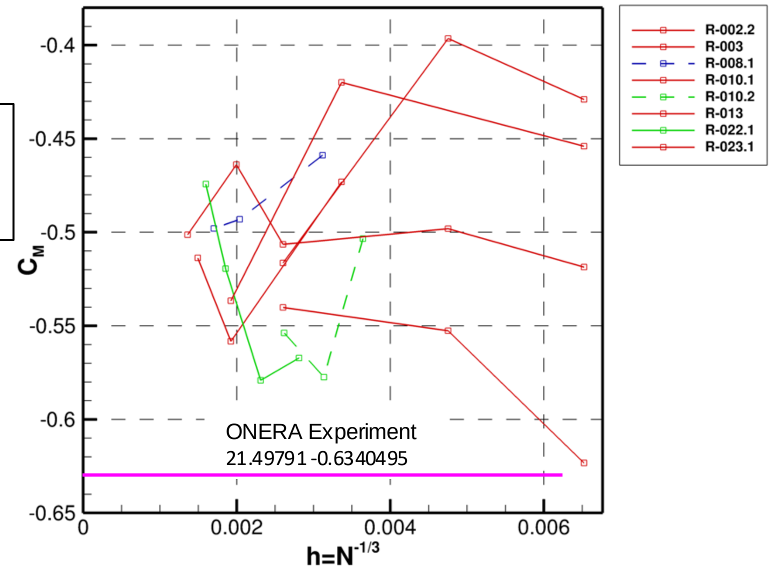

Skin-friction Contours in Selected SA Solutions, $\alpha = 21.5°$

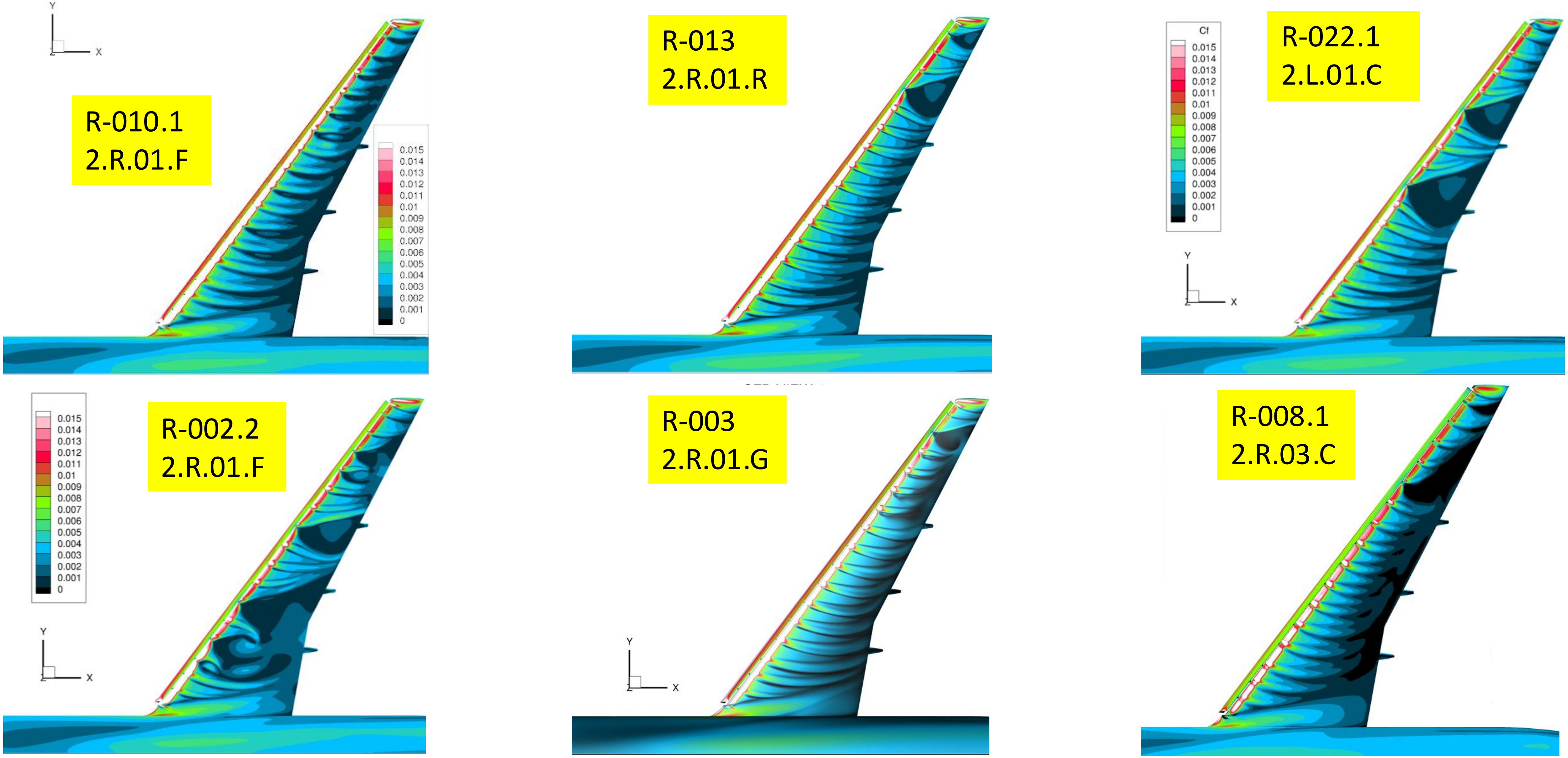

- Significant differences in skin-friction contours with "pizza" disturbances over entire wing
- R-003 and R-010.1 show relatively small "pizza" disturbances

No Solution Selected at α = 23.8°

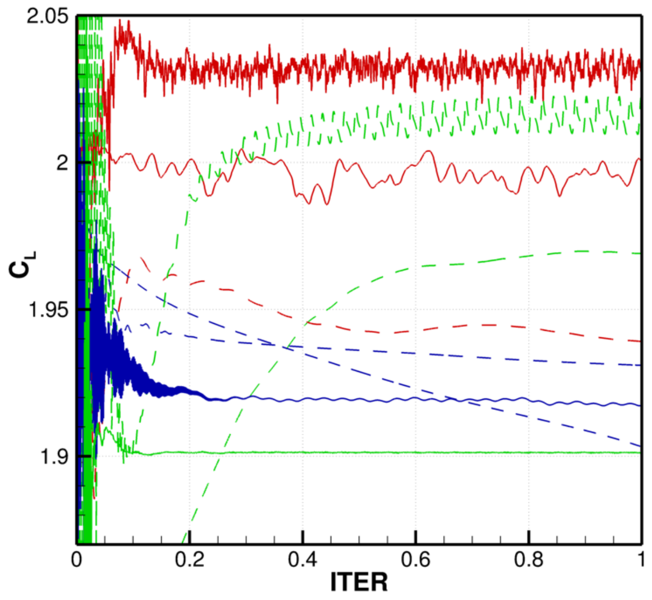

C_L: 17% range [1.81, 2.15]
C_D: 23% range [0.285, 0.355], 70 counts
C_M: 13% range [-0.66, -0.58]

No F&M grid convergence, no solution agreement

Red=2.R.01
Blue=2.R.03
Green=Other

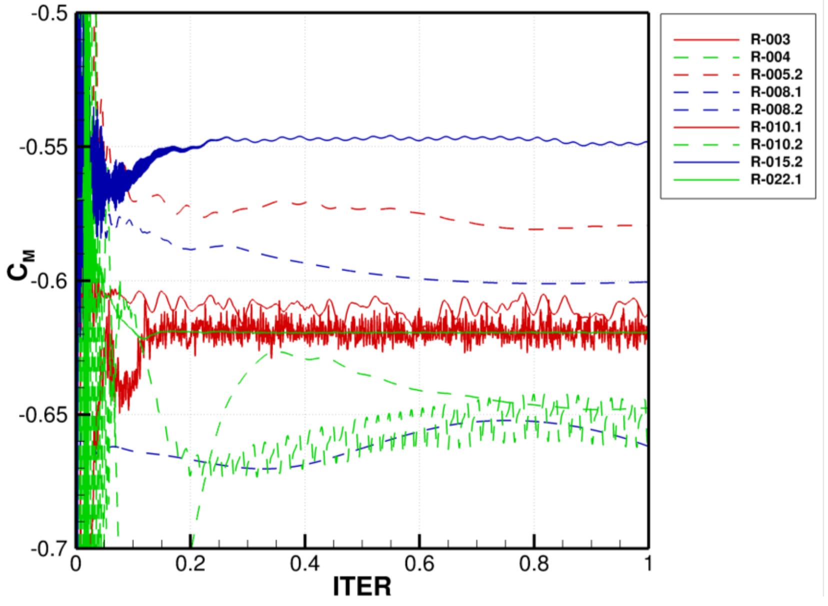

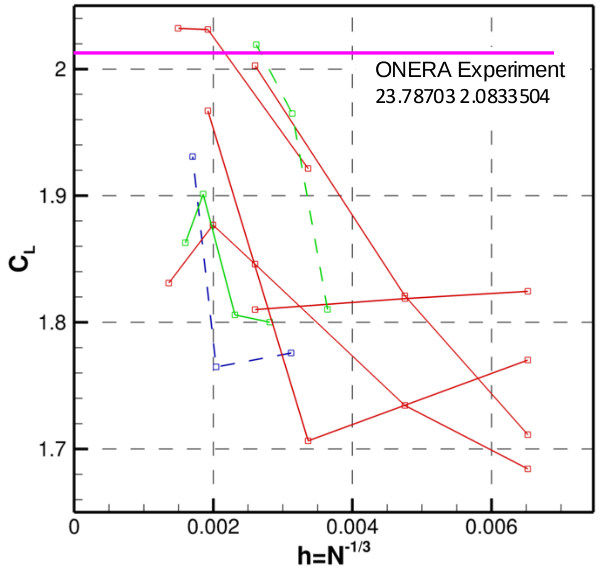

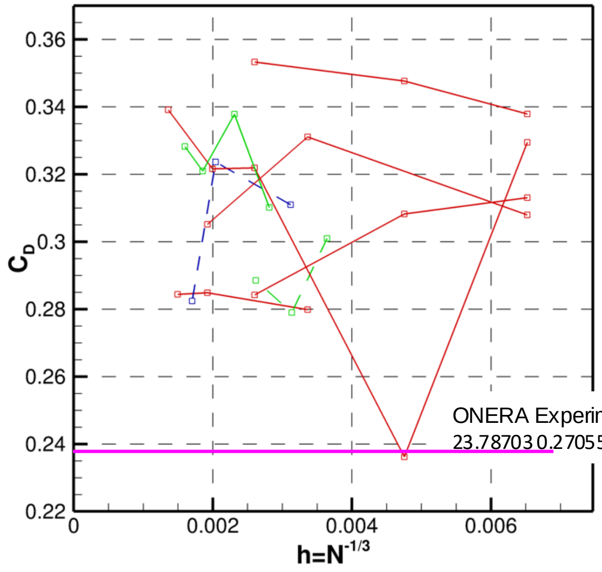

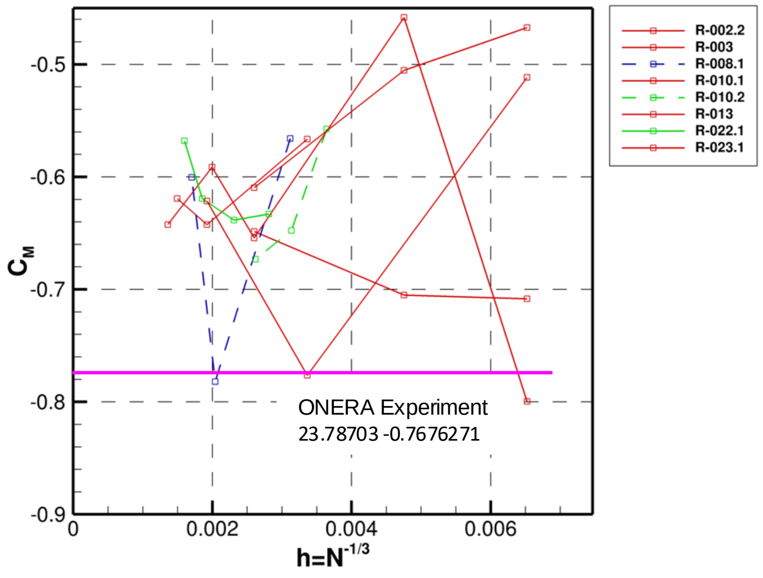

Skin-Friction Contours at α = 23.8°

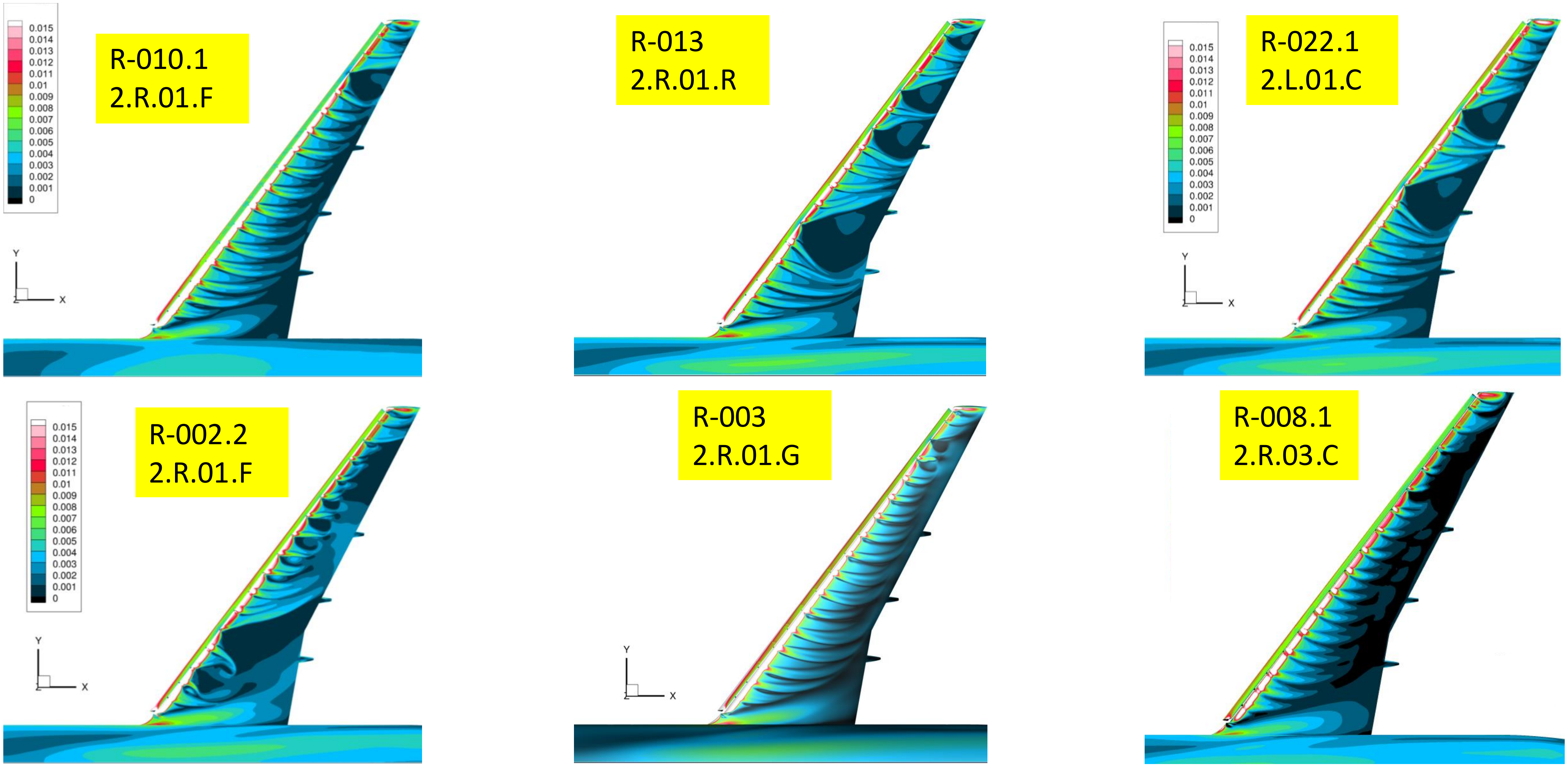

- Chaotic “pizza” disturbances over entire wing
- R-003 and R-010.1 show relatively small “pizza” disturbances

R-004 SA Solutions with Deep Residual Convergence

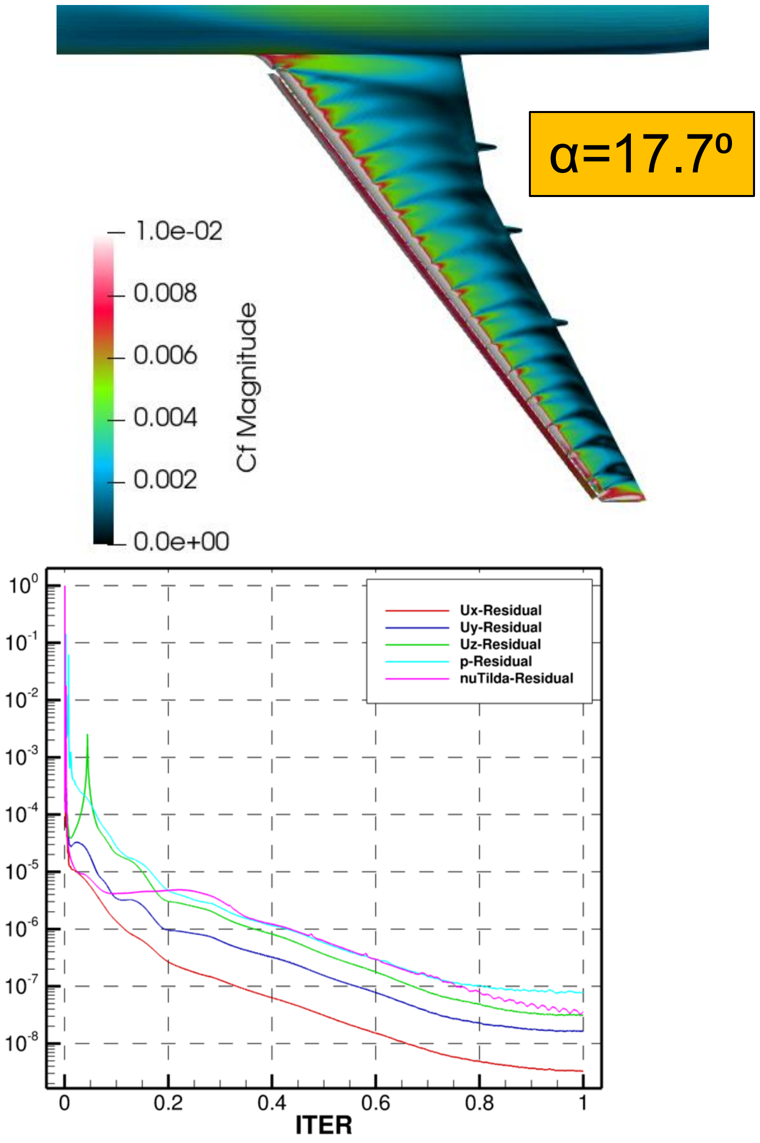

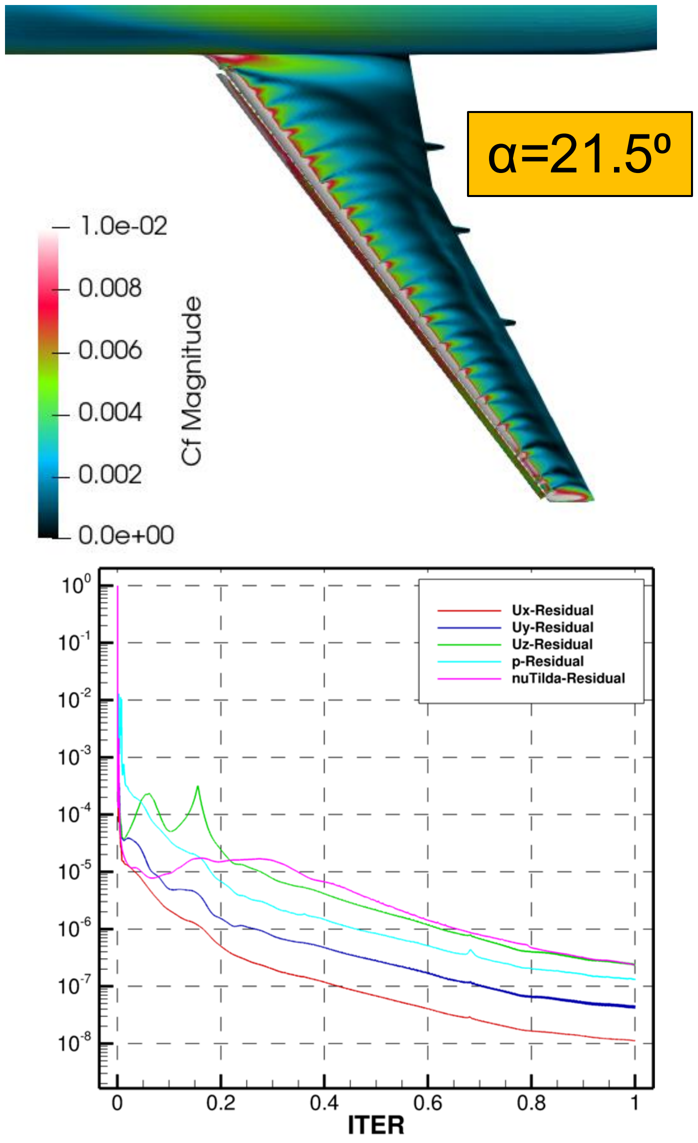

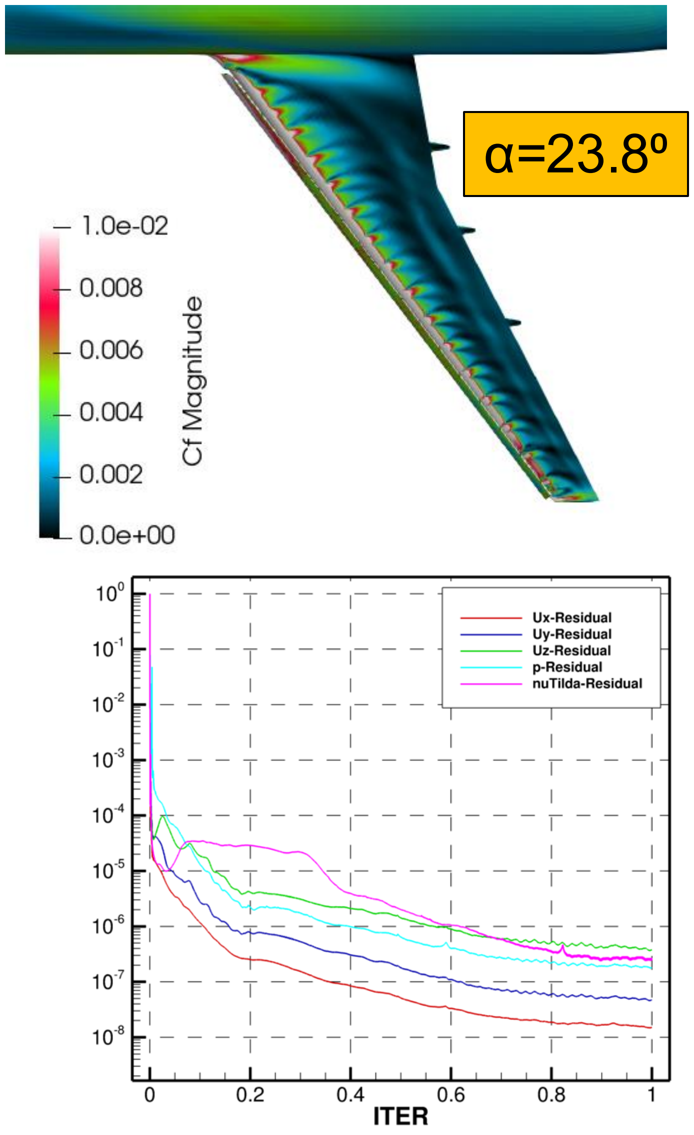

- Custom STAR-CCM+ grids with enhanced orthogonality
- No “pizza” disturbances at high angles of attack

Test Case 2.2: Summary

- **Iterative convergence is more challenging than for Case 2.1**
    - Many solvers arrive at steady state at low angles of attack
        - ✓ R-004 consistently reported deep residual convergence for all angles of attack and no “pizza” disturbances
    - At high angles of attack, most established solutions are oscillatory
        - ✓ In many solutions, “pizza” disturbances appear for $\alpha \geq 17.7°$, mostly outboard
        - ✓ Initiated at different slat brackets
- **Grid convergence is challenging for high angles of attack**
    - Selected SA solutions show grid convergence and good agreement for $\alpha \leq 10°$
        - ✓ F&M agreement improves on grids with 200M+ degrees of freedom
    - Agreement between solutions deteriorates for high angles of attack
        - ✓ Fewer selected solutions and insufficient data for solutions assessment
        - ✓ No grid convergence and no solution agreement at $\alpha = 21.5°$; no selected solutions at $\alpha = 23.8°$
- **Comparison with experiment**
    - Relatively good agreement at low angles of attack
    - At high angles of attack
        - ✓ C_L tends to be lower than experiment
        - ✓ C_D tends to be higher than experiment
        - ✓ C_M tends to be less negative than experiment
        - ✓ In some solutions, C_L and C_D are relatively close to experiment at all angles of attack
        - ✓ No solution shows C_M close to experiment

Case 2.3

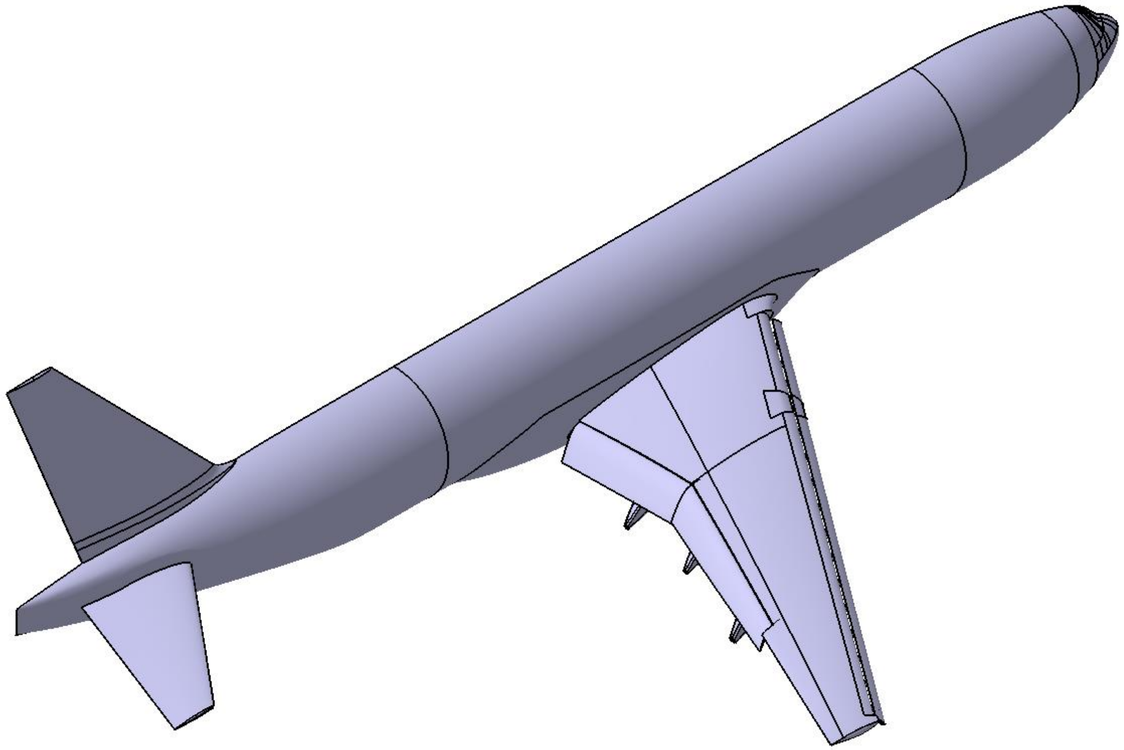

ONERA_LRM-WBSFHV

Flow Conditions: M_∞ = 0.2, Re_{MAC} = 5.9×10^6, T_{ref} = 518.67°R,

α = 6°,10°, 12°, 14°, 16°, 17.7°, 20.7°, 23.5°

F&M Polars on Nominal Grids, All RANS Solutions

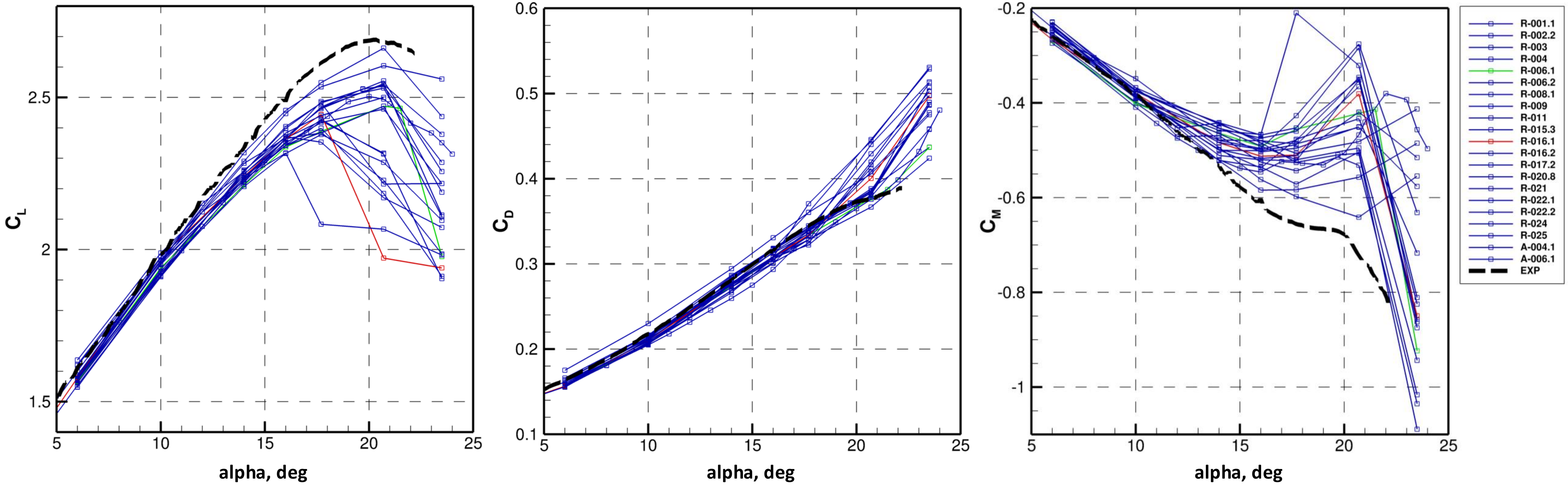

Blue = SA
Red = SA-R(c_{rot}=1)-QCR2000
Green = other

Global view:
- Some agreement between solutions for low angles of attack
- No agreement for high angles of attack

F&M Polars on Nominal Grids
Selected SA Solutions

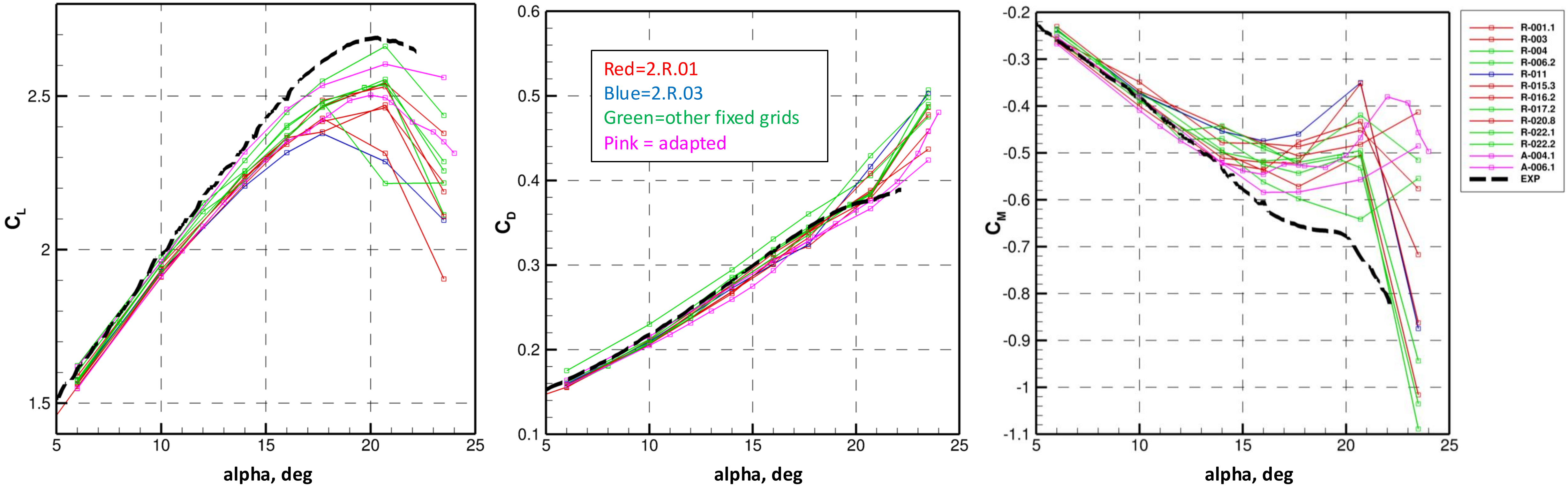

Global view:

- Poor iterative and grid convergence, especially at higher angles of attack
- Selected solutions have no benefits over all solution
- Usefulness of selection diminishes when iterative and grid convergence are lacking

Skin-Friction Contours, $\alpha = 10°$

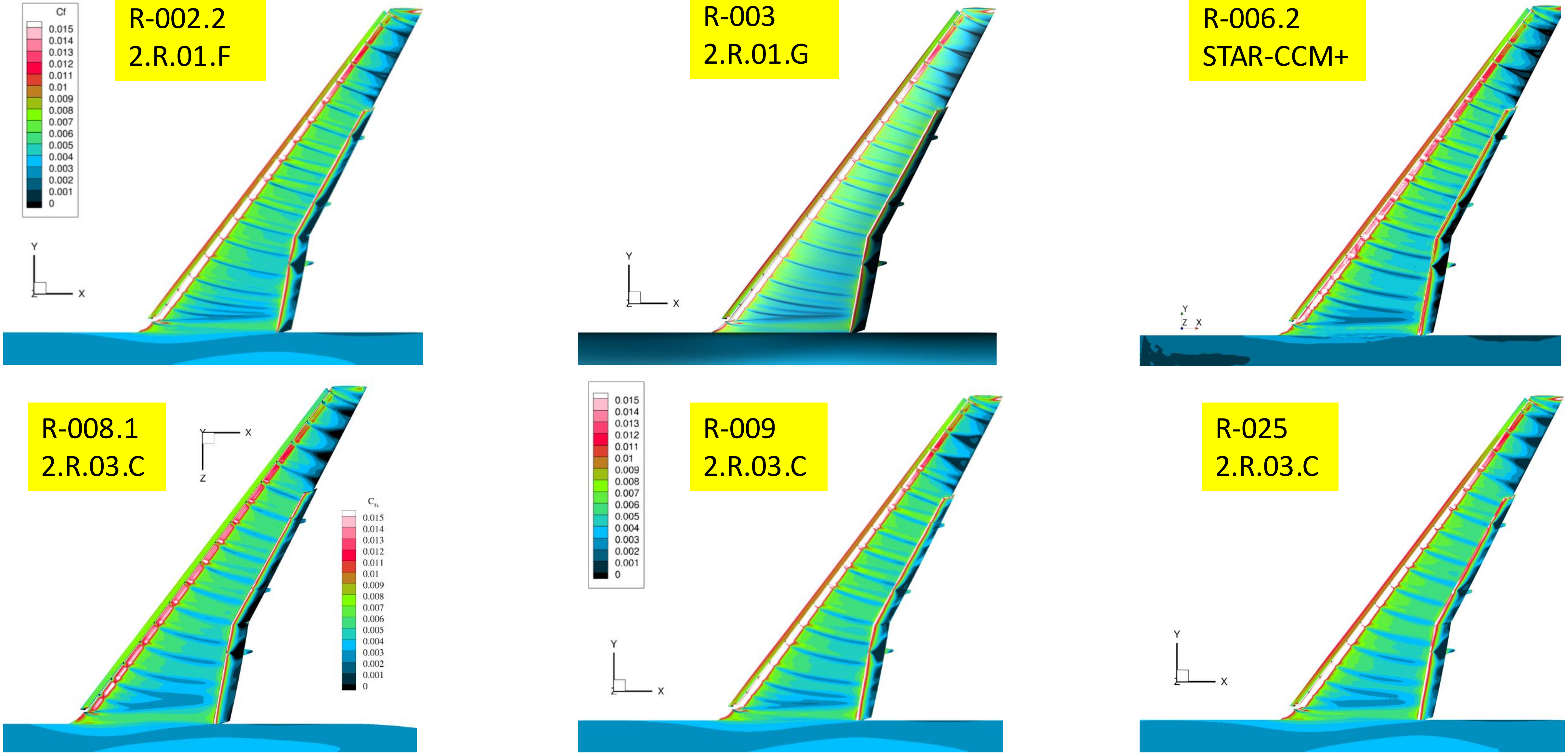

- Similar skin-friction patterns with separation outboard and on flaps

Skin-Friction Contours, $\alpha = 17.7°$

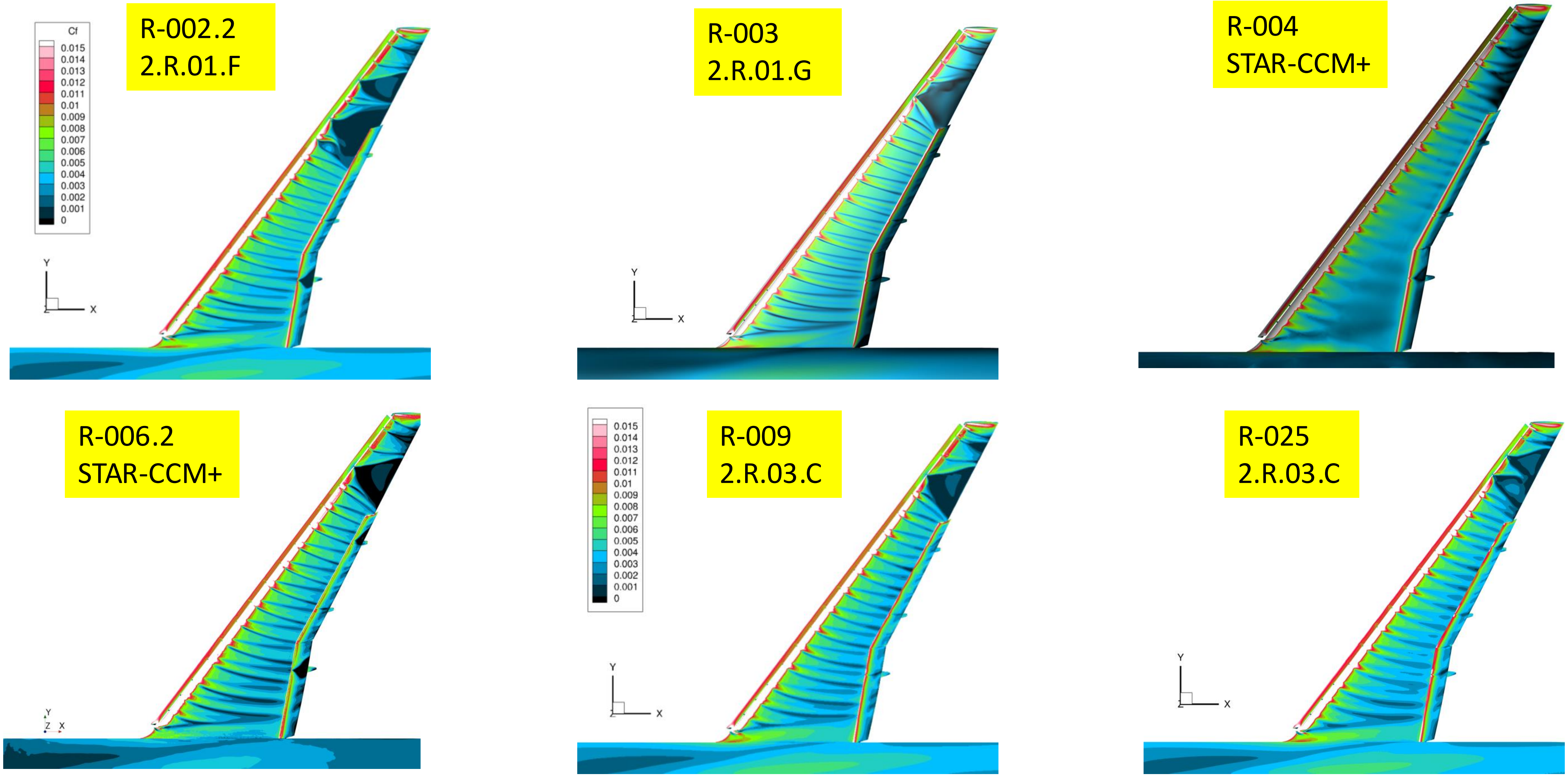

- Significantly different skin-friction patterns; outboard and flap separation

Skin-Friction Contours, α = 23.5°

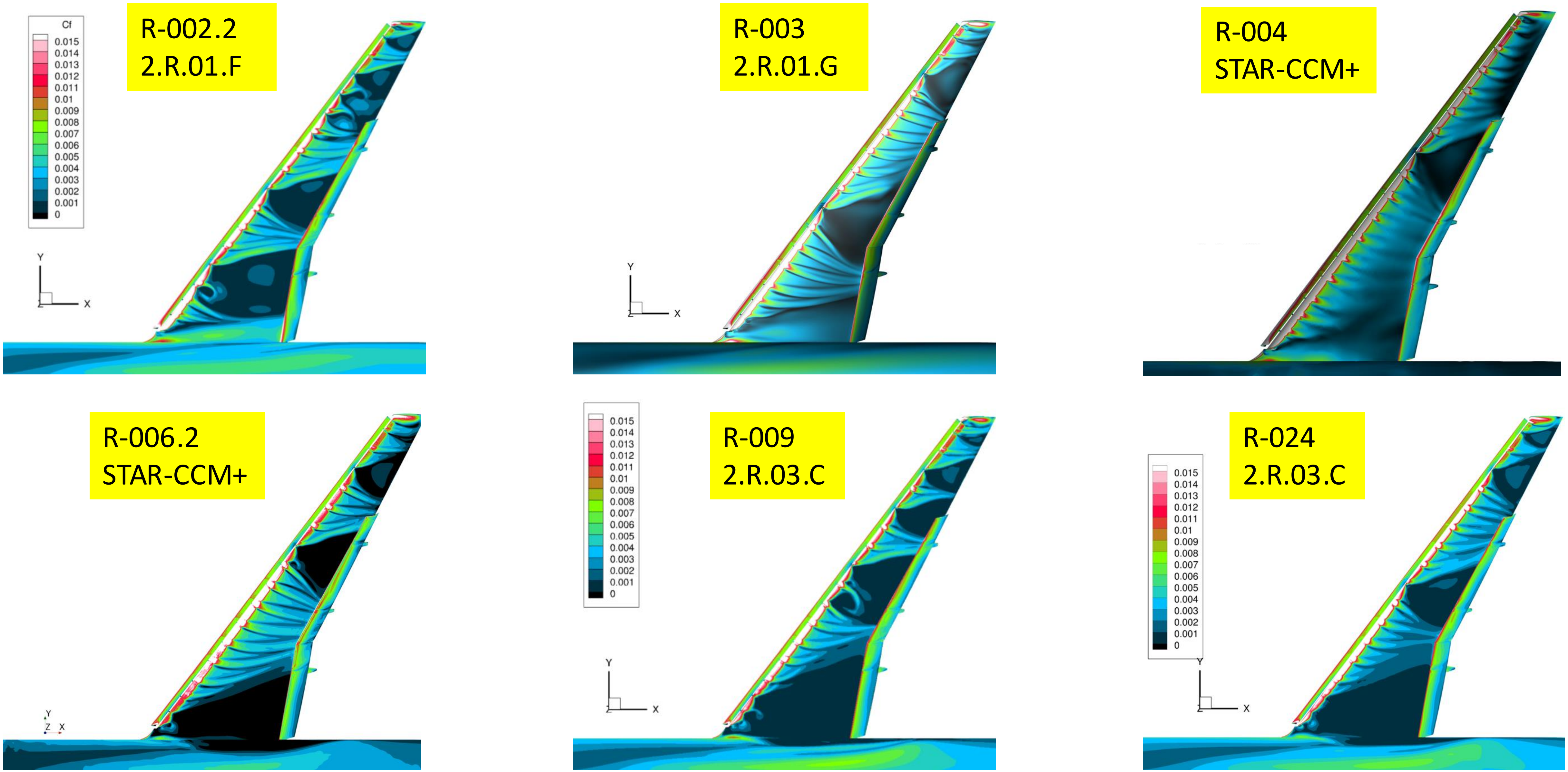

- Very different skin-friction patterns; large inboard separation

Test Case 2.3: Summary

- **No benefits from selection**
- **Reasonable agreement between solutions at $\alpha = 10°$**
- **Poor agreement at $\alpha = 17.7°$ and $\alpha = 23.5°$**

Case 2.4

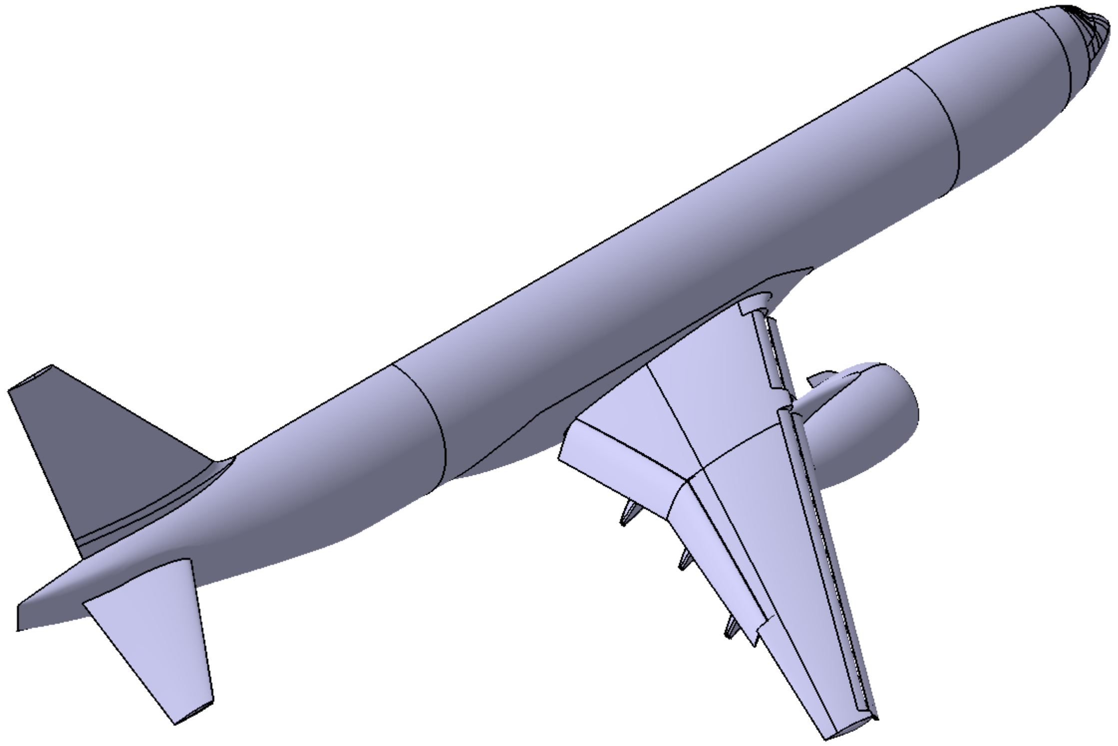

ONERA_LRM-LDG-HV

Flow Conditions: $M_\infty = 0.2$, $Re_{MAC} = 5.9\times10^6$, $T_{ref} = 518.67°R$,

α = 7.6°,10°, 14°, 16°, 17.7°, 19.7°, 23.6°

F&M Polars on Nominal Grids, All RANS Solutions

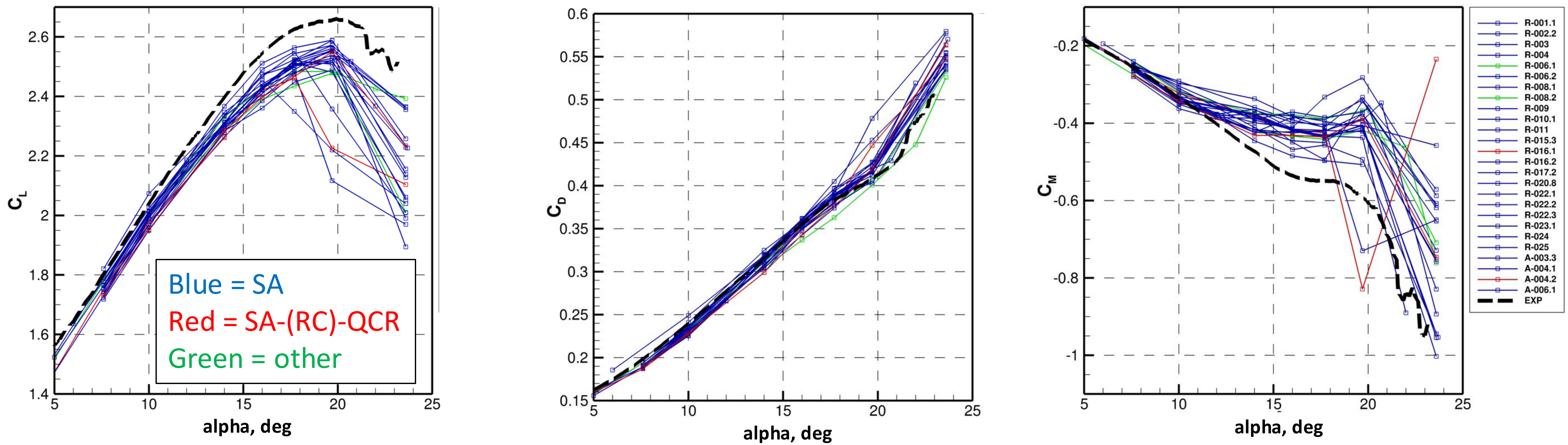

Global view:

- Some F&M agreement for low angles of attack
- C_L is lower than in ONERA experiment
- No good agreement for C_M for high angles of attack

Skin-Friction Contours, $\alpha = 10°$

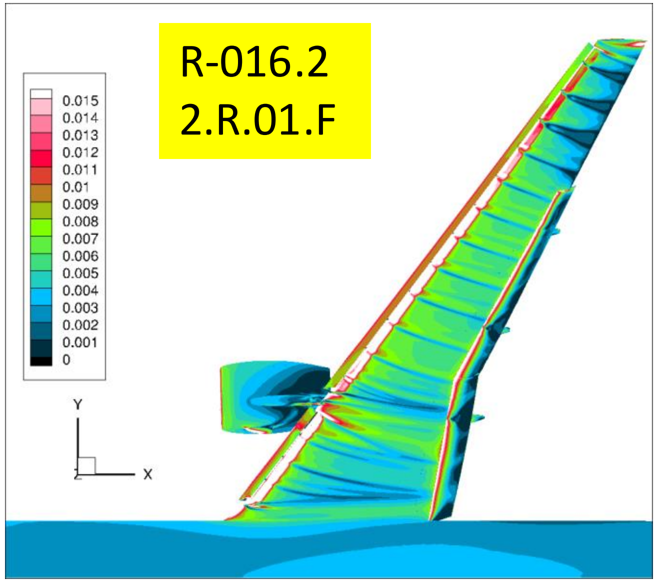

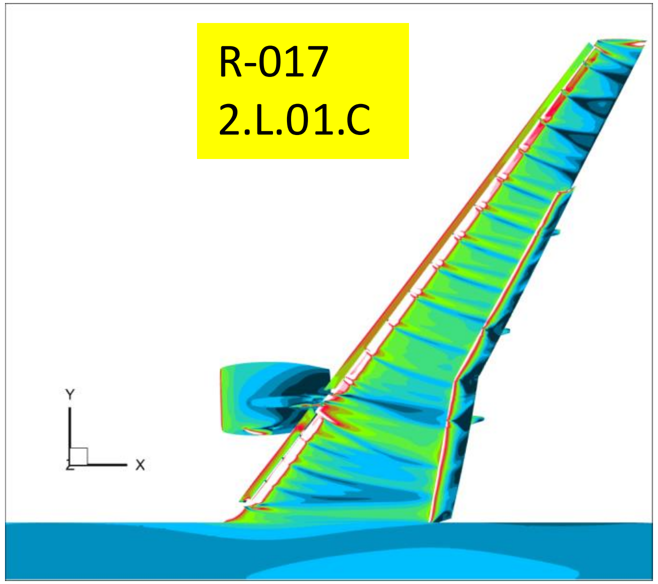

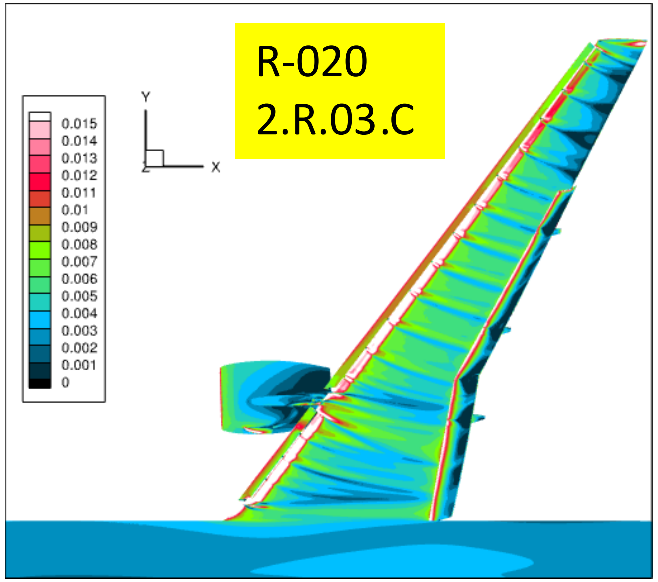

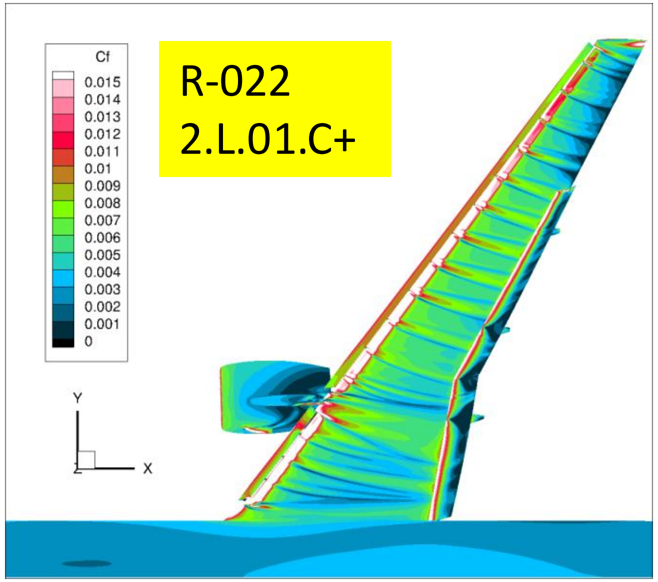

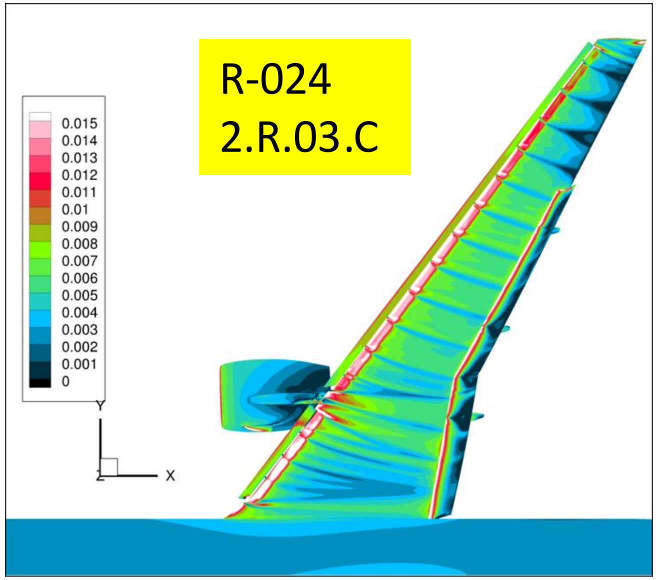

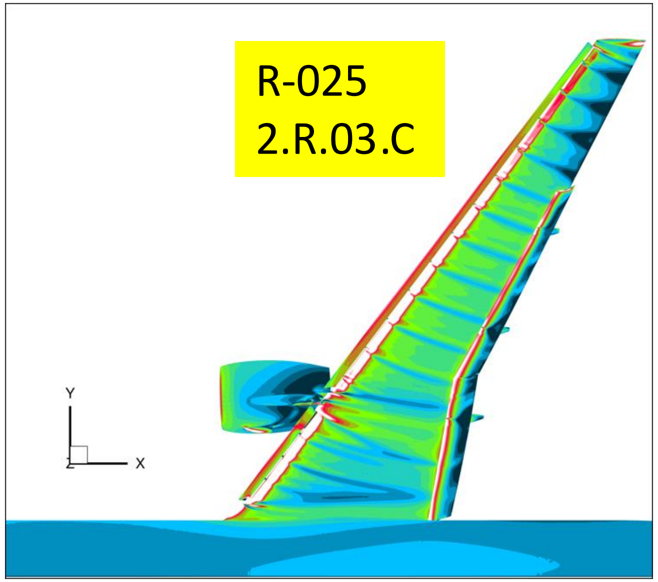

- Similar skin-friction patterns with separation outboard, on flaps, pylon, and nacelle

Skin-Friction Contours, $\alpha = 17.7°$

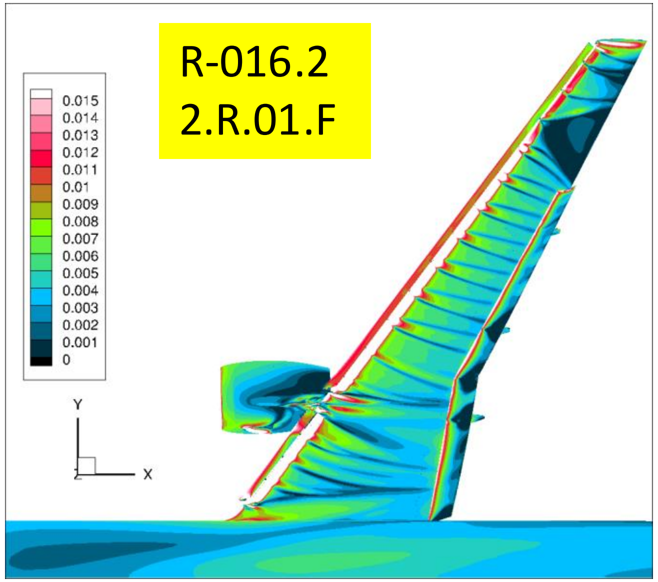

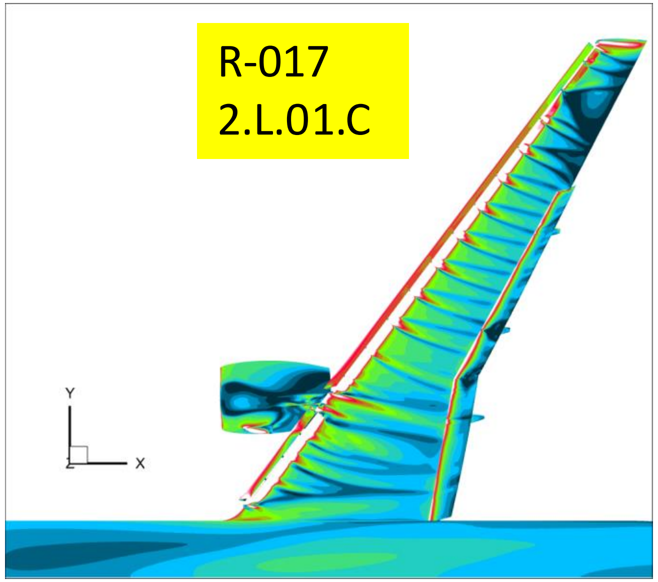

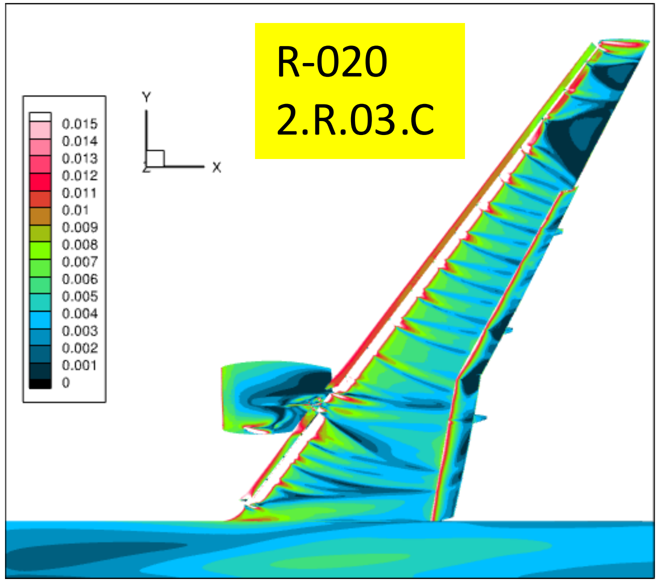

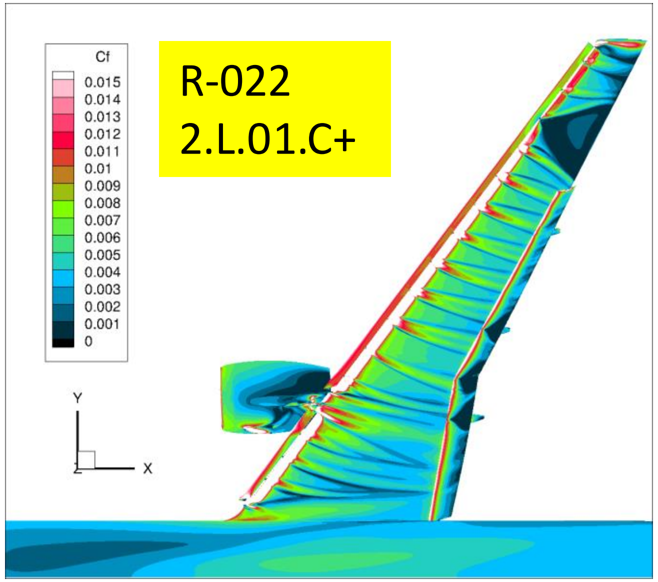

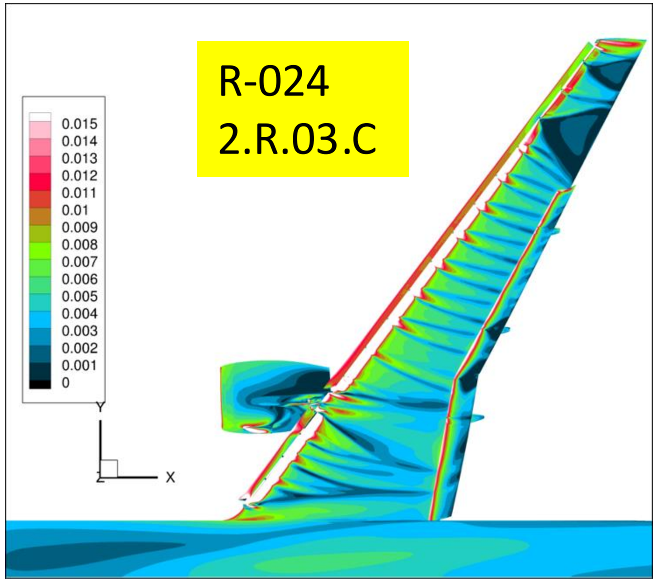

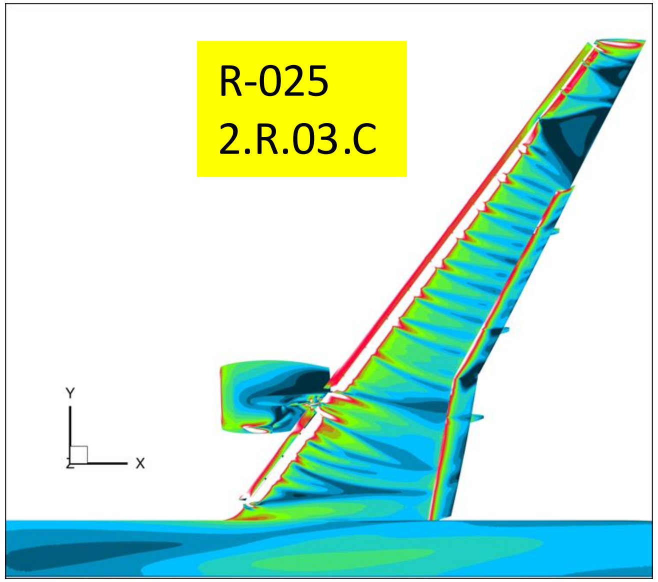

- Different skin-friction patterns with separation outboard, on flaps, pylon, and nacelle

Skin-Friction Contours, $\alpha = 23.6°$

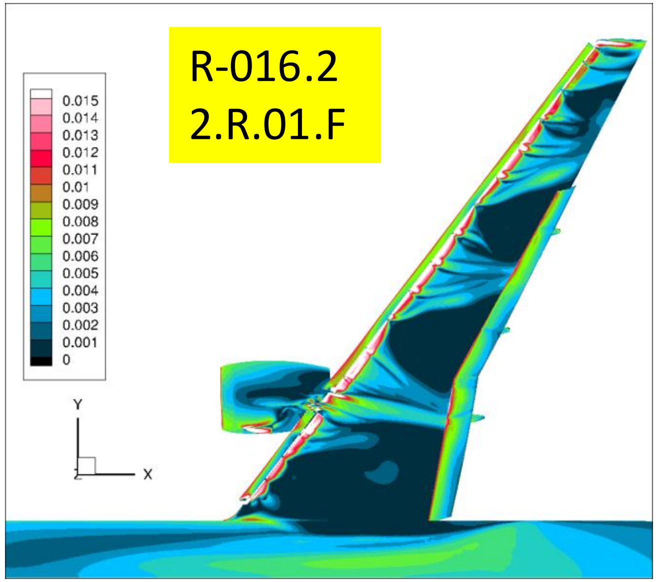

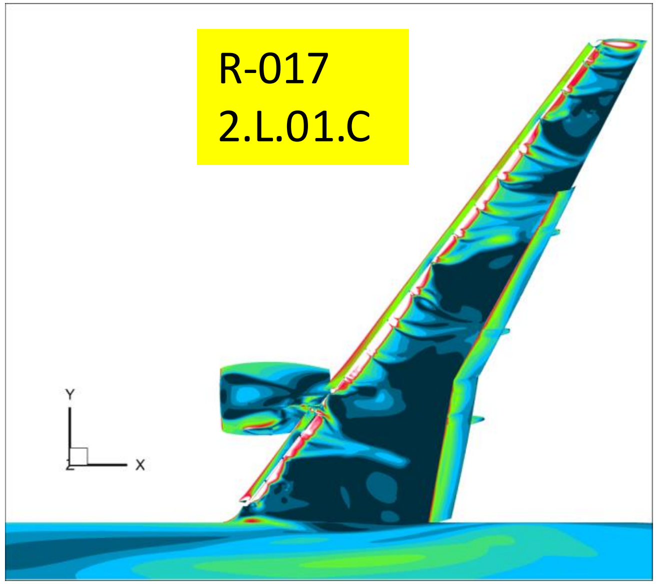

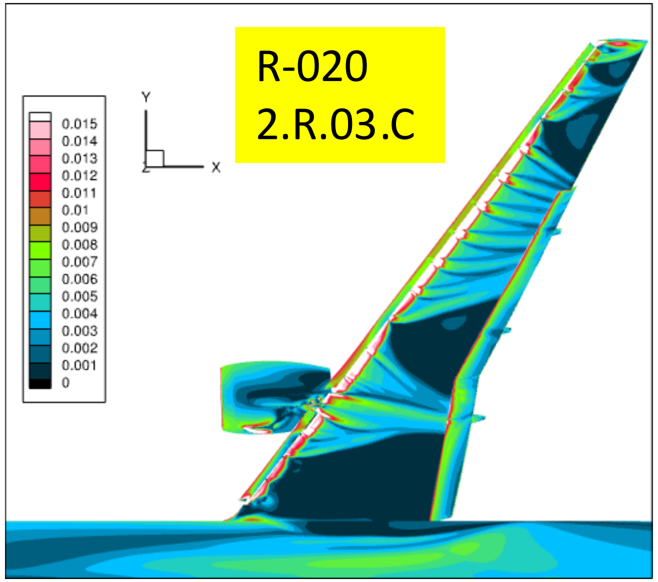

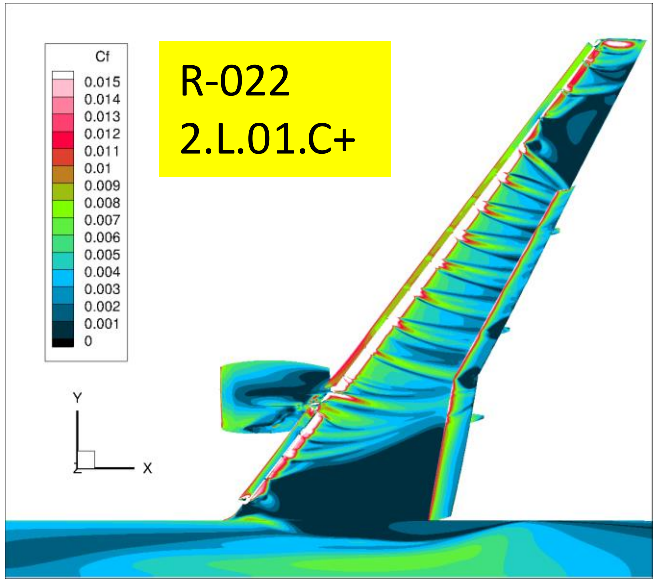

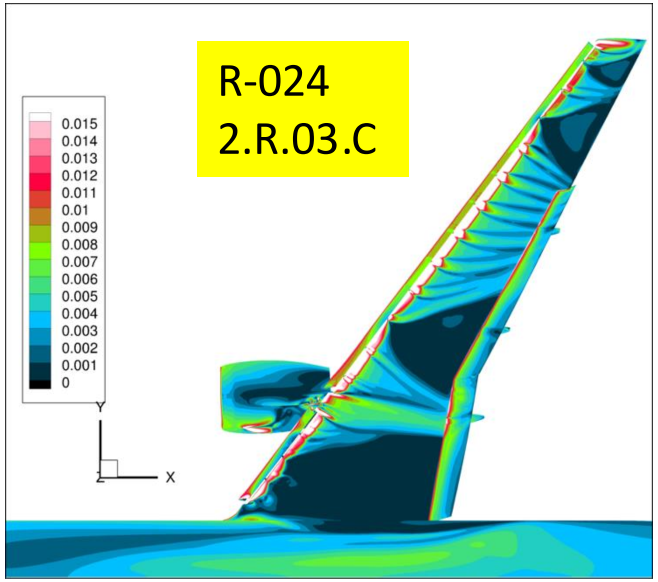

- Different skin-friction patterns; large inboard separation

Configuration Build-Up Effect on C_L

R-001.1, R-002.2, R-003, R-004, R-009, R-010.1, R-011, R-015.3

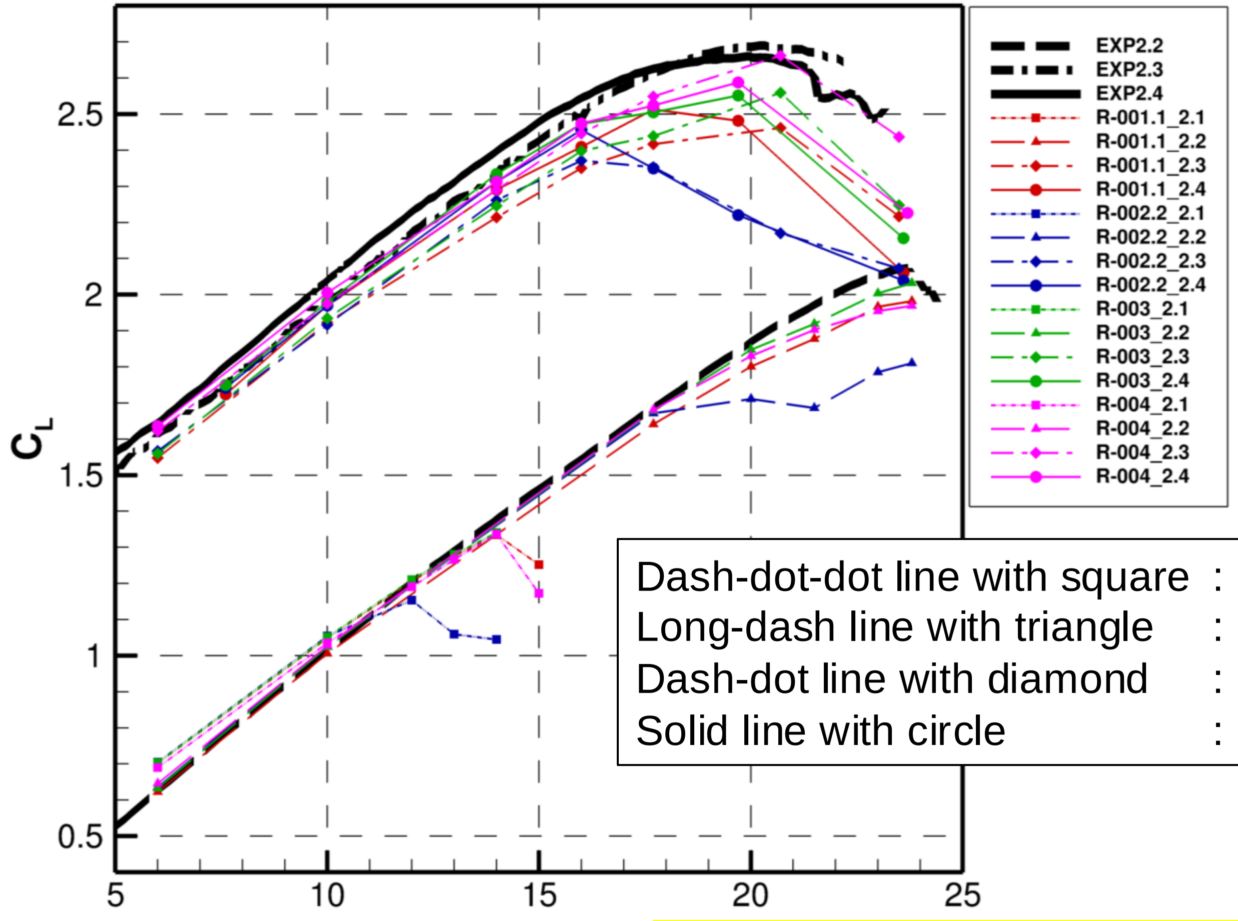

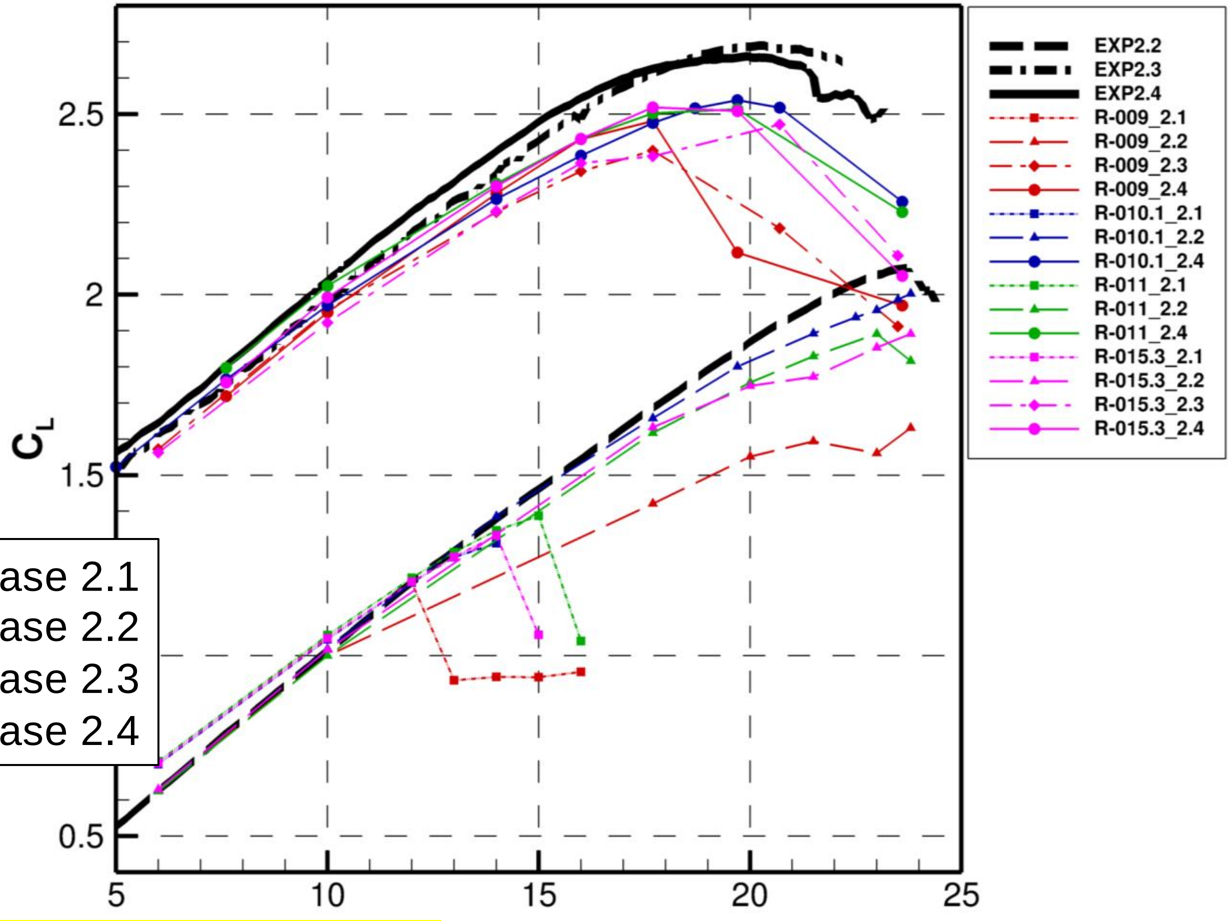

Dash-dot-dot line with square	: Case 2.1
Long-dash line with triangle	: Case 2.2
Dash-dot line with diamond	: Case 2.3
Solid line with circle	: Case 2.4

- C_L qualitatively follows configuration buildup trend:
  - C_L increases and $C_{L,\,max}$ angle decreases in Case 2.3 over Case 2.2
  - Small changes in Case 2.4 from Case 2.3
- Good prediction of angle of $C_{L,\,max}$ in most solutions
- $C_{L,\,max}$ underpredicted for all configurations

Configuration Build-Up Effect on C_L

R-017.2, R-022.1, R-023.1, R-024, R-025

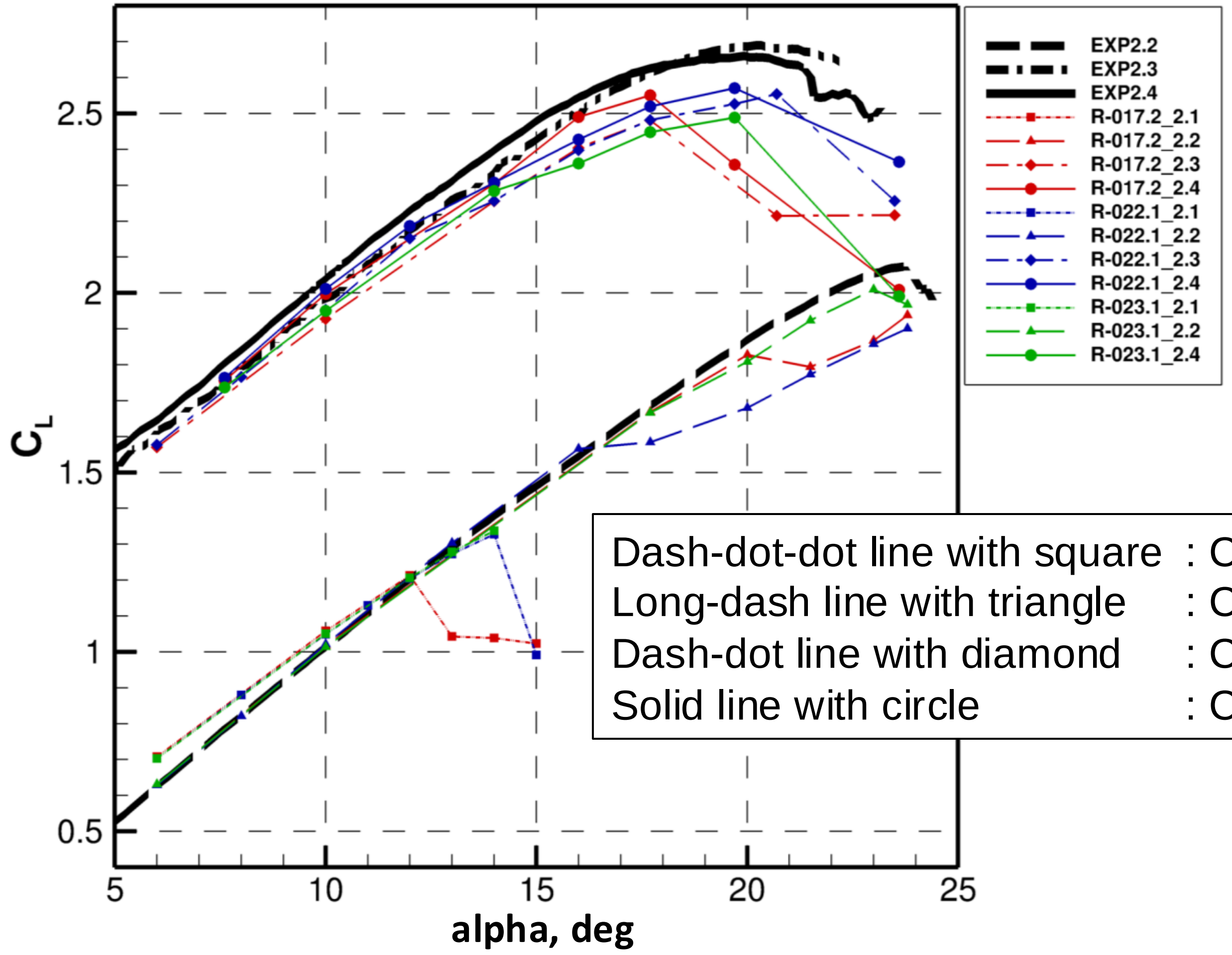

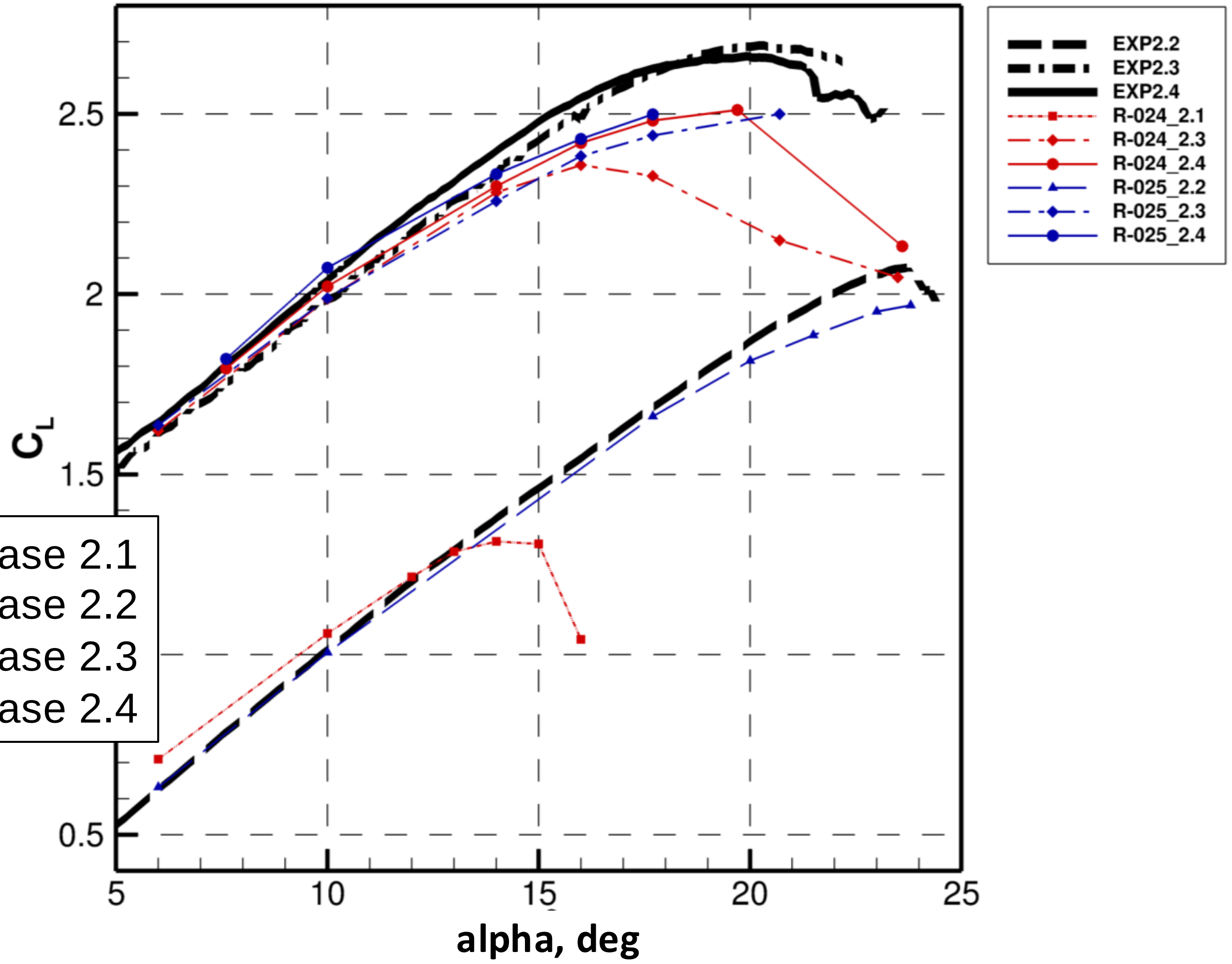

Dash-dot-dot line with square	: Case 2.1
Long-dash line with triangle	: Case 2.2
Dash-dot line with diamond	: Case 2.3
Solid line with circle	: Case 2.4

- C_L qualitatively follows configuration buildup trend
- $C_{L,\ max}$ underpredicted for all configurations

Turbulence Model and Configuration Build-Up Effects on C_L

R-006, R-008, R-016

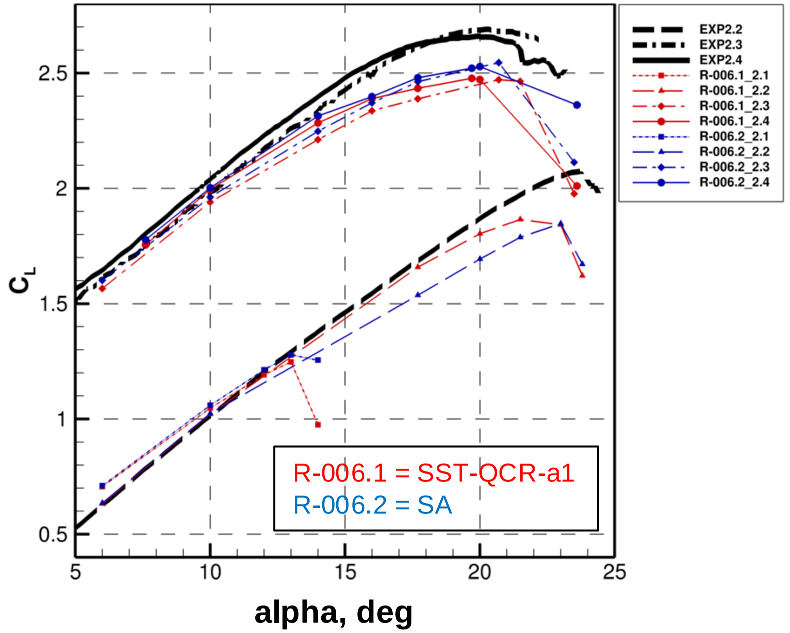

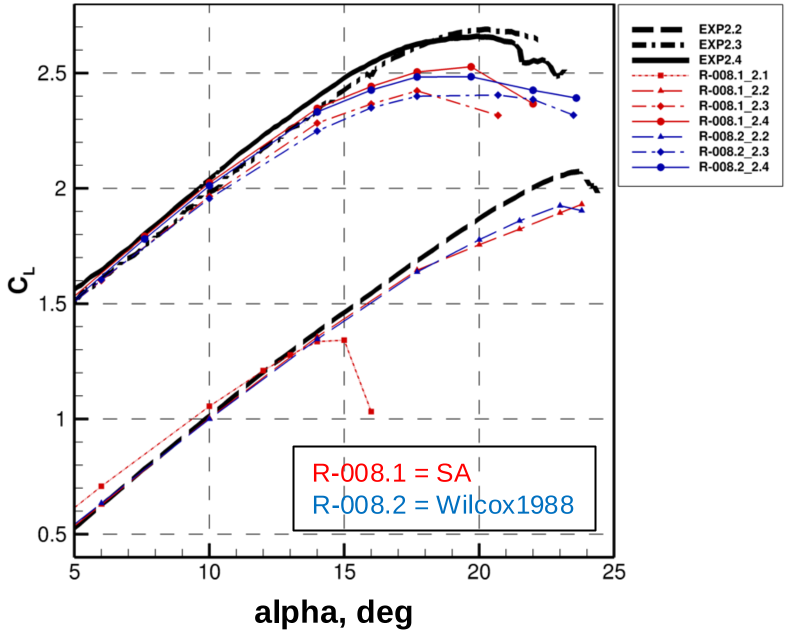

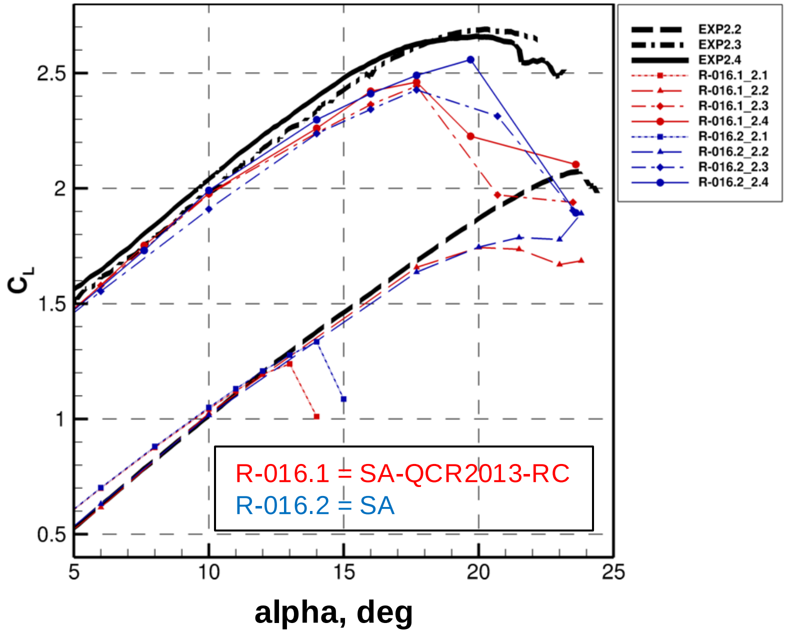

Dash-dot-dot line with square	: Case 2.1
Long-dash line with triangle	: Case 2.2
Dash-dot line with diamond	: Case 2.3
Solid line with circle	: Case 2.4

- No clear trend for turbulence-model variation
- C_L qualitatively follows configuration build-up trend
- $C_{L,\,max}$ underpredicted for all configurations

Test Case 2: Summary

- **Selected SA solutions agree to each other for Case 2.1 $\alpha \leq 14°$**
  - Iterative and grid convergence achieved
  - Experimental data needed to assess accuracy of RANS models for these flow conditions
- **Iterative and grid convergence are challenging for Cases 2.2, 2.3, and 2.4**
  - Qualitative agreement between solutions at low angles of attack
  - Modifications in geometry, RANS models, solvers, and grids may be needed to enable converged solutions and assessment of RANS model accuracy for high angles of attack
- **Qualitative comparison with ONERA experiment for Cases 2.2, 2.3, and 2.4**
  - Some agreement at low angles of attack
  - At high angles of attack
    - ✓ C_L tends to be lower than experiment
    - ✓ C_D has qualitative agreement with experiment
    - ✓ C_M tends to be less negative than experiment
- **F&M deltas qualitatively follow configuration buildup trend**

Test Case 3

Reynolds Number Study

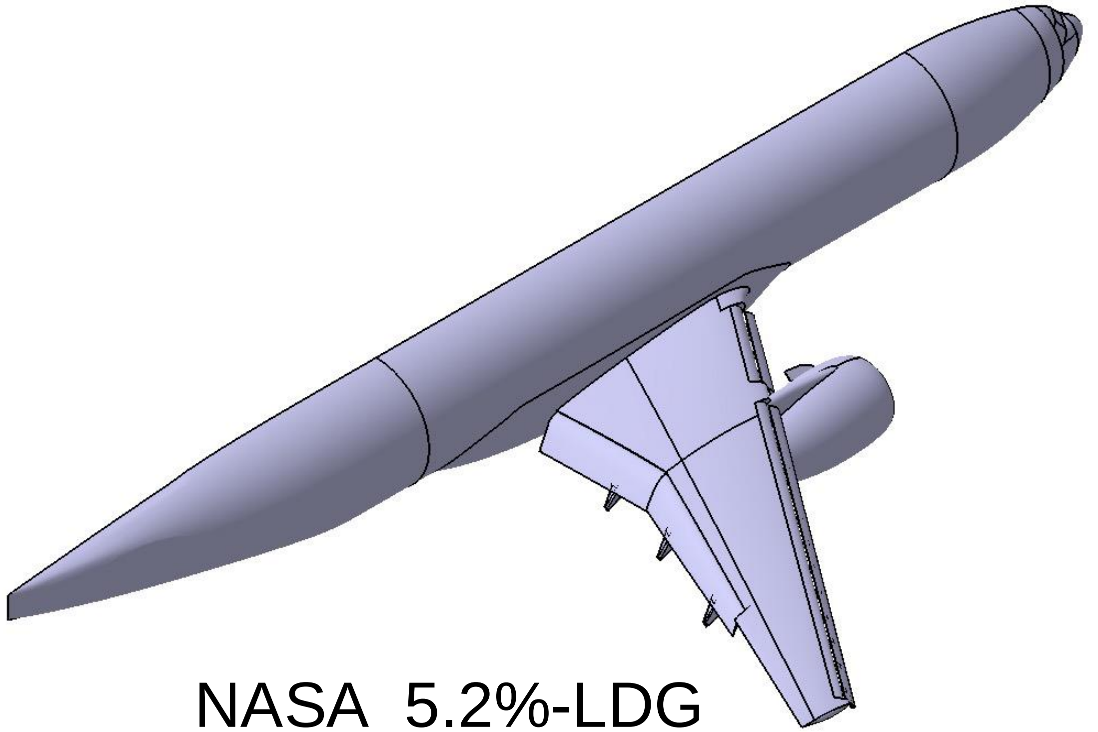

NASA_5.2%-LDG

3.1: $Re_{MAC} = 1.05 \times 10^6$

3.2: $Re_{MAC} = 5.49 \times 10^6$

3.3: $Re_{MAC} = 16.00 \times 10^6$

3.4: $Re_{MAC} = 30.00 \times 10^6$

$M_\infty = 0.2$, $T_{ref} = 518.67°R$,

α = 6°,10°, 14°, 16°, 18°, 19°, 20°, 22°

Case 3.1: F&M Polars on Nominal Grids, All RANS Solutions

Red = SA-notf2-R or SA-RC-QCR
Blue = SA

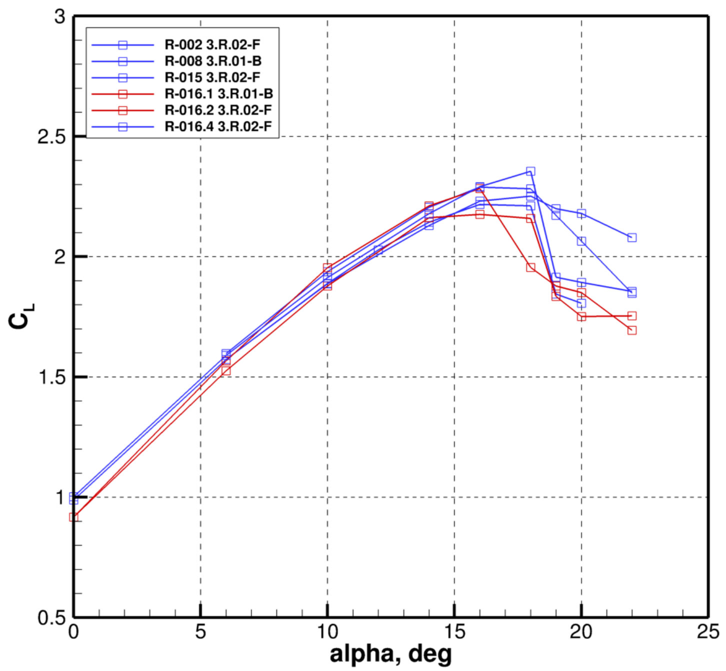

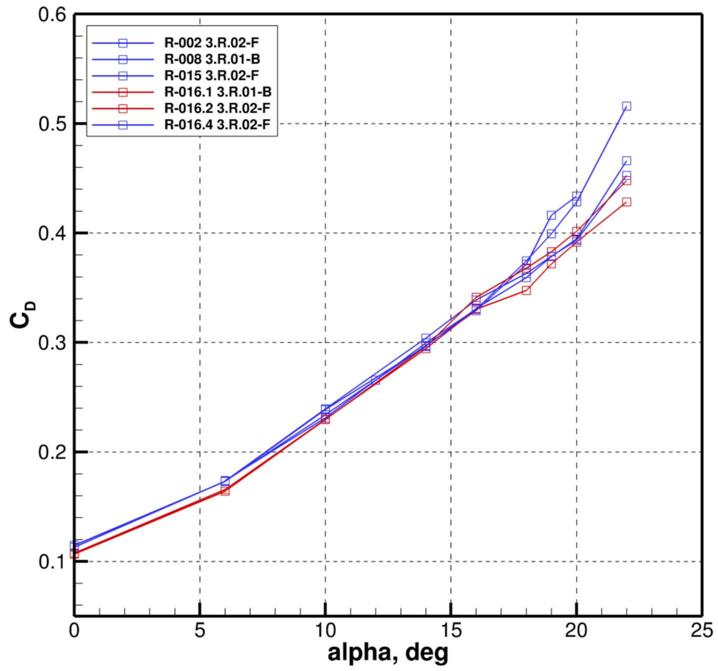

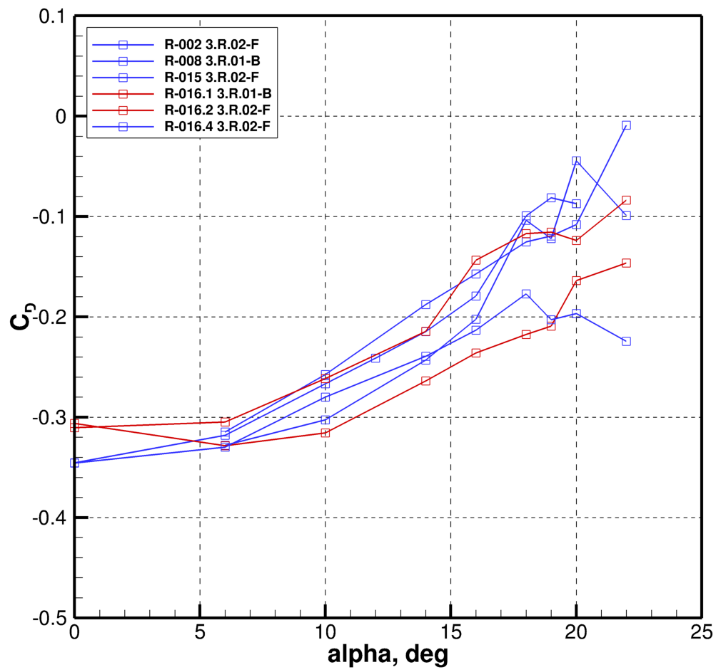

Global view:

- $C_{L,max}$ within [2.2, 2.35] achieved at 16° ≤ α ≤ 18°
- Some agreement between C_L coefficients at low angles of attack
- Agreement deteriorates for high angles of attack
- Some relative agreement between C_D coefficients at α ≤ 16°
- Poor agreement between C_M coefficients, more data needed

Case 3.2: F&M Polars on Nominal Grids, All RANS Solutions

Red = SA-notf2-R or SA-RC-QCR
Blue = SA

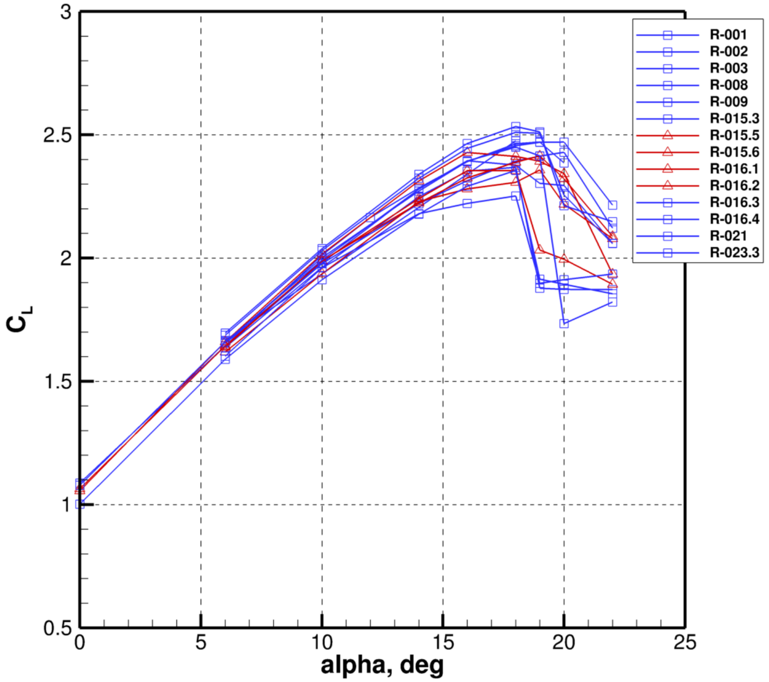

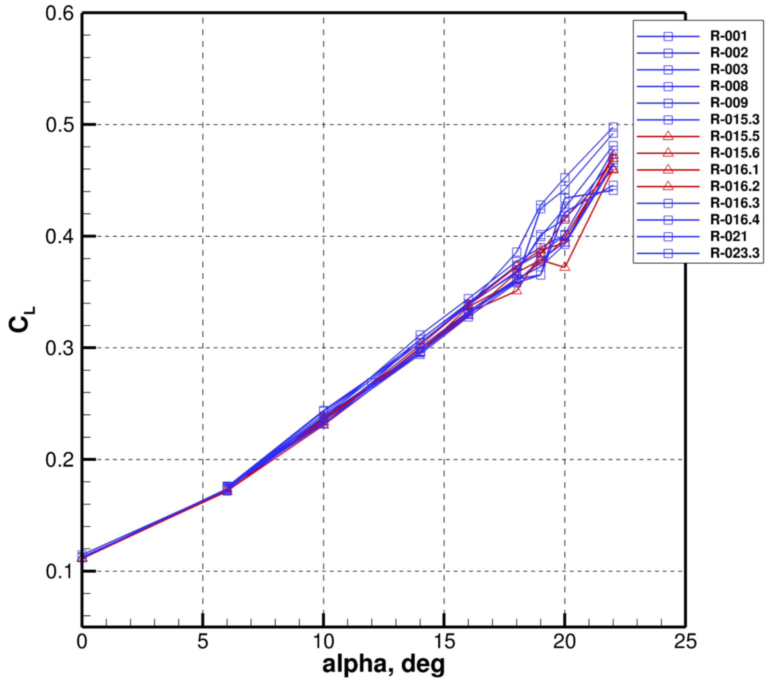

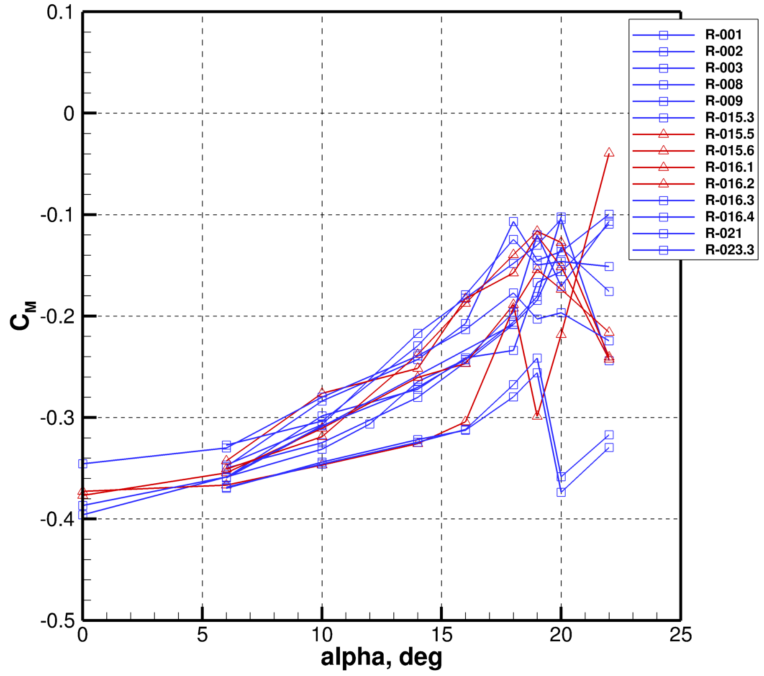

Global View:

- $C_{L,max}$ within [2.25, 2.52] achieved at 16° ≤ α ≤ 20°
- Poor agreement between C_L coefficients
- Some relative agreement between C_D coefficients at α ≤ 18°
- Poor agreement between C_M coefficients, more data needed

Case 3.3: F&M Polars on Nominal Grids, All RANS Solutions

Red = SA-notf2-R or SA-RC-QCR
Blue = SA

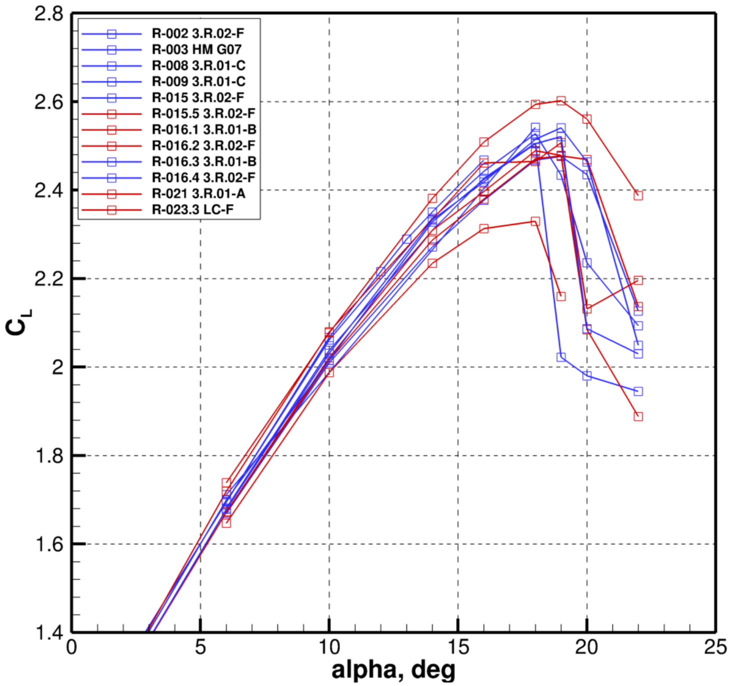

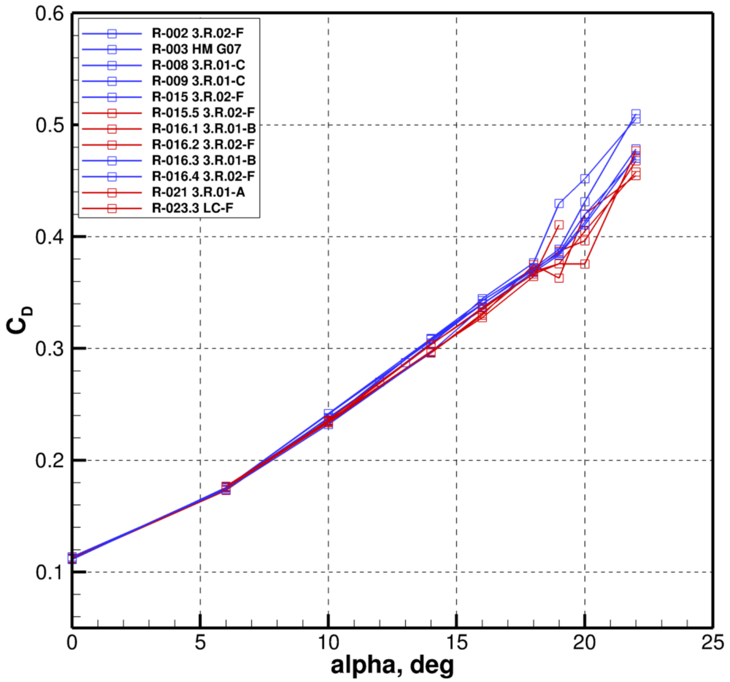

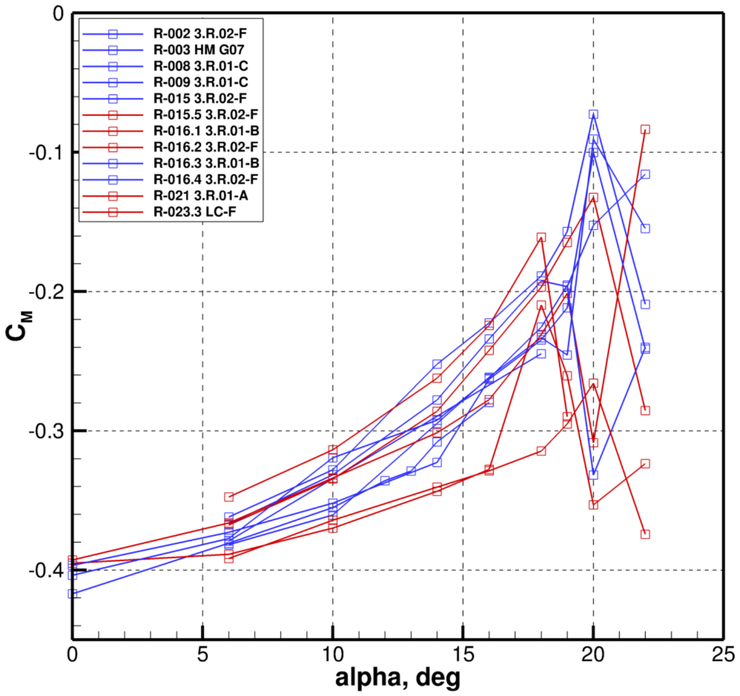

Global View:

- $C_{L,max}$ within [2.35, 2.60] achieved at 18° ≤ α ≤ 19°
- Poor agreement between C_L coefficients
- Some relative agreement between C_D coefficients at α ≤ 18°
- Poor agreement between C_M coefficients, more data needed

Case 3.4: F&M Polars on Nominal Grids, All RANS Solutions

Red = SA-notf2-R or SA-RC-QCR
Blue = SA

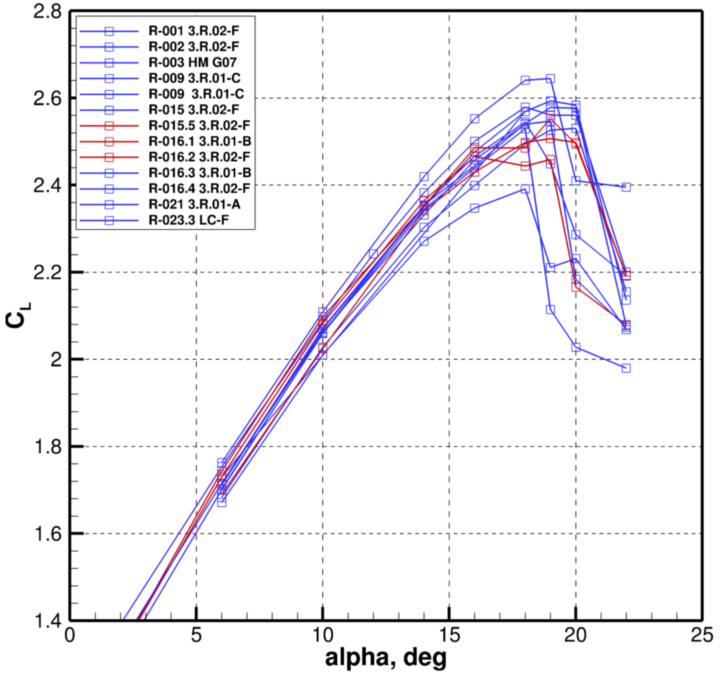

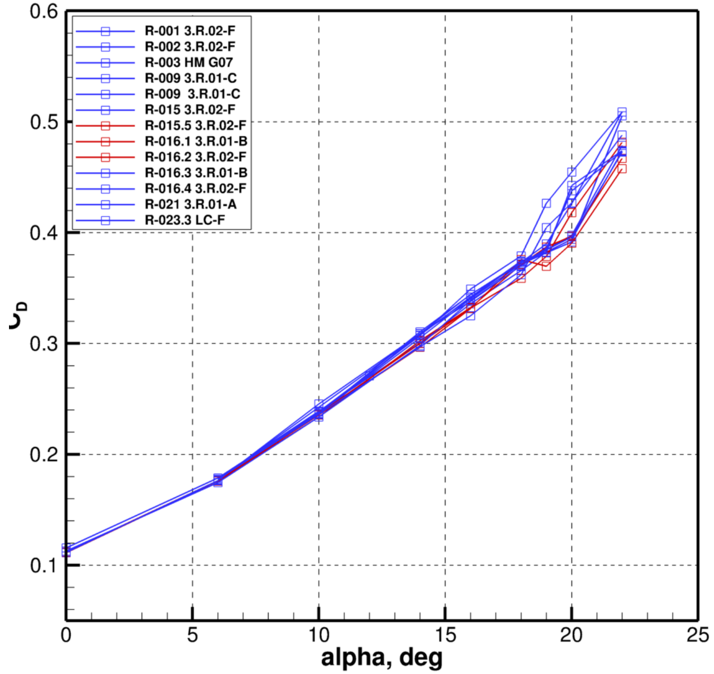

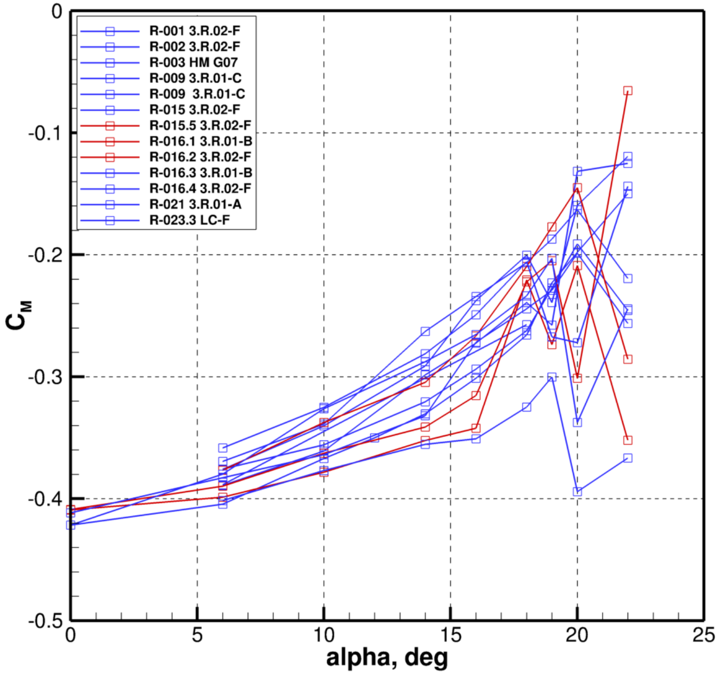

Global View:

- $C_{L,max}$ within [2.4, 2.7] achieved at 18° ≤ α ≤ 19°
- Poor agreement between C_L coefficients
- Some relative agreement between C_D coefficients at α ≤ 18°
- Poor agreement between C_M coefficients

Case 3.4: Skin-Friction Visualization at α=19°

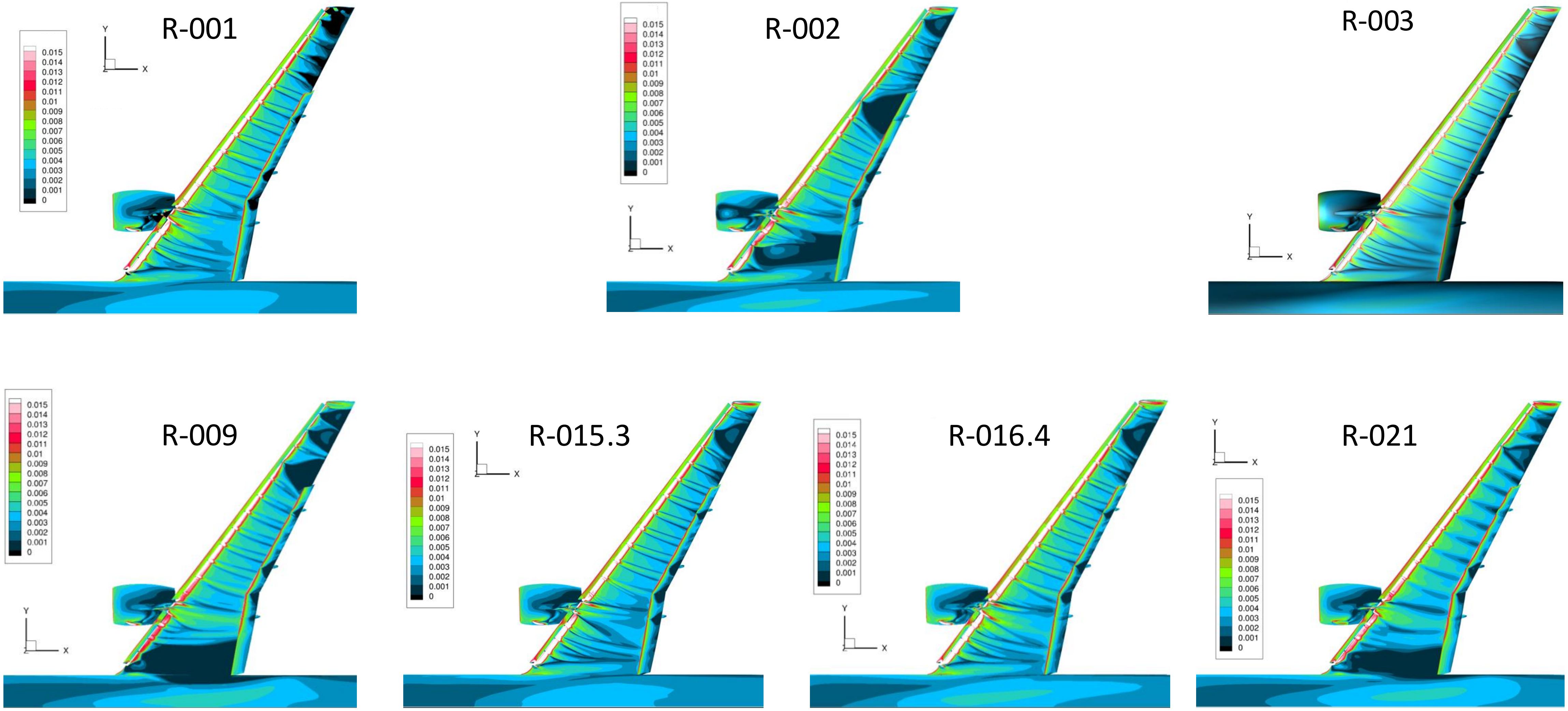

- Different skin-friction patterns
- “Pizza” disturbance appears outboard in all solutions
- Inboard separation observed in subset of submission

Case 3: Example (R-003) of Reynolds Number Effect

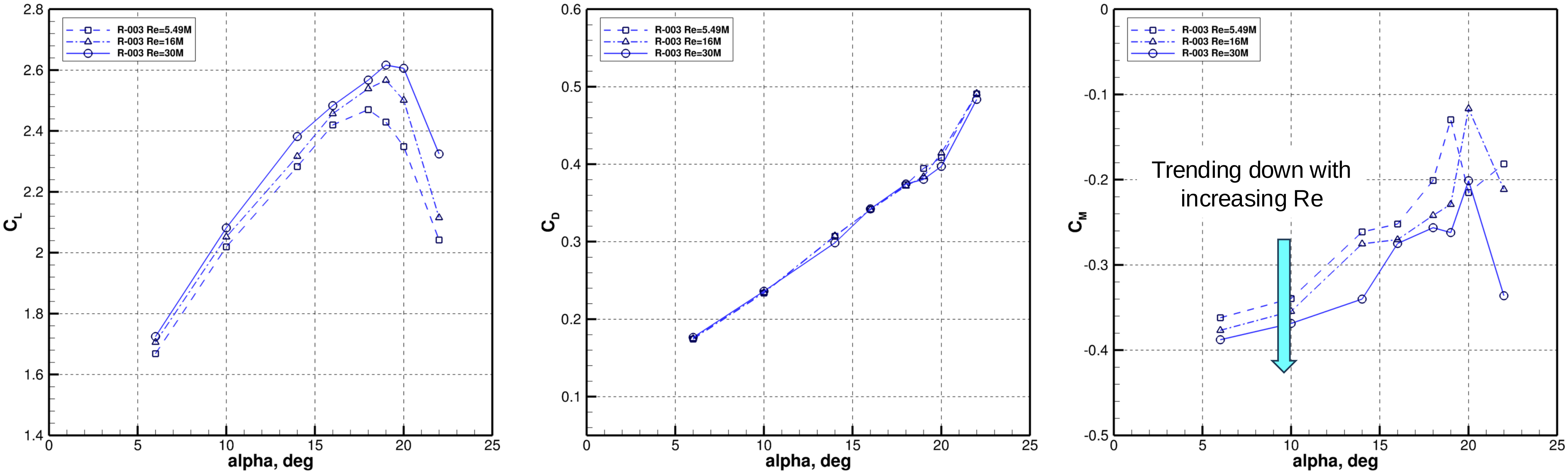

Effects of Reynolds number increase

- $C_{L,max}$ and corresponding angle of attack increase
- C_D has small relative change
- C_M becomes more negative

Long-dash line with square	: $Re_{MAC} = 5.49 \times 10^6$
Dash-dot line with triangle	: $Re_{MAC} = 16.00 \times 10^6$
Solid line with circle	: $Re_{MAC} = 30.00 \times 10^6$

Case 3: Reynolds Number Effect on C_L

R-001, R-002, R-003, R-008, R-015.3, R-015.5

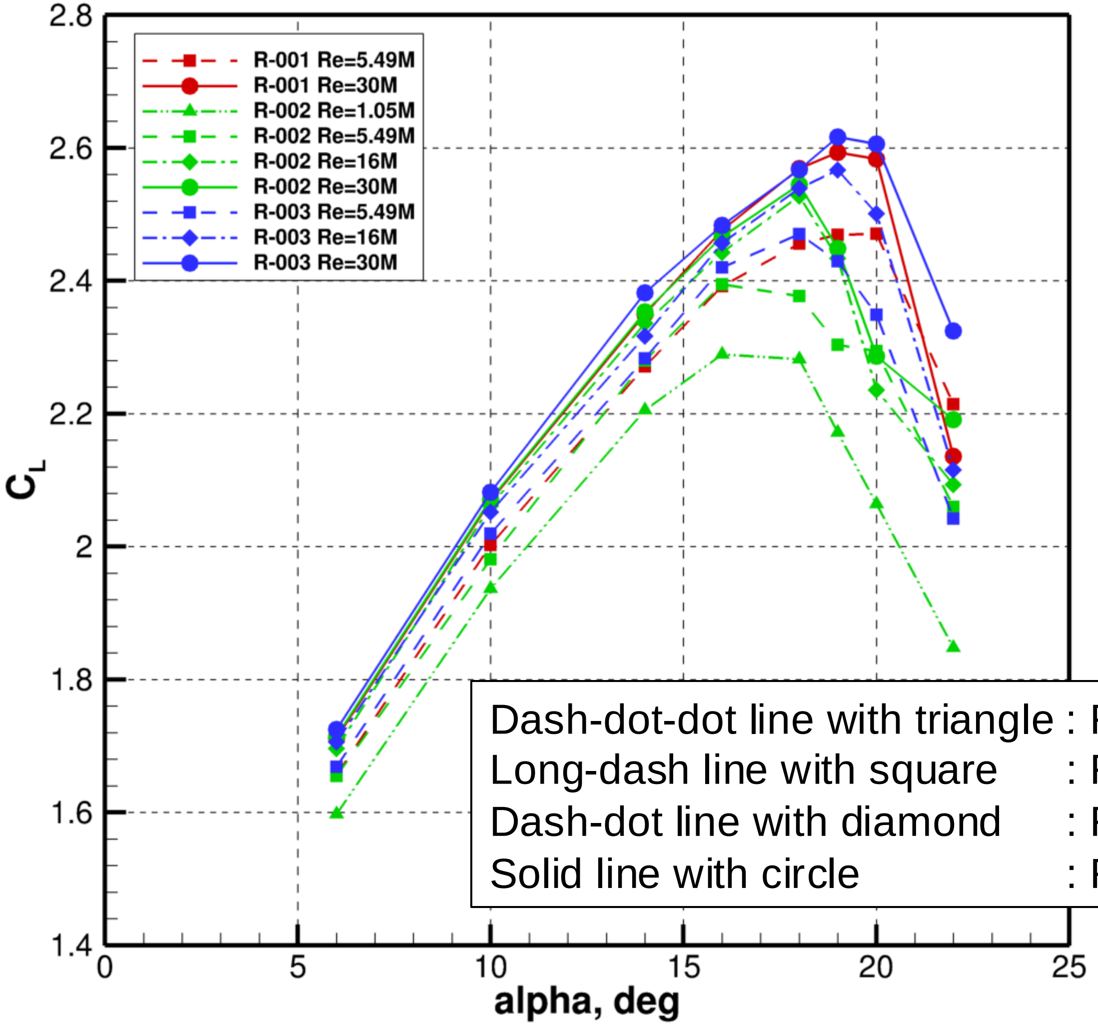

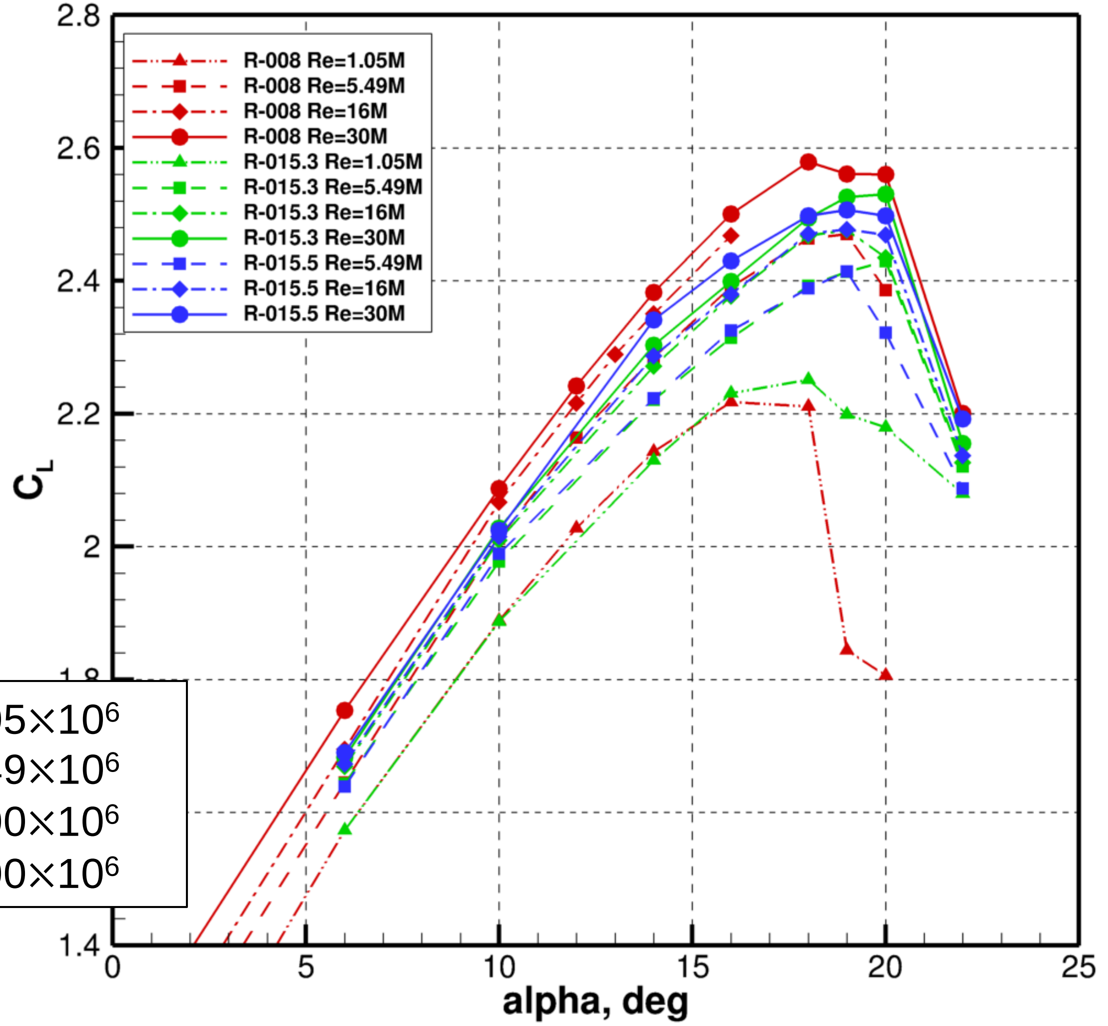

Dash-dot-dot line with triangle : $Re_{MAC} = 1.05\times10^6$
Long-dash line with square : $Re_{MAC} = 5.49\times10^6$
Dash-dot line with diamond : $Re_{MAC} = 16.00\times10^6$
Solid line with circle : $Re_{MAC} = 30.00\times10^6$

Case 3: Reynolds Number Effect on C_L

R-016.1, R-016.2, R-016.3, R-016.4, R-021, R-023

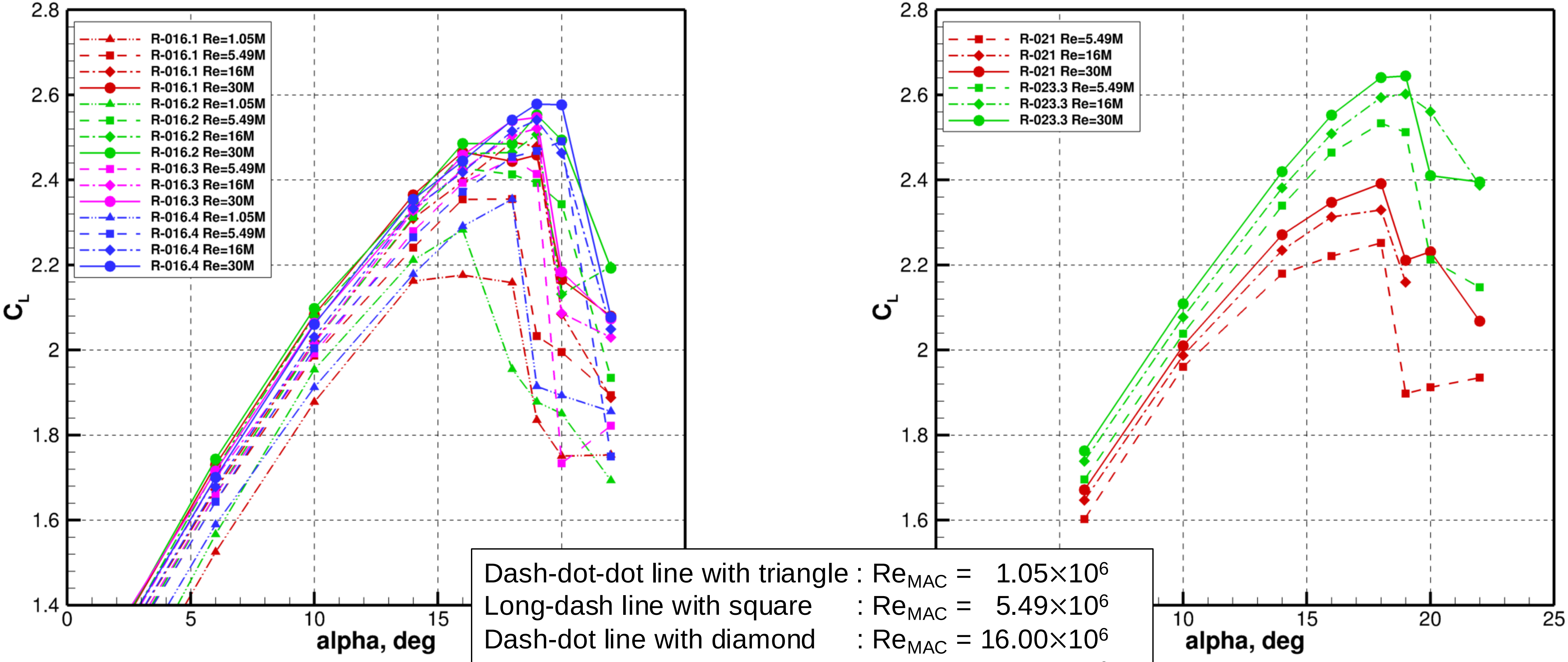

Dash-dot-dot line with triangle	: $Re_{MAC} = 1.05\times10^6$
Long-dash line with square	: $Re_{MAC} = 5.49\times10^6$
Dash-dot line with diamond	: $Re_{MAC} = 16.00\times10^6$
Solid line with circle	: $Re_{MAC} = 30.00\times10^6$

Case 3: Reynolds Number Effect on C_M

R-001, R-002, R-003, R-008, R-015.3, R-015.5

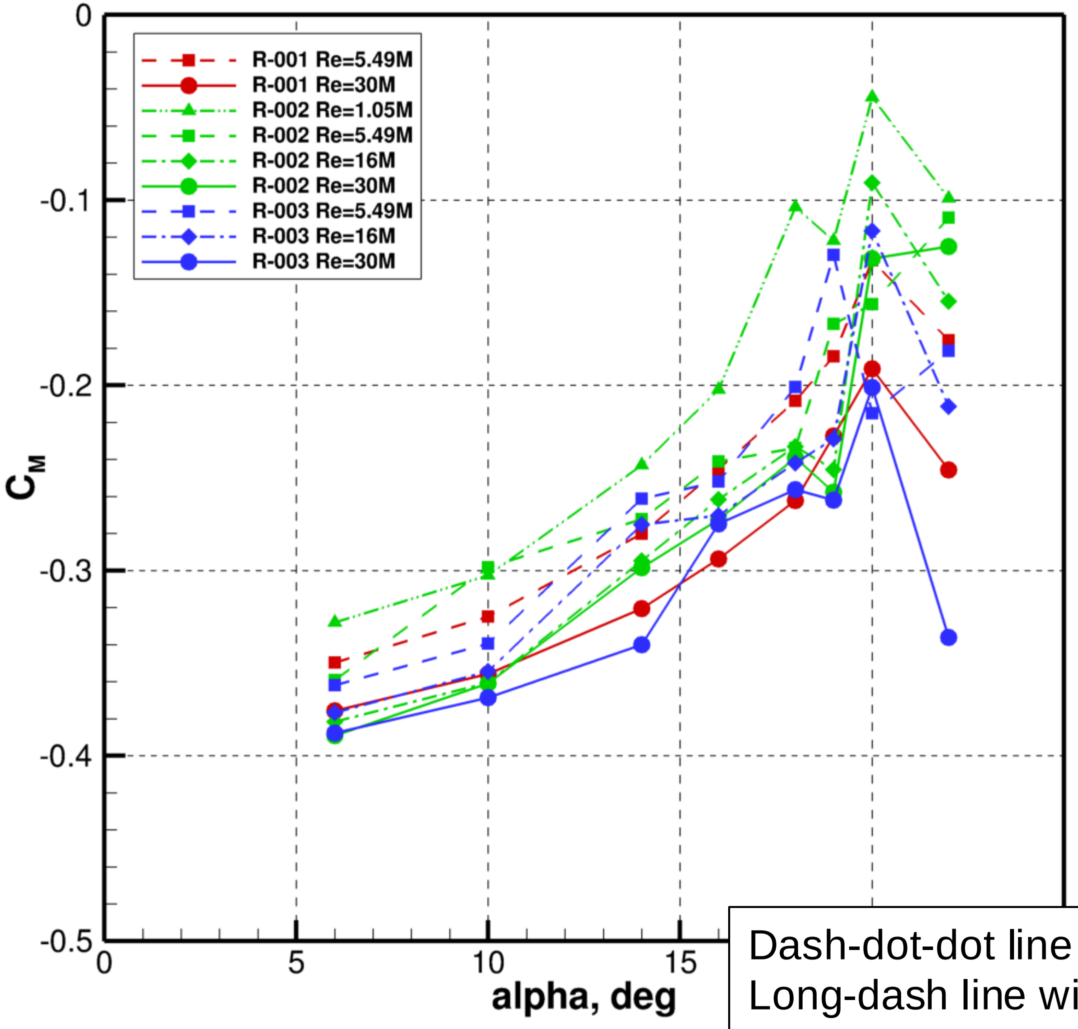

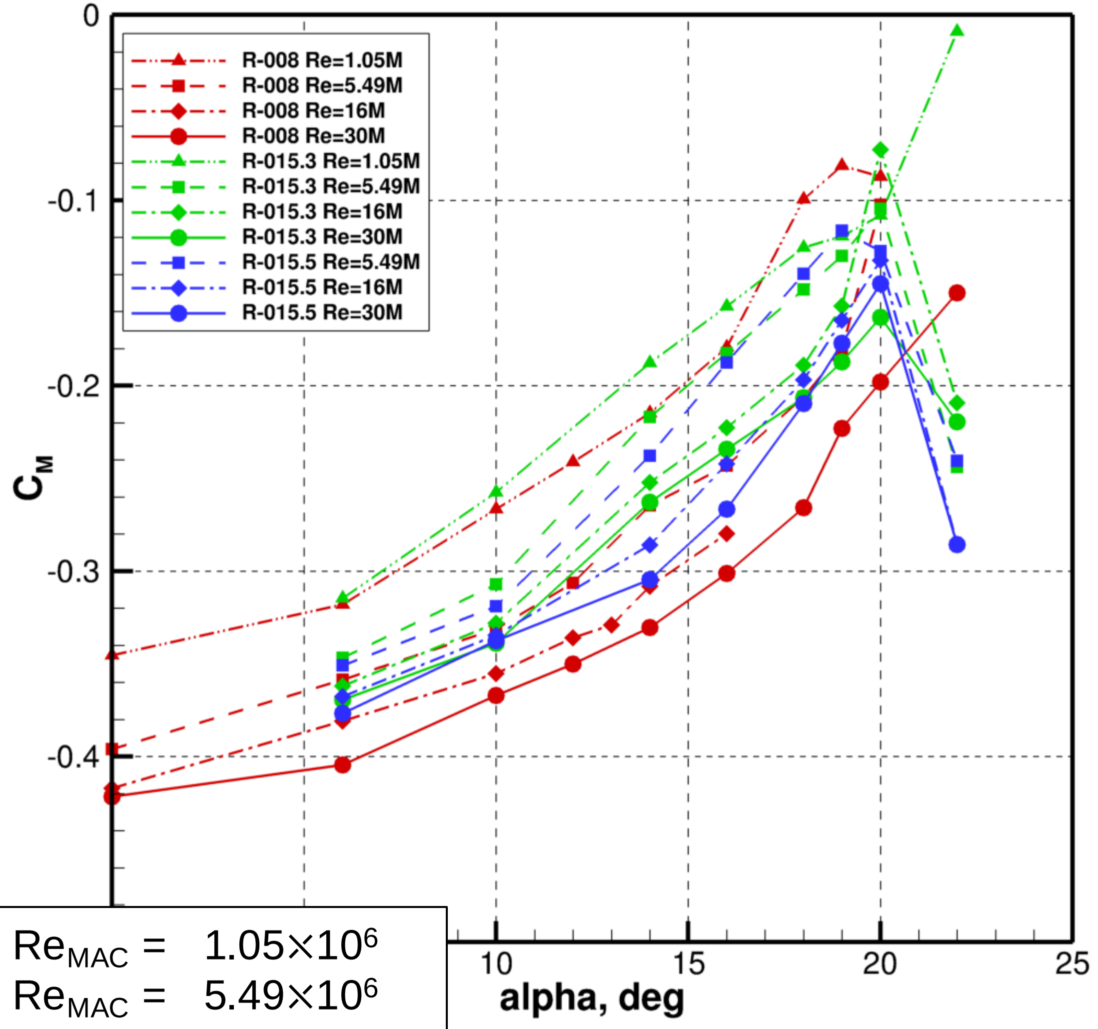

Dash-dot-dot line with triangle	: Re_{MAC} = 1.05×10⁶
Long-dash line with square	: Re_{MAC} = 5.49×10⁶
Dash-dot line with diamond	: Re_{MAC} = 16.00×10⁶
Solid line with circle	: Re_{MAC} = 30.00×10⁶

Case 3: Reynolds Number Effect on C_M

R-016.1, R-016.2, R-016.3, R-016.4, R-021, R-023

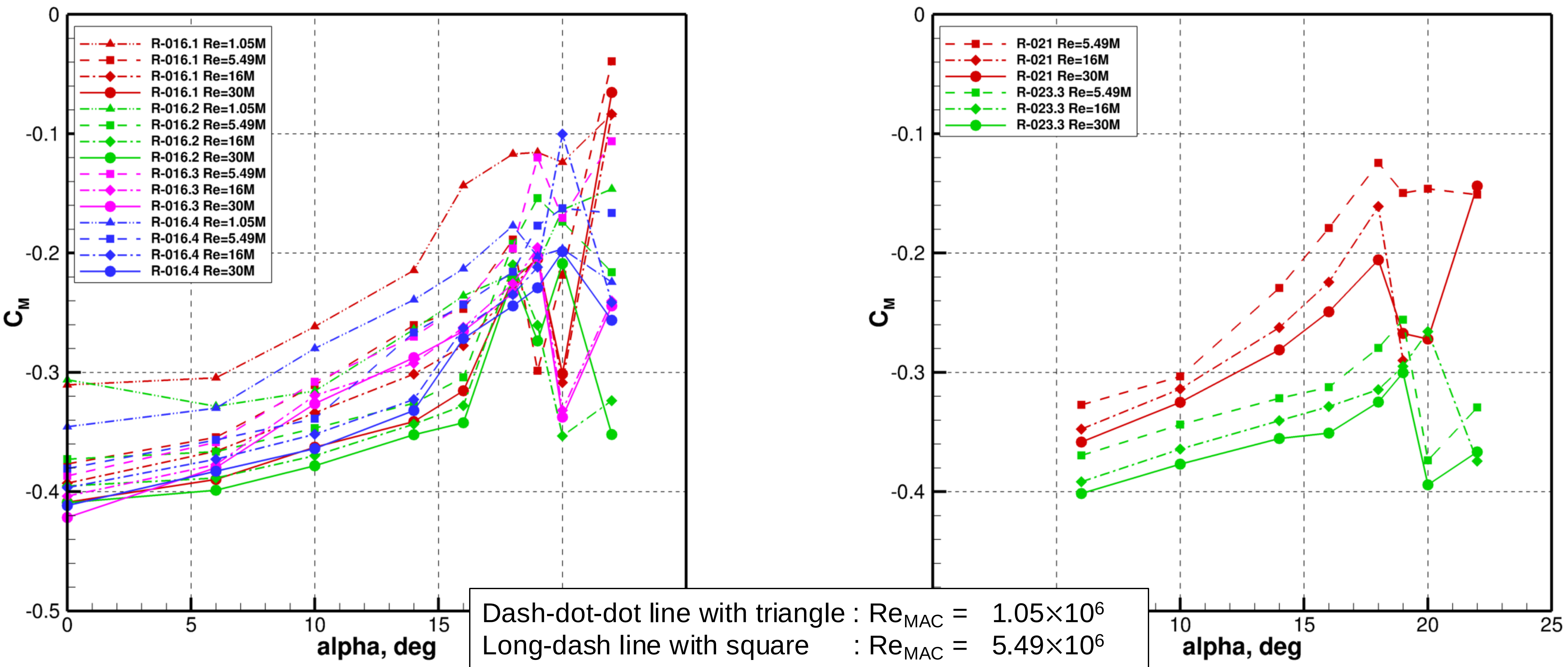

Dash-dot-dot line with triangle : Re_{MAC} = 1.05×10^6
Long-dash line with square : Re_{MAC} = 5.49×10^6
Dash-dot line with diamond : Re_{MAC} = 16.00×10^6
Solid line with circle : Re_{MAC} = 30.00×10^6

Test Case 3: Summary

- **No iterative or grid convergence observed**
  - No quantitative agreement between solutions
- **F&M deltas qualitatively support following trends corresponding to Reynolds number increase**
  - $C_{L,max}$ and corresponding angle of attack increase
  - C_D has small relative change
  - C_M becomes more negative

Effect of Slat Bracket Geometry and Gridding on RANS Solutions

Effect of Spatial Grid Resolution of Brackets

by Hidemasa Yasuda (Kawasaki Heavy Industries, Japan)

- **Effect of grid resolution of slat brackets for Cases 3.2, 3.3, and 3.4 at $\alpha = 6°$**
  - Current grid resolution does not resolve structure of vortex generated by slat bracket
  - Significantly different solutions (different separation patterns) for different grid resolutions
  - **Large sensitivity of RANS solutions to small changes in gridding of brackets and/or discretization scheme, even for low angles of attack**
  - **This sensitivity may be linked to insufficient spatial grid resolution to represent the bracket wake**

Iterative Convergence Sensitivity to Geometry and Grid Resolution

by Andrew Wick (Helden Aerospace)

- **Grid refinement on brackets at Case 3.4, $\alpha = 10°$**
  - Wake sources removed = slight improvement but drop in lift
  - Surface mesh on brackets refined = convergence is worse
  - Layer mesh refined = did not affect convergence
  - **Iterative convergence unaffected by mesh resolution**
- **Geometry modification**
  - Case 2.2, $\alpha = 10°$: Removing entire brackets = machine-zero residual convergence
  - Case 2.2, $\alpha = 10°$: Removing bracket mount = machine-zero residual convergence
  - Case 3.4, $\alpha = 10°$: Adding "filler" geometry into bracket gaps = residual convergence stalls on a single bracket in the middle of the wing
  - **Large sensitivity of RANS iterative convergence to bracket geometry**

Fixed-Grid RANS TFG Summary

- **Agreement between selected RANS solutions for Case 1 and Case 2.1 ($\alpha \leq 14°$)**
  - Iterative convergence and grid convergence for selected solutions
  - Importance of well-posed RANS models, grids that place degrees of freedom in right locations, and strong iterative solvers
  - Sufficient accuracy to distinguish between solutions corresponding to different RANS models
  - Experimental data for these flow regimes should allow assessment of RANS models
- **Today, RANS solvers do not agree on solutions for complex configurations (Cases 2.2 – 2.4 and 3.1 – 3.4) at high angles of attack**
  - RANS solutions (deltas) qualitatively follow trends for configuration buildup and Reynolds number increase
  - RANS model accuracy for these flow regimes cannot be assessed
    - Different separation patterns observed
    - "Pizza" disturbances prevent iterative convergence and grid convergence
  - Current gaps preventing quantitative assessment of RANS models
    - ✓ Lack of regularization of RANS models
    - ✓ Insufficient understanding of grid-resolution aspects
    - ✓ Insufficient robustness and efficiency of nonlinear solvers
    - ✓ Iterative-convergence sensitivity to small geometry features (e.g., slat brackets)

Fixed-Grid RANS TFG Summary

- **RANS predictions in comparison with ONERA experiment for Cases 2.2, 2.3, and 2.4**
  - Some agreement for low angles of attack
  - For high angles of attack
    - ✓ C_L is lower than experiment; some solutions show comparable C_L for Case 2.2
    - ✓ C_D has small relative difference from experiment; higher for Case 2.2
    - ✓ C_M is poorly predicted

- **Possible topics for future studies**
  - Isolate bracket-geometry issue from ability to predict separated flows
    - ✓ Focus on multiple angles of attack for Case 1 and/or higher angles of attack for Case 2.1
    - ✓ Use simplified bracket geometries for Cases 2.2-2.4
  - Modify RANS models, grids, and solvers for relevant flow conditions
    - ✓ Demonstrate iterative convergence and grid convergence
    - ✓ Establish reference solutions for RANS models in high-lift cases
    - ✓ Develop solver technology allowing iterative convergence for complex flows

Answers to Key Questions

- **Fixed-Grid RANS TFG Key Questions**
  - Can grid-converged solution be achieved with practical RANS solvers for high-lift configurations?
    - ✓ YES, RANS solvers can achieve grid-converged solutions on simple high-lift configurations
  - Can different solvers using the same RANS model agree on grid-converged solution?
    - ✓ YES, RANS solvers can agree on grid-converged solutions
  - What are requirements for different RANS solvers to agree on grid-converged solutions?
    - ✓ Verified implementation of the same well-posed turbulence model
    - ✓ Well-designed families of grids placing degrees of freedom in critical areas
    - ✓ Strong iterative solvers allowing iterative convergence for complex flows/configurations
  - What insight RANS solutions can provide for experiments and turbulence models?
    - ✓ Large sensitivity of iterative convergence to shape/gridding of slat brackets
    - ✓ Can we isolate effects of high angle of attack from effects of brackets?

Answers to Key Questions

- **HLPW-5 Key Questions**

- Case 1: Does consistency of integrated CFD forces/moments can be achieved for simple high-lift configurations?
  - ✓ YES, RANS solvers can achieve consistent solutions for simple configurations
- Case 2: Does consistency of CFD forces/moments change in configuration buildup?
  - ✓ Consistency for Cases 2.2, 2.3, and 2.4 at high angles of attack is worse than consistency for Case 2.1.
  - ✓ Deterioration of iterative convergence may relate to fidelity of bracket resolution
  - ✓ Some RANS solvers achieve converged solutions for configuration with brackets (Case 2.2)
  - ✓ Iterative and grid convergence may be facilitated by simpler slat bracket shape or modifications in turbulence models
- Case 3: Does consistency of CFD forces/moments change with variation of Reynolds number?
  - ✓ Do not have sufficient data
- Are there unique CFD modeling requirements (e.g., mesh, solver, etc.)?
  - ✓ Consistent use of turbulence models
  - ✓ Grids that place degrees of freedom in critical areas
  - ✓ Strong iterative solver allowing iterative convergence for complex cases
  - ✓ Ability to demonstrate iterative convergence and grid convergence

Many Thanks to Fixed-Grid RANS TFG Participants!!!

Questions?